

**Annual Report FY 2000**

**平成 1 2 年度 活動報告**

**Institute for Geothermal Sciences**

Graduate School of Science  
Kyoto University

京都大学  
大学院理学研究科

**附属地球熱学研究施設**

Institute for Geothermal Sciences  
Graduate School of Science, Kyoto University

京都大学 大学院理学研究科  
附属地球熱学研究施設



Beppu Geothermal Research Laboratory

Noguchibaru, Beppu 874-0903, Japan

Telephone: +81-977-22-0713

Facsimile: +81-977-22-0965

別府

〒874-0903 大分県別府市野口原

電話: 0977-22-0713

ファックス: 0977-22-0965

Homepage: <http://www.vgs.kyoto-u.ac.jp/>

Aso Volcanological Laboratory

Choyo, Aso, Kumamoto 869-1404, Japan

Telephone: +81-9676-7-0022

Facsimile: +81-9676-7-2153

阿蘇（火山研究センター）

〒869-1404 熊本県阿蘇郡長陽村

電話: 09676-7-0022

ファックス: 09676-7-2153

Homepage: <http://w3.vgs.kyoto-u.ac.jp/>



Front Cover Image:

The strombolian explosion in the 1st crater of Mt.Nakadake, Aso volcano in October 1979.

(Photograph: M.Sako)

表紙の写真:

1979年10月の阿蘇中岳第1火口のストロンボリ式噴火の様子  
(迫幹雄撮影)

Editorial compilation by Y. Furukawa

Printing by Meibundo Printing, Inc.

September 2001

## 目 次 Contents

序 Preface	iv
構 成 員 Member	1
研 究 活 動 Research Activities	
研究報告 Scientific Reports	2
公表論文 Publications	33
学会発表 Conference Presentations	35
共同研究 Collaboration	38
定常観測 Routine Observations	40
観測・実験システム Observation and Experimental Systems	46
教 育 活 動 Education	
学位・授業 Academics	52
セミナー Seminars	53
学 会 活 動 Activities in Scientific Societies	55
社 会 活 動 Public Relations	55
装置・設備 Instruments and Facilities	56
研 究 費 Funding	58
来 訪 者 Visitors	59

## Preface

Fiscal Year 2000, covering the period between April 2000 and March 2001, was the transformative time marking an epoch for university people; the Ministry of Education, Culture, Sports, Science and Technology was newly established by reorganization of Japanese Government, and also the juridical personalization of national universities started to materialize. Such movements urge us to think about what is expected and what can be done. Publication of our annual report started in 1997 when the Institute was established. Various records accumulated in the four reports including this volume should give us basic data to think and act towards the future.

Some changes in staff occurred in the Institute. Firstly, Dr. T. Ohkura took up his position of Associate Professor in Research Section for Volcanic Structure on 16 October 2000, coming from the Faculty of Integrated Human Studies, Kyoto University. Secondly, Professor Y. Tatsumi retired from the Institute on 31 December 2000 to work in Japan Marine Science and Technology Center. Although he held the post shorter than three years and half, he inspired staff with leading ideas on the Earth Sciences, and consolidated the research organization and experimental facilities in the Institute. I would like to express my cordial gratitude for his intensive contributions. For visiting professors, Professor Udo O. Fehn (University of Rochester) joined us from 1 April to 30 September, 2000 working on an investigation entitled "Determination of I-129 in geothermal and volcanic waters in Japan: a search for the presence of marine sediments in subduction zones". From 1 October 2000, Dr. Gary M. Thompson (University of Hong Kong) has taken the position carrying on his investigation entitled "Evolution of the deep mantle inferred from Re-Pt-Os isotopes". In addition to the twelve regular faculty members, two teaching associates, one JSPS research fellow, four special research fellows, one visiting researcher, six graduate students worked at the Aso and/or the Beppu facilities.

Mr. T. Hoka, Technician, retired from Kyoto University by reaching retirement age on 31 March 2001. Over the last 42 years, he has made many important contributions to various observations and to the maintenance of the facilities at the Aso Laboratory. On the same day, Ms. M. Yamamoto, Secretary, left the Beppu Laboratory. I would like to express my cordial gratitude to them.

Under changing circumstances inside and outside the Institute, we must strengthen our efforts even more. I hope that this annual report will contribute to the mutual understanding among the members of the Institute, as well as present their activities to a broader audience. I would like to invite all people to investigate our activities through this report and am looking forward to hearing comments and advise concerning the further development of the Institute.

May 2001

Yuki Yusa, Director in Fiscal Year 2000

## 序

20 世紀から 21 世紀へと移る平成 12 年度は、大学に籍を置き、研究と教育にたずさわる私たちにとって、文部科学省が発足するとともに、国立大学の法人化への動きが具体化するという、節目の年であったと思います。そうした激動の中で、私たちは、何を期待されているのか、何をなすことができるのかを常に考えていくことが要求されているように思われます。当施設が発足した平成 9 年度から発行が始まった本施設の年報は、今回で第 4 号となりますが、それらに盛られている活動記録は、将来に向けて考え・行動する上での基盤的資料になるものと信じます。

平成 12 年度においても、施設人員の異動等がありました。教官では、平成 12 年 10 月 16 日付で、京都大学総合人間学部より大倉敬宏助教授が着任されました。同助教授は阿蘇を主勤務地として、火山構造論研究分野を担当しています。これにより、施設の教官定員（12 名）が充足しましたが、平成 12 年 12 月 31 日付で、巽好幸教授が退職され、海洋科学技術センター（JAMSTEC）に異動なさいました。同教授の在任は 3 年半足らずの短期間ではありましたが、本施設に新風を吹き込み、

地球物質科学に関連した研究組織と実験設備の整備・充実を推進されました。ここに深く感謝の意を捧げたいと思います。外国人客員研究員には、平成 12 年 4 月 1 日から 9 月 30 日まで Udo O. Fehn 教授が就任し、「日本の地熱及び火山水中に含まれる沃素 129 の測定：沈み込み帯における海成堆積物存在の探索」の研究を行い、次いで、平成 12 年 10 月 1 日からは Gary M. Thompson 助教授が就任し、「Re-Pt-Os 同位体から推定される深部マントルの進化」の研究を行っています。以上に加えて、教務補佐員 2 名、日本学術振興会特別研究員 1 名、特別予算による非常勤研究員 4 名、研修員 1 名、大学院生 6 名が研究活動を行いました。

行政職では、昭和 34 年度から 42 年間の長きにわたって、阿蘇における観測と施設の維持管理をご支援いただいた外輝明技官が、平成 13 年 3 月 31 日をもって定年により退官なさいました。また、同日付けで、別府の事務を担当していただいた山本美由紀事務補佐員が退職されました。これらの方々に、深く感謝を申し上げます。

先に述べた大学法人化を始めとする変革の潮流の中にあって、研究を始めとする諸活動のいっそうの活発化が望まれます。この活動報告が、施設全員の相互理解と研鑽の抛り所として活用されることを願い、また、施設外の方々には、私たちの活動をご理解いただき、ご指導ご助言をたまわりますよう、お願い申し上げます。

平成 13 年 5 月  
平成 12 年度地球熱学研究施設長  
由佐 悠紀

## 構 成 員 Member

### 教 授 *Professors*

田中 良和 Yoshikazu Tanaka  
巽 好幸 Yoshiyuki Tatsumi  
平成12年12月 退職  
由佐 悠紀 Yuki Yusa  
(施設長 Director)

### 助 教 授 *Associate Professors*

古川 善紹 Yoshitsugu Furukawa  
大倉 敬宏 Takahiro Ohkura  
平成12年10月 着任  
大沢 信二 Shinji Ohsawa  
須藤 靖明 Yasuaki Sudo

### 助 手 *Assistant Professors*

橋本 武志 Takeshi Hashimoto  
川本 竜彦 Tatsuhiko Kawamoto  
小野 博尉 Hiroyasu Ono  
柴田 知之 Tomoyuki Shibata  
鈴木 勝彦 Katsuhiko Suzuki

### 外国人研究員 *Visiting Faculty*

Gary Thompson  
平成12年10月 着任  
Fehn Udo  
平成12年9月 退職

### 技 官 *Technical Professionals*

外 輝明 Teruaki Hoka  
馬渡 秀夫 Hideo Mawatari  
迫 幹雄 Mikio Sako  
吉川 慎 Shin Yoshikawa

### 教務補佐員 *Research Assistant*

芳川 雅子 Masako Yoshikawa

### 研究支援推進員 *Technical Assistant*

増田 秀晴 Hideharu Masuda  
平成12年11月 着任  
Bogdan S. Vaglarov

### 事務補佐員 *Secretaries*

今村 町子 Machiko Imamura  
山本 美由紀 Miyuki Yamamoto  
米沢 由佳 Yuka Yonezawa

### 臨時用務員 *Temporal Assistant*

増田 秀晴 Hideharu Masuda  
平成12年10月 退職  
山崎 咲代 Sakiyo Yamasaki

### 非常勤研究員 *Research Associates*

熊谷 一郎 Ichiro Kumagai (JSPS)  
松影 香子 Kyoko Matsukage  
平成12年12月 着任  
下田 玄 Gen Shimoda  
宇津木 充 Mitsuru Utsugi

### 大学院生 *Graduate Students*

網田 和宏 Kazuhiro Amita D4  
長谷 英彰 Hideaki Hase D3  
John Makario D2  
中坊 真 Makoto Nakaboh D4  
山田 誠 Makoto Yamada D1  
吉川 美由紀 Miyuki Yoshikawa D2

## Compressional wave velocity of granite and amphibolite up to melting temperature at 1 GPa

*Y. Aizawa and K. Ito*

Compressional wave velocities ( $V_p$ ) at above-solidus temperatures and at 1 GPa were obtained for an granite and amphibolite, which are considered to be major constituents of the continental crust. The temperature variation of velocities showed that the  $V_p$  values of granite decreased with raising temperature, but substantially increased beyond the melting temperature (850-900°C). Such an increase may be caused by the  $\alpha$ - $\beta$  transition of quartz (Fig. 1 (a)). The present results, together with estimated geotherms corresponding to the heat flow value, beneath the southern Tibet, suggest that the thickening of the felsic crust would lead to raise the temperatures within the crust sufficient to cause partial melting, yielding a low velocity and subsequent increase of the velocity due to the quartz transition (Fig. 2 (a)). The velocities of amphibolite decreased linearly with increasing temperature and dropped sharply at temperatures above the solidus (700°C), indicating that partial melting of amphibolite acts to significantly lower the seismic velocities (Fig. 1 (b)). Taking the density of the crust into account, the low average seismic velocities beneath central Andes, may be explained by the presence of partially molten amphibolite, which is probably originated from basaltic magmas underplated at the base of the crust (Fig. 2 (b)).

### References

- Owens, T.J. and Zandt, G. (1997) Implications of crustal property variations for models of Tibetan Plateau evolution, *Nature*, 387, 37-43.
- Wigger, P. J. and 10 others (1994) Variation in the crustal structure of the southern Central Andes deduced from seismic refraction investigations, In: K-J. Reutter, E. Scheuber and P. Wigger (Eds), *Tectonics of the Southern Central Andes*. Springer, Berlin, pp. 23-48.

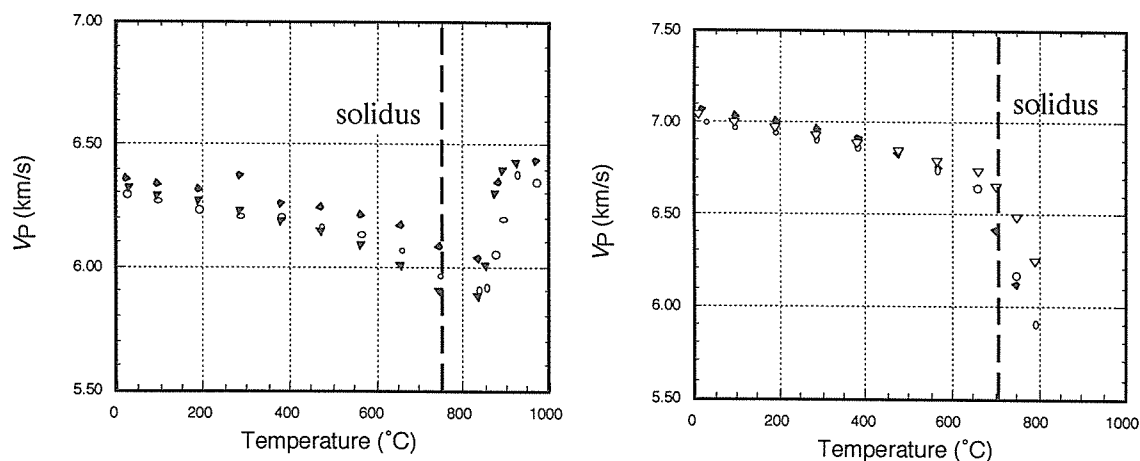


Fig. 1 Compressional wave velocity ( $V_p$ ) of granite; (a) and amphibolite; (b) as a function of temperature.

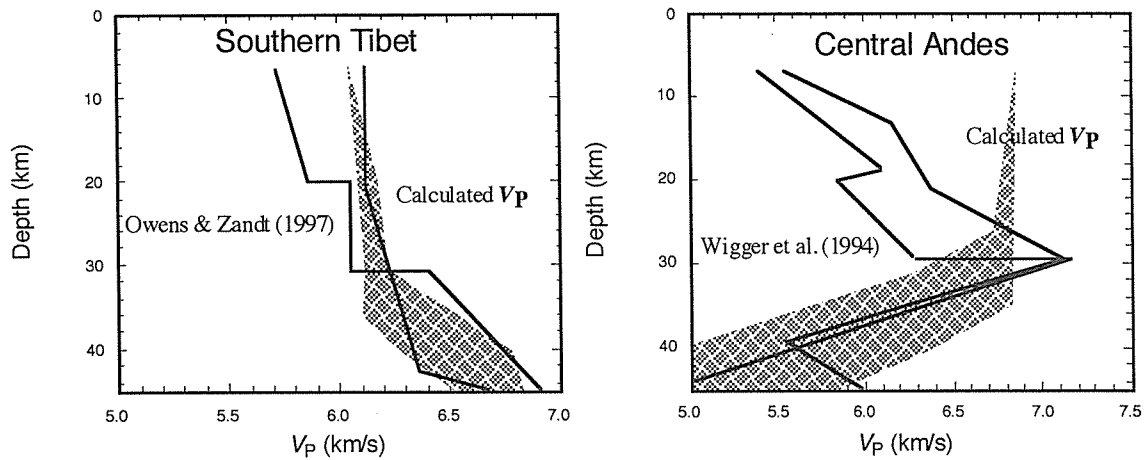
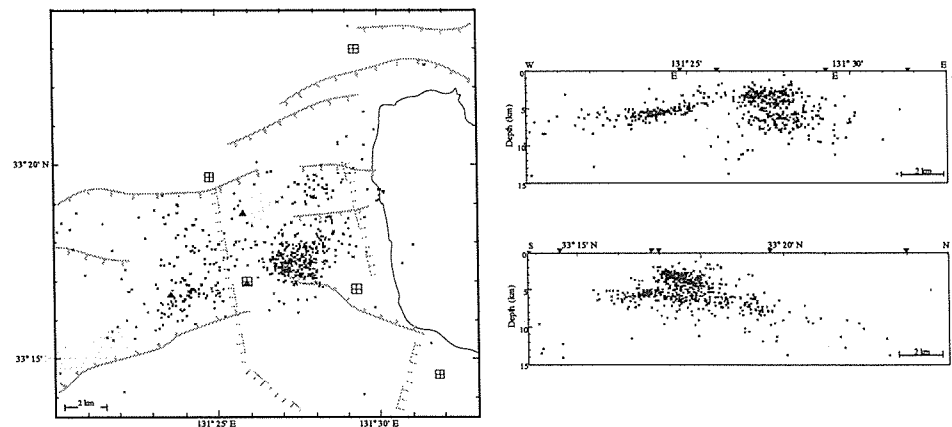


Fig. 2. Velocity ( $V_p$ )-depth relation of granite and amphibolite (this study), together with P-wave velocity data for southern Tibet (Owens and Zandt (1997)) and central Andes (Wigger et al. (1994)).

### Seismic Activity in the Beppu graben, Kyushu, Japan: implications for earthquakes triggered by magmatic fluids

*Y. Furukawa, H. Mawatari, and T. Ohkura*

The Beppu graben is located at the eastern end of the Beppu-Shimabara rift zone in Southwest Japan, where E-W striking normal faults are dominated. In this graben we have installed five seismic stations and monitored seismic activity since March 1993. Focal distribution in this graben shows the following features: (1) there is an aseismic zone in the eastern flank of the Quaternary volcanoes: Mt. Garan and Mt. Tsurumi, (2) most of earthquakes in this graben have occurred in a region around the aseismic zone, (3) focal distribution shows a parabolic form in which focal depths increase with the distance from the aseismic zone, while seismicity is active at shallower depths between the Kannawa and the Asamigawa faults through which hydrothermal circulation of meteoritic water is very active. These features could be explained by high temperatures of the magmatic body in the aseismic zone and migration of magmatic and meteoritic fluids around the magmatic body. The deeper limit of the seismicity probably corresponds to an isotherm of the brittle-ductile transition of granitic rocks. Magmatic fluids from the magmatic body migrate upward, which causes seismicity with the parabolic focal distribution above the isotherm. In the area of the shallow seismicity between the Kannawa and the Asamigawa faults hydrothermal circulation of meteoritic water is very active, which could be the cause of the shallower seismicity.





Left: Epicenter distribution located in the period from April 1993 to Dec. 1999 for events with magnitude greater than 1.0. The shaded oval represents the location of the estimated high electric conductivity body. Fault structures estimated from gravity survey are also shown as shaded straight lines. Open rectangles and filled triangles denote seismic stations and volcanoes, respectively.

Right: Vertical cross sections of focal distribution in the N-S and E-W directions. The solid triangles denote the location of the seismic stations.

### **Self-potential measurements on the central cones of Aso Volcano (3)**

*H. Hase, T. Hashimoto, M. Utsugi, and Y. Tanaka*

We have conducted self-potential (SP) surveys since 1998 on the central cones of Aso Volcano, southwestern Japan. As a result of the survey until last year, we detected some characteristic positive anomalies: (i) a regional anomaly, which centers on the Nakadake crater (+800mV); (ii) local anomalies around the hot spring areas (Jigoku-Tarutama, Yoshioka and Yunotani, +200mV); (iii) local anomalies around Mt. Kishima and Mt. Ojo (+300mV).

We also detected local positive anomalies on Mt. Eboshi and Mt. Neko. Positive SP anomalies are often considered as a sign of subsurface hydrothermal activity. Mt. Eboshi and Mt. Neko were formed about 25,000 and 100,000 years ago, respectively. They are older than most of other cones belonging to Aso Volcano. Besides, geothermal activity on the ground surface cannot be seen in these areas. Considering these matters above, it is difficult to attribute the cause of these positive anomalies to subsurface hydrothermal upflows around these areas. More plausible mechanism for the anomalies is the effect of impermeable layer in the vicinity of these peaks that interferes the water flow. Thus, positive anomalies of small scale appear there due to the canceling of topographic effects. In the case of (iii), we also recognize the same effect.

### **Geomagnetic variation and heat discharge at Aso volcano**

*T. Hashimoto, Y. Tanaka, M. Utsugi, S. Sakanaka, and H. Masuda*

Thermomagnetic changes and its mechanism of Aso Nakadake volcano was investigated using geomagnetic changes observed in 1991-2000 near the active crater with special attention to the heat budget of geothermal system including the crater lake. The heating and cooling rate below the crater was estimated based on the thermomagnetic model. The heating/cooling rate at the 'thermal reservoir' inferred from geomagnetic changes was revealed to have decreased to one fifth after 1994. In addition, the rate during calm stage of the volcano was found to be about one tenth of the discharging energy from the crater lake. The authors maintain that the crater lake functions as a large heat radiator which suppress the temperature variation of the system during a calm stage and that the crater lake should not be regarded as a 'thermal cap' as had been considered by Tanaka (1993). The 'thermal reservoir' below the crater lake during a calm stage works as a field of efficient heat transport from depths to the lake rather than as an accumulator of the heat. Therefore the heat-transport system including the crater lake tends to keep a quasi-equilibrium during the calm stage of volcanic activity. The authors consider that the equilibrium is broken and an active stage starts when the efficient heat-transport process is lost.

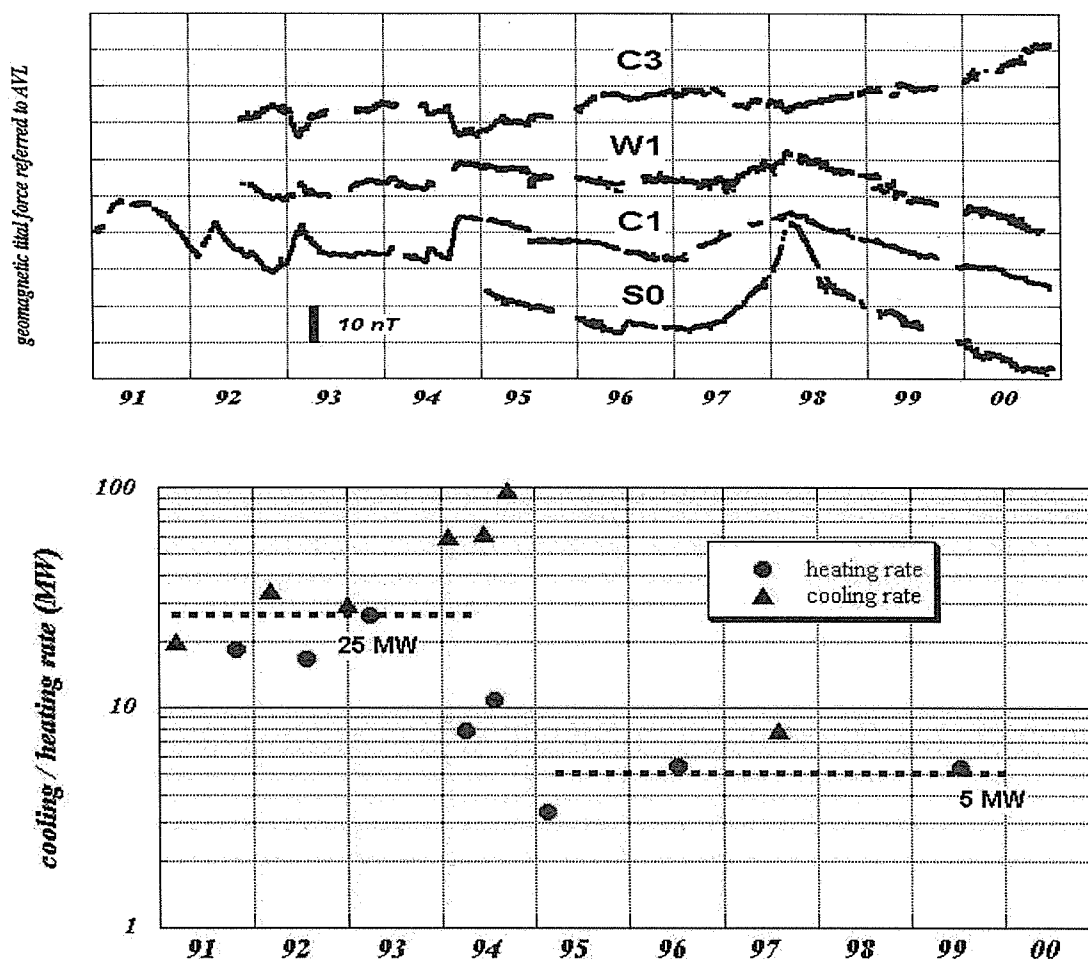


Figure1: (upper) Temporal change in geomagnetic total force observed at Aso volcano (daily values). (lower) Heating/cooling rate deduced from geomagnetic changes and powerloss from the surface of the crater lake.

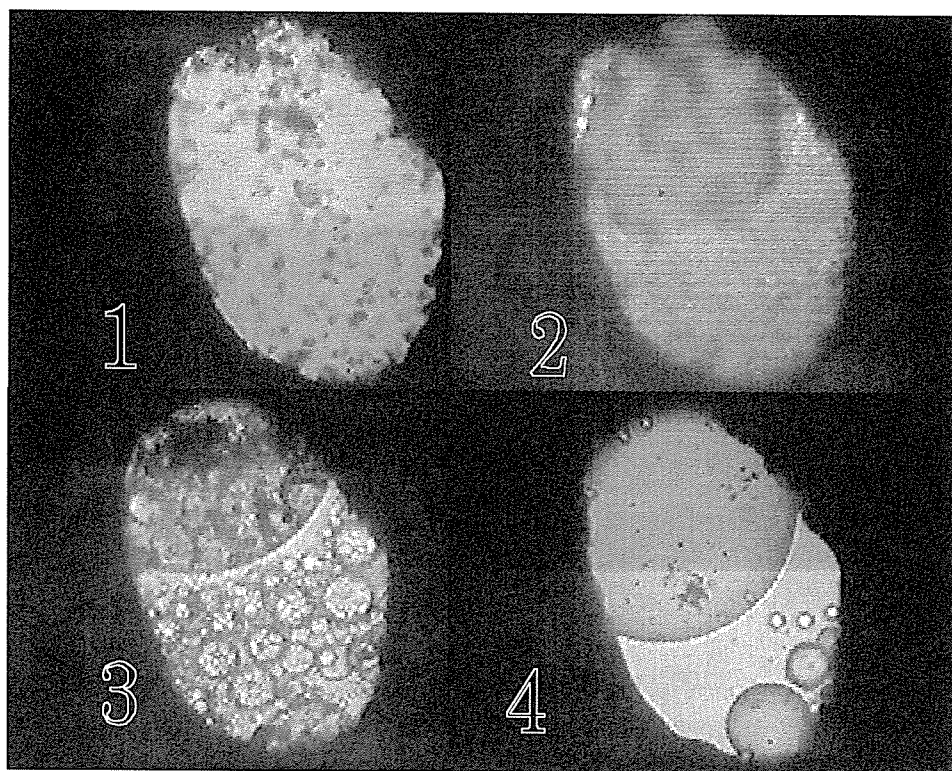
## Direct Observation of Complete Miscibility Between Andesitic Magma and H<sub>2</sub>O at High Temperature and Pressure Conditions

*T. Kawamoto*

Knowledge of structures of magmas is important to model the evolution of the earth's interior. Much efforts has been made to understand structure of magmas by measuring properties of glasses quenched from high temperature and pressure conditions. Properties of silicates melts have been found to be different from those of quenched glasses (1). Therefore, the direct measurement of melts at high temperature and pressure conditions is desirable. Based on chemistry of partial melts of H<sub>2</sub>O-saturated mantle peridotite, we have suggested structures of hydrous melts should change drastically with an increasing pressure (2). A series of direct observation of complete miscibility in H<sub>2</sub>O and an island arc andesite has been conducted using Bassett's type externally heated diamond anvil cell (DAC, (3)). The starting material is an andesitic scoria which was erupted from the east flank of Fuji volcano at 1707 (Ho-2). There is less than 1 volume % crystals in the sample. Chemical characteristics of the andesite (61.2 weight % SiO<sub>2</sub>, 0.97 % TiO<sub>2</sub>, 16.45 % Al<sub>2</sub>O<sub>3</sub>, 7.25 % Fe<sub>2</sub>O<sub>3</sub>\*, 0.14 % MnO, 2.29 % MgO, 5.7 % CaO, 3.9 % Na<sub>2</sub>O, 1.8% K<sub>2</sub>O, 0.3 % P<sub>2</sub>O<sub>5</sub>) is calc-alkaline andesite of Miyashiro, and of high alumina basalt series of Kuno, and medium K of Gill. Hydrous glasses were produced through melting of Fuji 1707 andesite powders and 2 weight % water at 1 GPa and 1300 °C for 1 hour with piston cylinder type high

pressure apparatus. For direct observation using DAC, chips of the quenched glass were loaded into a sample room of Rhenium gaskets with distilled water and an air bubble. Upon heating the air bubble is found to diminish into the H<sub>2</sub>O fluid at a homogeneous temperature, depending on a bulk density of H<sub>2</sub>O. This allows us to estimate the pressure and temperature path inside of the sample room using equation of state of H<sub>2</sub>O. Subsequent heating produces a single fluid phase with a small amount of crystalline phases left (Figure 1). Upon decompression or cooling, at around 1 GPa and 950 °C, the single supercritical fluid suddenly becomes milky (Figure 2) and is separated into two fluids (Figure 3), and they are coalesced to larger globules of H<sub>2</sub>O rich andesitic melts surrounded by silicate rich H<sub>2</sub>O fluid (Figure 4). Such a supercritical behavior has been reported in the albite and H<sub>2</sub>O system (4) and the SiO<sub>2</sub>-Al<sub>2</sub>O<sub>3</sub>-Na<sub>2</sub>O-K<sub>2</sub>O-CaO-MgO system (5). Whether such a supercritical behavior occurs between H<sub>2</sub>O fluids and magmas equilibrated with mantle peridotite system remains uncertain. This study is the first observation of a supercritical behavior of natural andesite. It is difficult to melt basaltic compositions in Bassett type DAC due to its temperature limitation of 1050 °C. The Fuji 1707 eruption produced ejecta in a compositional range from basalt to rhyolite (49 SiO<sub>2</sub> weight % to 70). We will examine the supercritical temperature and pressure conditions from andesite to rhyolite in order to estimate the PT conditions of possible supercritical fluid in the basalt-H<sub>2</sub>O system.

- (1) Stebbins, J. F., McMillan, P. F., and Dingwell, D. B. ed., 1995, Reviews of Mineralogy, 32, Mineral. Soc. Am.
- (2) Kawamoto, T. and Holloway J. R., 1997, Science, 276, 240-243.
- (3) Bassett, W. A., Shen, A. H., Bucknum, M. J., I-Ming Chou, 1993, Rev. Sci. Instrum., 64, 2340-2345.
- (4) Shen, A. H., and Keppler, H., 1997, Nature, 385, 710-712.
- (5) Bureau, H. and Keppler, H., 1999, Earth Planet. Sci. Lett., 165, 187-196.



Figures. Supercritical behavior of H<sub>2</sub>O and andesitic melt at around 1 GPa and 950 °C. A homogeneous fluid phase with a small amount of crystalline phases (1) becomes milky (2) and is separated into two fluids (3). Coalesced globules of H<sub>2</sub>O rich andesitic melts are surrounded by silicate rich H<sub>2</sub>O fluid (4). This sample room is 300 x 550 micrometers.

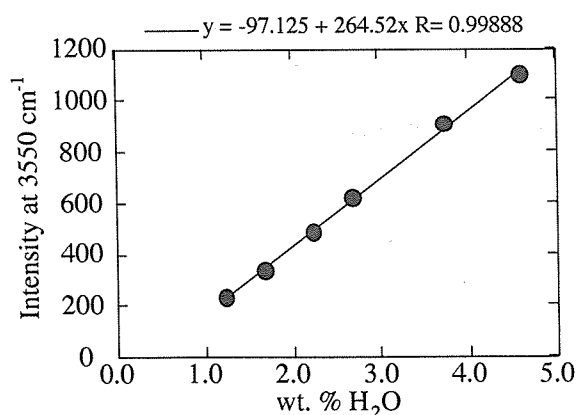
## Determination of H<sub>2</sub>O abundances in Andesitic glasses by micro-Raman spectroscopy

T. Kawamoto and S. Yamashita\*

(\*Institute for Study of the Earth's Interior, Okayama University at Misasa Campus)

H is the most abundant and important volatile element to affect differentiation processes of earth forming materials. However, H<sub>2</sub>O in deep-seated magmas escapes during ascending to the surface and is lost eventually at a moment of eruption, because H<sub>2</sub>O solubility in silicate melts decreases with decreasing pressure to zero at the atmospheric pressure. Therefore much efforts have been made to determine H<sub>2</sub>O concentrations of melt inclusions which can possess H<sub>2</sub>O in the depths. Recently Thomas (2000) performed Raman spectroscopy with rhyolitic compositions and concluded that Raman microscope is a vital tool to determine H<sub>2</sub>O concentrations of small melt inclusions. Raman microscope has a higher spatial resolution of a few micrometers than 10 micrometer of infra red microscope and SIMS and requires a single side polished section. We here report our results of Raman spectroscopy for hydrous andesitic glasses. The starting material is an andesitic scoria that was erupted from the east flank of Fuji volcano at 1707 (HoTa-1). Chemical characteristics of the andesite (58.21 weight % SiO<sub>2</sub>, 1.12 % TiO<sub>2</sub>, 16.92 % Al<sub>2</sub>O<sub>3</sub>, 8.45 % Fe<sub>2</sub>O<sub>3</sub>\*, 0.17 % MnO, 2.97 % MgO, 6.6 % CaO, 3.76 % Na<sub>2</sub>O, 1.47 % K<sub>2</sub>O, 0.33 % P<sub>2</sub>O<sub>5</sub>) is calc-alkaline andesite of Miyashiro, and of high alumina basalt series of Kuno, and medium K of Gill. Hydrous glasses were synthesized through melting of Fuji 1707 andesite powders and desired water contents at 1 GPa and 1300 degree C for 1 hour using piston cylinder type high pressure apparatus at Beppu. Quenching rate of 200 degree C per a minute was achieved by switching off a power supply. We used Au<sub>75</sub>Pd<sub>25</sub> capsule in order to minimize iron loss to the capsule material. Quenched glasses were crushed and separated to be used for density measurements and then H<sub>2</sub> manometry, and doubly polished thin sections originally for FTIR analysis. H<sub>2</sub> manometry was conducted by S. Y. at Misasa. Unpolarized Raman spectra of the andesitic glasses were measured with Raman microscope (Keiser HoloLab 5000 system) composed of 532 nanometer YAG laser, holographic transmission gratings, and CCD detector for 100 – 4500 cm<sup>-1</sup> Raman shift. Low frequency region at 250-1250 cm<sup>-1</sup> is characterized by bands from bending and stretching vibrations of Si – O – Si (Al). High frequency region is characterized by band at 3550 cm<sup>-1</sup> from Si (Al) – OH and molecular H<sub>2</sub>O. Absolute Raman intensity is difficult to obtain (Zotov and Keppler 1998). Therefore, we normalized the Raman spectra requiring that the integrated area in the range 250 – 1250 cm<sup>-1</sup> equals to 1,000,000. We obtained a linear relationship between normalized intensity of 3550 cm<sup>-1</sup> and total H<sub>2</sub>O concentrations determined by manometry (Figure). We are now investigating Raman spectra of hydrous rhyolite and basalt glasses with known H<sub>2</sub>O concentrations (Yamashita et al., 1997) and preliminary results show that we can use micro-Raman spectroscopy in a wide range of chemical compositions to determine 1 weight % or more H<sub>2</sub>O concentrations. FTIR can provide us with information about the speciation of OH and molecular H<sub>2</sub>O but require double polished section and the spatial resolution can be more than 10 micrometer. In order to know total water concentration of small melt inclusions micro-Raman spectroscopy can be a more useful tool than FTIR.

References: Thomas, R., 2000, *Am. Mineral.*, 85, 868-872., Yamashita, S., Kitamura, T., Kusakabe, M., 1997, *Geochem. J.*, 31, 169-174., Zotov, N. and Keppler, H., 1998, *Am. Mineral.*, 83, 823-834.



# Identification of iron-titanium oxides in a block-and-ash-flow deposit at Yufu Volcano, Southwest Japan: implication for lava dome collapse processes

T. Saito<sup>1</sup> and T. Kawamoto

<sup>1</sup> Graduate School of Human and Environmental Studies, Kyoto University

Since the 1990-95 eruption at Unzen Volcano, Southwest Japan, lava dome eruptions have been attracting many researchers in the field of volcanology. We have studied the Ikeshiro pyroclastic-flow deposit at Yufu Volcano in order to understand processes generating block-and-ash flows by dome collapse. By using paleomagnetic and rock-magnetic methods, we classified samples from the Ikeshiro pyroclastic-flow deposit into two types. Each type showed different magnetic properties. In this study, we characterized iron-titanium (Fe-Ti) oxides in samples of each type with an optical microscope in reflected light and an electron microprobe analyzer. We determined chemical compositions of Fe-Ti oxides with a JEOL JXA-8800K electron microprobe analyzer.

As a result, one type (type A) includes homogeneous titanomagnetite (TM) with  $x \approx 0.2$  and TM attached to titanohematite (TH) with  $y \approx 0.7$ . Equilibrium conditions are estimated to be temperatures of 840°C and  $fO_2$  of  $10^{-6}$  atmospheres. Fe-Ti oxides in the other type (type B) show complex textures and composition. TH20 lamellae within TM10 grain indicates that deuteric oxidation occurred in type B samples. Equilibrium condition estimated from compositions of this grain is temperatures of 760°C and  $fO_2$  of  $10^{-1}$  atmospheres. Another grain consisting of TH50, rutile and pseudobrookite indicates that type B was oxidized extremely (figure). In addition, existence of TH50 indicates that samples were quenched from high temperature (above 700°C). These suggest that Fe-Ti oxides in type B samples suffered from strong oxidation at lava dome before generation of the Ikeshiro pyroclastic-flow, while type A samples did not.

On the basis of these results, we propose the generation of the Ikeshiro pyroclastic-flow as follows. Lava blocks exposed on the dome surface (type B) were strongly oxidized and variable lamellae textures were formed, while lava blocks at the dome core (type A) were hardly oxidized. Collapse of the lava dome generated the Ikeshiro pyroclastic-flow and lava blocks were quenched from high temperature.

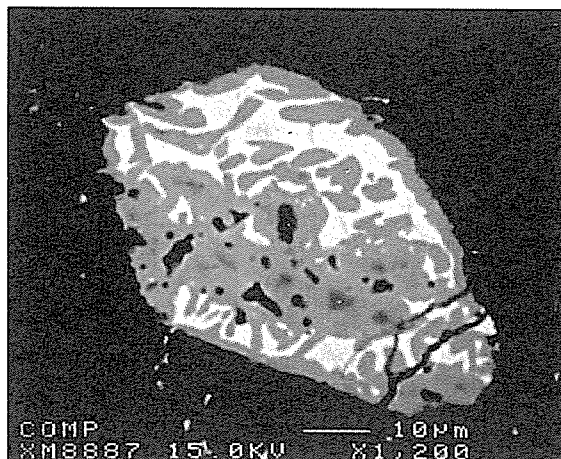


Figure. Photomicrograph of oxidized Fe-Ti oxides in type B samples. This grain consists of titanohematite with  $y \approx 0.5$  (white), pseudobrookite (light gray) and rutile (dark gray).

## NMR evidence for a new water dissolution mechanism in depolymerized silicate melts: results for hydrous diopside composition

X. Xue\*, T. Kawamoto, M. Kanzaki\*

(\*Institute for Study of the Earth's Interior, Okayama University at Misasa Campus)

The dissolution of water in silicate melts significantly affects their phase relations, and physical/thermodynamic properties. The mechanism of water dissolution is thus a subject of intensive interest in earth sciences and has been studied by various spectroscopic techniques. However, almost all the studies thus far have been on relatively polymerized systems, from fully polymerized silicates (e.g.  $SiO_2$ ) to disilicate compositions (e.g.  $Na_2Si_2O_5$ ). These studies have shown that water is dissolved in either molecular  $H_2O$  or  $SiOH$

at least for Al-free systems. More depolymerized silicate melts, such as metasilicate compositions are also geologically important, because mantle-derived magmas are known to become less silica-rich with depth of generation. Such magma could be particularly important during the early evolution of the earth's mantle. We have studied a hydrous diopside ( $\text{CaMgSi}_2\text{O}_6$ ) glass (quenched melt) using  $^{29}\text{Si}$  and  $^1\text{H}$  NMR in an attempt to understand the water dissolution mechanism in a depolymerized system. The sample contains about 3.85 wt%  $\text{H}_2\text{O}$  and has been synthesized at 1 GPa and 1500 °C in a piston cylinder apparatus. Both single-pulse  $^{29}\text{Si}$  and  $^1\text{H}$ - $^{29}\text{Si}$  cross-polarization (CP) MAS NMR yield a single, asymmetric peak near -82 ppm, resembling that of anhydrous diopside glass. The  $^1\text{H}$ - $^{29}\text{Si}$  CP time constant has been found to be 0.39 ms, similar to those of SiOH in other hydrous silicate glasses and crystals. Thus at least some of the dissolved water are in the form of SiOH. The  $^1\text{H}$  NMR spectra (both single pulse and spin-echo) contain two partially resolved peaks at 1.3 and 4.5 ppm. The 4.5 ppm peak is broader and asymmetric with a broad shoulder near 14 ppm. This peak and its shoulder are similar to those observed in more polymerized hydrous silicate glasses, such as  $\text{BaSi}_2\text{O}_5$ , and can be ascribed to SiOH and/or molecular  $\text{H}_2\text{O}$  with a range of H-bonding strengths. The 1.3 ppm peak is narrower and somewhat taller than the 4.5 ppm peak. The chemical shift of this peak indicates that it is due to OH groups that are not hydrogen-bonded. Peaks at this position has not been observed in any Al-free hydrous silicate glasses thus far and are not likely to be due to SiOH or molecular  $\text{H}_2\text{O}$ . On the other hand, MgOH in low-pressure hydrous magnesium silicates, such as talc, and CaOH in calcium silicate hydrates (CSH) are known to yield similar  $^1\text{H}$  NMR chemical shifts. We may thus assign this peak to MgOH/CaOH, suggesting that a substantial part of the dissolved water are in the form of free OH. Therefore the water dissolution mechanisms in silicate melts/glasses seem to change from molecular  $\text{H}_2\text{O}$ +SiOH in more polymerized systems to free OH groups plus SiOH/molecular  $\text{H}_2\text{O}$  in metasilicate compositions. Any model for water dissolution in depolymerized silicate melts/glasses must take this fact into consideration.

## **Salad dressing tells us differentiation of the Earth: laboratory experiments on differentiation process of multiphase fluids**

*I. Kumagai and T. Yanagisawa*

After shaking a bottle of salad dressing, the oil separates from the other ingredients such as water, soy sauce and sometimes sesames. This is analogous to differentiation process of the magma ocean that consists of multiphase fluids and solid particles. In order to identify the main parameters that control the rate of differentiation and the mode of separation, we have conducted laboratory fluid experiments on differentiation process of the multiphase fluids (olive oil, syrup and water mixture, perfluorocarbon) with varying density, viscosity and volume fraction. At present we attempt to construct a model for differentiation process and also consider stirring effect of multiphase fluids, because the rate of differentiation in the Earth's interior depends on the competition between processes tending to differentiate components and other tending to homogenize everything such as mantle convection. This connects with production and removal of geochemical heterogeneities in the Earth's mantle.

## **Anatomy of mantle plumes**

*I. Kumagai*

Recent developments of seismological studies have a great success in detecting much smaller structure of geological units such as mantle plumes. For example, the seismic images for P- and S-waves under Iceland show a cylindrical region of low velocity, extending from the surface to the core-mantle boundary. Not only the

external structure of the plumes but their anatomy (internal structure) are focused because geochemical studies about mantle plume products have revealed that they consist of more than two components of geochemically distinct sources. This multi compositional structure is generally interpreted as a product by the entrainment and mixing between plume sources and ambient mantle materials.

Here, laminar entrainment of starting plumes with a compositionally buoyancy has been explored based on laboratory experiments. Two types of starting plumes are identified in viscosity ratio 10.4 to 856 of the ambient to the buoyant fluid. The first is “vortex ring” type for a small viscosity ratio (11). The plumes entrain the ambient fluids and form a multi-layered and swirled structure within their heads. This is similar to the well-known structure as observed in the thermal starting plumes with the fluids having a strong temperature-dependent viscosity. In contrast, the second one, “chaotic mixing” type is observed for a higher viscosity ratio (104-856). No report has been published on this type. At the earlier stage, the plume head forms a double-layered structure by the entrainment, having a buoyant fluid as the upper layer and an entrained fluid as the lower. Thereafter, the shear-flow at the interface between the layers promotes the shear instability and produces a mixing layer between them. This mixing layer grows with time and finally all fluids in the plume head mingle together. Depending on the viscosity ratio, the resultant internal structure of the plume head is different: layered structure preserving the initial compositions vs. chaotically mixing tending to homogenize everything. The anatomy of the plume heads presented here will provide a new point of view for the spatial and temporal variation of the geochemical data obtained from mantle plume products.

## **Melting of Dry Peridotite KLB-1 Revisited: Precise Determination of Phase Relations and Composition of Solids**

*K. Matsukage, K. Kubo and E. Takahashi*

Nearly all-melting experiments on mantle peridotite so far were designed primarily to determine melt compositions. In this study, we report an attempt to determine equilibrium solid composition and their modes in the mantle melting. To search the most suitable sample container, we tested three different materials, Re, graphite and Pt. Sample assemblies were designed to minimize the loss of Fe and Ni and to maintain the oxygen fugacity close to that of the Earth's upper mantle (about FMQ buffer). Powder peridotite, KLB-1 (spinel lherzolite; Takahashi, 1986), was used as starting material. The starting material was dried with a 1atm furnace at 1000 °C under oxygen fugacity controlled at NNO ~ FMQ buffer using CO<sub>2</sub>/H<sub>2</sub> gas mixture. The high-pressure experiments were carried out using a piston cylinder apparatus with 1/2 inch-diameter furnace assembly including talc, pyrex glass outer sleeves and AlSiMg inner sleeve with straight graphite heater.

At 1.5GPa, the experiment with Pt capsule near the solidus (1375 °C) shows highly variable Mg# (=Mg/(Mg + Fe) atomic ratio) of olivine from 0.9 (center of capsule) to 0.99 (margin of capsule). On the other hand, the Mg# of olivine is homogeneous around 0.9 in the Re/Pt and graphite/Pt double capsules. At the 1425 °C (about 15% melting), the Mg# of olivine is 0.91 in graphite/Pt, 0.92 in Re/Pt and 0.95 in Pt. Oxygen fugacity of the run products was calculated from the reaction (Bryndzia and Wood, 1990): 6Fe<sub>2</sub>SiO<sub>4</sub>(olivine) + O<sub>2</sub> = 3Fe<sub>2</sub>Si<sub>2</sub>O<sub>6</sub>(opx) + 2Fe<sub>3</sub>O<sub>4</sub>(spinel). The calculated delta FMQ (= log(fO<sub>2</sub>)-log(FMQ)) of the run products with Pt, Re and graphite are 4 to 5, -2 to 0 and <-10, respectively. Accordingly the Re/Pt double capsule is found to be most suitable for melting experiments of dry peridotite at high temperature (above 1350 °C) and the oxygen fugacity of the Earth's upper mantle.

Using the Re/Pt capsule, melting experiments of KLB-1 were made at pressures between 1.0 to 2.5 GPa, temperatures between 1250 and 1600 °C and the phase relation and mineral chemistries were determined by EPMA. An important difference was observed between our experiment and natural mantle peridotites in the stability field of chromian spinel. Spinel, which is common in natural mantle peridotite regardless of the bulk chemistry (e.g., lherzolite, harzburgite, and dunite), disappeared at much lower degree of melting in our

experiments (Fig. 1). It appears that the lithological and chemical variation of natural peridotite cannot be formed by simple batch melting but are the results of more complex melting processes (fractional melting and/or influx melting).

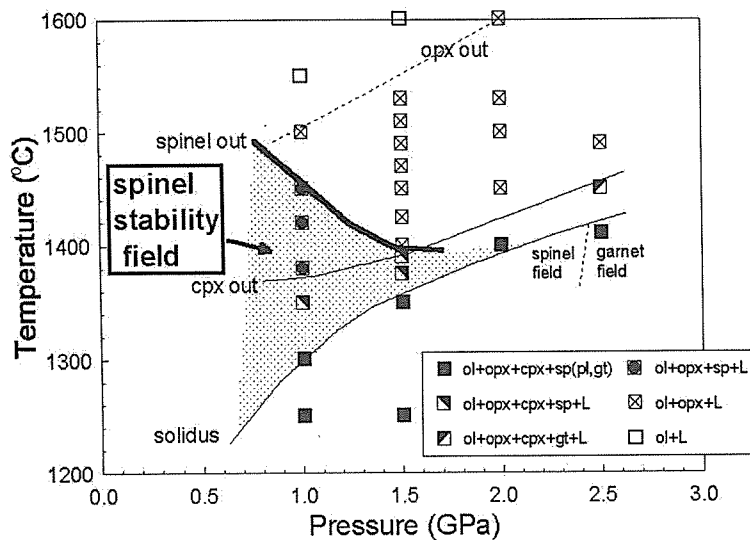


Fig.1. Phase relation of above solidus for lherzolite (KLB-1). Note that the stability field of chromian spinel significantly decreases with increase in pressure. ol, olivine; opx, orthopyroxene; cpx, clinopyroxene; sp, chromian spinel; gt, garnet; pl, plagioclase; L, liquid.

#### References

- Bryndzia, L.T., and Wood, B.J. (1990) Oxygen thermobarometry of abyssal spinel peridotites: the redox state and C-O-H volatile composition of the earth's sub-oceanic upper mantle. *American Journal of Science*, 290, 1093-1116.
- Takahashi, E. (1986) Melting of a dry peridotite KLB-1 up to 14 GPa: implications on the origin of peridotitic upper mantle. *Journal of Geophysical Research*, 91, 9367-9382.

## Ground deformation detected by EDM at Kuju Volcano

*M. Nakaboh, H. Ono, and M. Sako*

We have repeated EDM survey at Kuju Volcano since Oct. 1995 when a phreatic eruption occurred at the east flank of Mt. Hossho. There are geothermal region called Ioyama. New craters opened about 500m south from the pre-existing geothermal region. The fumarolic activity at pre-existing geothermal region activated after the phreatic eruption.

We constructed EDM network around the geothermal region, and extended the network step by step. The slope distance around Ioyama contracted rapidly in first a few months after the phreatic eruption. The contraction trend is still continued for more than 5 years since the phreatic eruption in 1995. For example, the slope distance of SGM-HSS contracted 67cm for about 5.5 years. The deflation source of Mogi model was located in a part of existing geothermal region where was the most active fumarolic region. The depth of source is about 800m from surface.

We infer that the ground deformation around Ioyama is caused by depression of the geothermal reservoir at deflation source by fumarolic activity. Because there are a good correlation between the temporal variations of the fumarolic activity and the slope distance.





We started GPS survey to locate the center of the deflation source in 1999. The first survey was carried out in February 1999. The second survey was in February and March 2001. Fig.1 shows the horizontal displacement of ground deformation. In this case, the station AVL is fixed. Most of the points moved to West. At stations, SKM and KBM, the displacement is large (about 2cm west against AVL). Fig.2 shows the horizontal displacement at the case of AVL moving 1.0cm to east and 0.2cm to south. In this case, the location of deflation source is near the center of descending area detected by leveling survey.

There are another three permanent GPS station constructed by GSI (Geographical Survey Institute) in Aso Caldera. We will analyze the location of deflation source together with GSI data in the near future.

## GPS Observation of Crustal Movements in the Macolod Corridor, Philippines

*T. Ohkura, G.M. Besana, T. Nakano, M. J. Sicat, Y. Hosono, E. Mangao, I. Geraldo, M. Ando, and R. S. Punongbayan*

GPS measurements were undertaken in order to detect crustal movements related to the origin of the Macolod Corridor in the Luzon island, Philippines. We established thirteen stations and made five campaigns from April 1996 to April 1998.

Most of the stations were found to be moving toward NW or WNW at 4-6 cm/yr with respect to the stable interior of the Eurasian plate. Moreover, the stations in the southern regions are moving noticeably toward ENE or East at about 2-3 cm/yr relative to northwestern part.

If we take into consideration the block motion determined through a recent paleomagnetic research and the young ages of volcanic, the obtained movements could be closely related to the formation of the Macolod Corridor caused by the collision of the Mindoro and Palawan blocks. The movements of these blocks may have been reactivated by the initiation of subduction of the Philippine Sea plate along the Philippine trench around 4 Ma.

Fig.1 a)

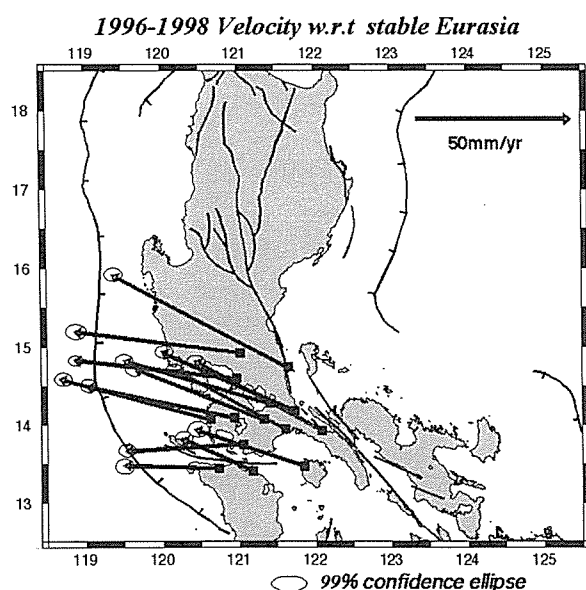


Fig.1 b)

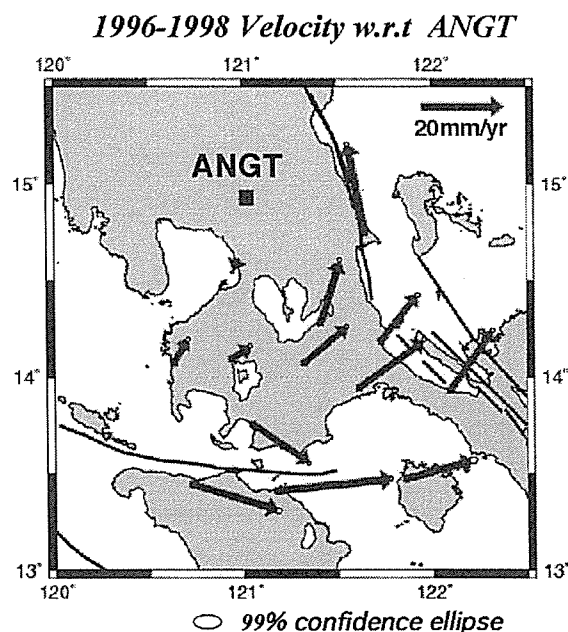


Fig.1 a) Velocity vectors at thirteen stations and Manila are shown with respect to stable Eurasia. The 99%

confidence ellipse is shown at the tip of each vector. b) Velocity vectors obtained by data analysis from April 1996 to April 1998. In this figure, ANGT is fixed. The 99% confidence ellipse is shown at the tip of each vector.

### **Rayleigh scattering by aqueous colloidal silica as a cause for the blue color of hydrothermal water**

*S. Ohsawa, T. Kawamura, N. Takamatsu and Y. Yusa*

Thermal waters in hydrothermal ponds, bathing pools and the brines of geothermal electric power plants commonly have a characteristic blue color. Although many researchers have assumed that the blue color is due to a colloidal suspension and/or absorption by dissolved ferrous iron or by water itself, there has been no specific effort to identify the physical nature of this phenomenon. We have tested, in synthetic and natural solutions, whether aqueous colloidal silica is responsible for the blue color. Aqueous colloidal silica is formed by silica-polymerization in thermal waters of the neutral-chloride type which contain initially monomeric silica in concentrations up to 3 times above the solubilities of amorphous silica. The hue of the blue thermal waters in the pools tested agrees with that of a synthesized colloidal silica solution. Grain size analyses of aqueous colloidal silica in the blue colored thermal waters demonstrate that the color is caused by Rayleigh scattering from aqueous colloidal silica particles with diameters (0.1-0.45 $\mu\text{m}$ ) smaller than the wavelengths of visible radiation.

(Submitted to JVGR)

### **Some geochemical features of hyper-acid brine of the summit crater lake on Aso Volcano, Japan**

*S. Ohsawa, Y. Onda, K. Amita, G. Shimoda,  
M. Yamada and K. Iwakura,*

On August 4 in 2000, water samples for chemical and isotope analyses were collected from Yudamari crater lake formed in the 1st crater of Mt. Nakadake, Aso Volcano, central Kyushu, Japan. The lake water has very high acidity (below pH 1) and contains chloride and bisulfate ions in large quantities. After sampling, gypsum precipitated from the sampled waters at an ambient temperature. Calculation of gypsum saturation indices with a modified SOLVEQ indicates that the lake water is near saturation with gypsum at the lake water temperature (ca. 55°C) and gypsum becomes supersaturated as the result of increase of activity of sulfate ion by dissociation of bisulfate ion as the sample water is cooled. Aqueous SiO<sub>2</sub> concentration of the lake water samples (430mg/L) is extremely higher than saturation value with respect to the most soluble SiO<sub>2</sub> mineral (amorphous silica) at the temperature of lake water. Dissolved sulfate enriched in <sup>34</sup>S ( $\delta^{34}\text{S}$ ; ca. +16‰) is probably formed by SO<sub>2</sub> disproportionation and/or hydrolysis of elemental sulfur at an elevated temperature. These may be signs that sublimic hydrothermal environment has been established under the lake. Temperature of the hydrothermal system is inferred to be about 160°C from oxygen isotopic equilibration between dissolved sulfate and lake water.

(Submitted to Geochemical J.)

## **Simplified analysis of stable carbon isotopic composition of dissolved inorganic carbon in hydrological samples**

*S. Ohsawa*

Recently, source and behavior of dissolved inorganic carbon (DIC;  $\text{CO}_2 + \text{HCO}_3^- + \text{CO}_3^{2-}$ ) in groundwater and river water, etc. have been actively discussed based on the investigation about its stable carbon isotope ratio and concentration. This study proposes a simplified preparation method for the carbon isotope measurement of DIC in hydrological samples. In this method,  $\text{SrCO}_3$  for the isotope measurement is directly precipitated from the sample water by adding carbonate-free  $\text{Sr}(\text{OH})_2$ . In spite of boiling of the treated sample water and exposure to atmospheric- $\text{CO}_2$  through the preparing process, it was shown that this isotopic analysis has constant systematic error ( $-0.5\text{‰} - -0.6\text{‰}$ ) no more than precision of the mass-spectrometry (less than  $\pm 0.1\text{‰}$ ). A linear relationship between reciprocal of concentration and  $\delta^{13}\text{C}$  value of DIC:  $\delta^{13}\text{C} = 6.59 \times 1/\text{DTC} - 21.8$ , is recognized by the application of the established method to river water samples from 8 small rivers in the Shimabara Peninsula, Nagasaki Prefecture. This relationship is likely to indicate that the river waters are mixture of groundwater equilibrated with soil  $\text{CO}_2$  and surface water equilibrated with atmospheric  $\text{CO}_2$ , and/or are soil  $\text{CO}_2$ -equilibrated groundwater interacted with atmospheric  $\text{CO}_2$  while the river waters flow through the drainage basins.

(Submitted to Japanese J. Limnology)

## **Cenozoic volcanism in northern Sikhote Alin, Far East Russia and its implication for the opening of the Japan Sea**

*K. Sato, R.T. Arai, Y. Tatsumi, T. Sano, T. Tagami, and V.S. Prikhodko*

K-Ar ages and major/trace element compositions were obtained from 59 fresh lavas from the northern Sikhote Alin, Far East Russia, in order to document the secular variation in volcanism and upper mantle processes during backarc opening. This region is distinct in that it was the home of the NE Japan arc sliver before the opening of the Japan Sea backarc basin. Also, the distribution of lavas from the coastal region to the inner part of the continent is the characteristic feature of this region. Northern Sikhote Alin can be divided into two volcanic belts, that is, the East Sikhote Alin volcanic belt (ESAVB) along the Japan Sea coast, the West Sikhote Alin volcanic belt (WSAVB).

The volcanic activity in the north Sikhote Alin took place during 40-25 Ma and 20-5 Ma, and was separated by a marked hiatus in volcanism during 25-20 Ma, which is synchronous to the period of the major rifting event in the Japan Sea backarc basin. It should be stressed that the volcanic activity during the pre-rifting stage of the Japan Sea occurred in the entire ESAVB along Japan sea, whereas no volcanism in the WSAVB. Such an arc-like distribution of volcanism may suggest the location of a continental arc-trench system in this region before the formation of the backarc basin. On the other hand, the volcanism during 20-5 Ma exhibits "spot-like" distributions both in the WSAVB and ESAVB.

All lavas erupted in the ESAVB during 40-25 Ma have compositions typical of subduction-zone magmas, implying that the ESAVB formed a continental-margin arc before the opening of the Japan Sea. It is further suggested that the backarc rifting is initiated at the volcanic front, not in the backarc region. Thus, the present data clearly demonstrate that the opening of the Japan Sea initiated at least 25-20 Ma, earlier than 15 Ma as suggested previous based on paleomagnetic data. On the contrary, the arc magma chemistry is not confirmed for any lava erupted during 20-5 Ma, indicating that such subduction-related volcanism was terminated due to the opening of the Japan Sea. During 20-5 Ma, intraplate-type lavas with typical hotspot magma compositions typifies the Sikhote Alin volcanism and may be caused by mantle upwelling beneath the Cenozoic intraplate basalt province in the northeast China and Far East Russia.

# Faraday cup efficiency in a multicollector mass spectrometer, Finnigan MAT 262 at Beppu Geothermal Research Laboratory

*T. Shibata, M. Yoshikawa and Y. Furukawa*

## Abstract

Relative Faraday cup efficiencies in the Nd isotope analysis with static multicollection technique were determined to eliminate the difference in Faraday cup efficiencies by measuring the Nd isotope ratio with nine different cup configurations. The result shows that a part of Faraday cups in thermal ionization mass spectrometer of BGRL were already damaged and correcting calculation with relative Faraday cup efficiencies is necessary to obtain reliable isotope ratios by static multicollection technique.

## Introduction

The development of the technology of mass spectrometer with static multicollection mass spectrometry (SMCMS) (e.g. Wagner et al., 1984), in which multiple collectors measure all isotopes concerned simultaneously, has realized the improvement of the analytical precision and reduction of the time for data acquisition (e.g. Noble et al., 1990; Thirlwall, 1991). In this technique, Faraday cup efficiencies (FCEs) of each Faraday cup must be same within the analytical error, because FCEs of each collector are assumed to be equal when the static multicollection technique is applied. However, it is well known that large ion beams damage Faraday cups resulting the change and instability of FCE. This change and instability of FCE induce systematic errors in analytical result (Makishima and Nakamura, 1991). Therefore, we determined RFCEs of thermal ionization mass spectrometer (TIMS) at BGRL following the method described in Makishima and Nakamura (1991) to obtain reliable isotope ratios by SMCMS.

## Experiment

TIMS of Finnigan MAT 262<sup>®</sup> was employed in this report. This TIMS is equipped with 8 movable Faraday cups and fixed one. In order to eliminate the difference in the characteristics between amplifiers attached to the individual collectors, amplifier gain factors (A-Gain) were measured for SMCMS prior to data acquisition by supplying a uniform current into the amplifiers. Accelerating voltage was adjusted to 10 kV.

Table 1. Faraday cup configurations for the Nd isotope static analysis.

Configuration No.	Faraday Cup No.							
	Col. 1	Col. 2	Col. 3	Col. 4	Col. 5	Col. 6	Col. 7	Col. 8
1				146		144	143	
2			146		144	143		
3		146		144	143			
4	146		144	143				
5	146	144	143					
6		146	144	143				
7				146	144	143		
8					146	144	143	
9						146	144	143
Isotope ratio	R1	R2	R3	R4	R5	R6	R7	R8

La Jolla standard was used as a standard of Nd isotope composition. The detailed procedure of the Nd isotope measurement was described in Yoshikawa et al. (in this issue). As given in Table 1, <sup>143</sup>Nd/<sup>144</sup>Nd ratios were measured with nine different cup configurations. The obtained results with different configurations are denote as Ri (i= 1, 2, ....., 9). In each cup configuration, three separate runs were made.

## Result and discussion

The Nd isotope ratios measured with different nine cup configurations are shown in table 2. The averaged values of three measurements (Ri) for each cup configurations are also shown in Table 2. The range of Ri is 0.511821 (R5) to 0.511858 (R3). The difference of R3 and R5 apparently exceeds the analytical errors. Similar result was observed by Makishima and Nakamura (1991), and they concluded the diversity was caused by the difference in FCE. They further established the method to calculate the RFCEs for individual cups using the measured ratios of Ri. Following their method, we calculated RFCEs in TIMS at BGRL. Our TIMS have nine Faraday cups, and we determined RFCEs for seven of eight cups against Col. 4. The equations of RFCEs can be described as follows:

$$f_1/f_4 = R1^{-2} \times R2^{-2} \times R3^{-2} \times R5^2 \times R6^2 \times R9^2$$

$$f_2/f_4 = R1^{-2} \times R2^{-2} \times R6^2 \times R9^2$$

$$f_3/f_4 = R1^{-2} \times R6^2$$

$$f_5/f_4 = R0^2 \times R7^{-2}$$

$$f_6/f_4 = R0^3 \times R1^2 \times R2^{-1} \times R5 \times R6^{-3} \times R7^{-3} \times R9$$

$$f_7/f_4 = R0^{3.5} \times R1^5 \times R2^{-3.5} \times R5^{2.5} \times R6^{-6.5} \times R7^{-4.5} \times R9^{3.5}$$

$$f_8/f_4 = R0^{3.45} \times R1^{8.5} \times R2^{-5.25} \times R5^{4.25} \times R6^{-10.25} \times R7^{-5.25} \times R8^{-1} \times R9^{5.25}$$

Table 2. Analytical results of Nd isotope ratios with eight different cup configurations

Configuration No.	<sup>143</sup> Nd/ <sup>144</sup> Nd	
1	0.511861±21	
	0.511844±17	
	0.511831±11	a.v. 0.511845±15 (R1)
2	0.511849±17	
	0.511855±13	
	0.511857±12	a.v. 0.511854±04 (R2)
3	0.511848±13	
	0.511870±12	
	0.511856±09	a.v. 0.511858±11 (R3)
4	0.511822±14	
	0.511850±11	
	0.511821±11	a.v. 0.511831±16 (R4)
5	0.511829±11	
	0.511820±11	
	0.511815±11	a.v. 0.511821±07 (R5)
6	0.511815±11	
	0.511841±08	
	0.511829±09	a.v. 0.511828±13 (R6)
7	0.511824±10	
	0.511837±09	
	0.511852±10	a.v. 0.511829±14 (R7)
8	0.511850±14	
	0.511854±10	
	0.511867±08	a.v. 0.511857±09 (R8)
9	0.511838±09	
	0.511828±12	
	0.511841±08	a.v. 0.511836±07 (R9)

Table 3. Calculated RFCEs against Col. 4.

RFCE	
$f_1/f_4$	0.999977
$f_2/f_4$	0.999988
$f_3/f_4$	0.999937
$f_5/f_4$	1.000004
$f_6/f_4$	1.000094
$f_7/f_4$	1.000192
$f_8/f_4$	1.000302

From those equations, RFCEs were calculated and listed in Table 3. We can also calculate the true value of <sup>143</sup>Nd/<sup>144</sup>Nd (R), and the result was 0.511846. This value of R is same as presented by Makishima and Nakamura (1991) with different mass spectrometer. The result shows that the RFCEs of Col. 1 to 3 are less than unity, and those of Col. 5 to 8 are more than unity. This indicates that Col. 1 to 3 are less sensitive compared to Col. 5 to 8, may be caused by the damaged with large ion beams. Using those RFCEs, we can eliminate difference of FCEs in TIMS for the measured isotope ratios.

## Volcanic short-period tremor at Aso Volcano Its amplitude variation and ratio variation of characteristic frequency bands

*Y. Sudo and M. Sako*

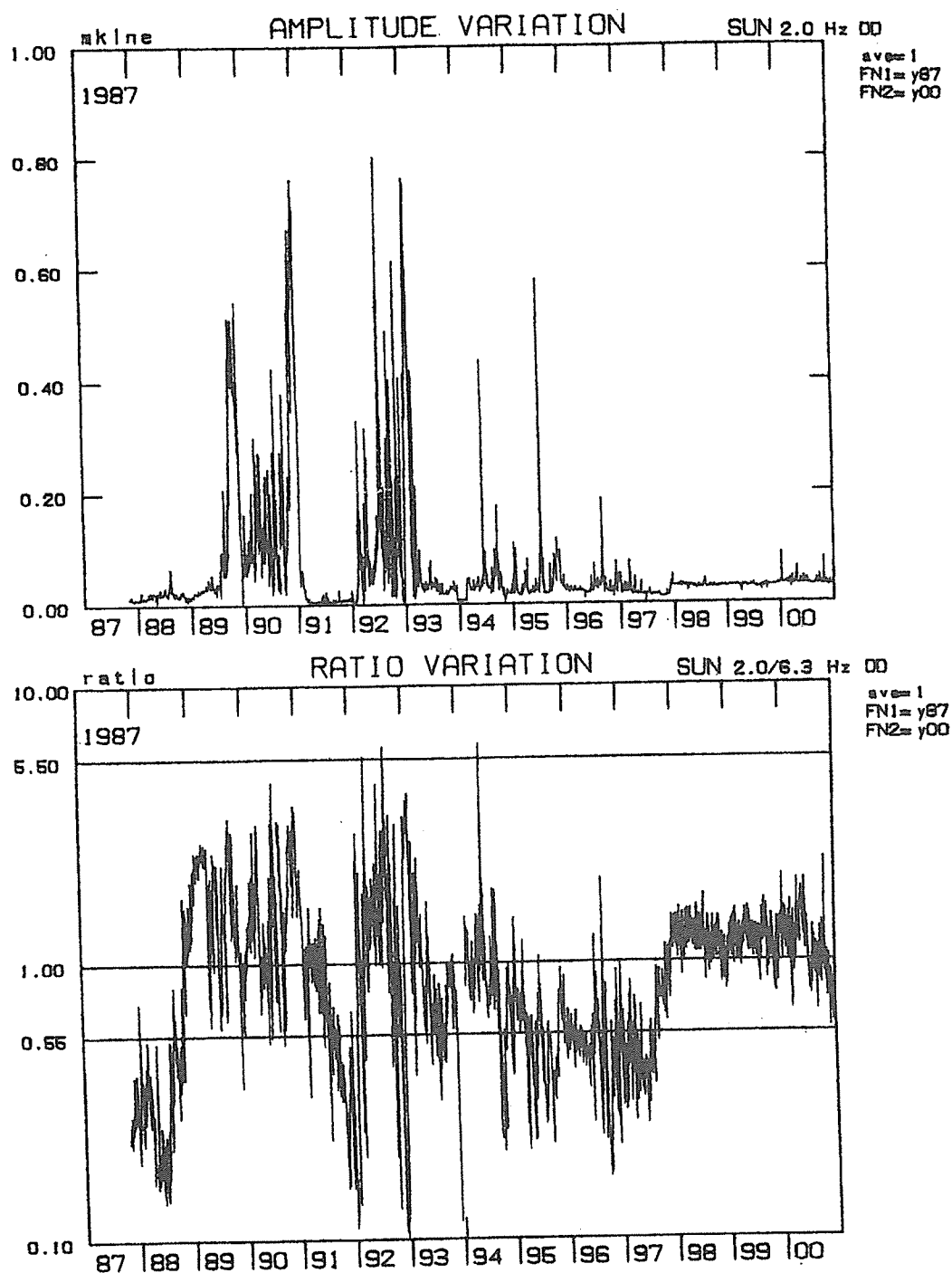
### *Comparison with Volcanic Activity*

At Aso Volcano, the changes in volcanic short-period tremor amplitude closely correspond to the volcanic activity. The top of figures shows the amplitude variation of tremor, of which the frequency band was 2.0Hz, observed at Station SUN, about 1km south from the center of the active crater. This figure is a good indication of

the state of volcanic activity. The volcanic states in the crater had been observed in this period, i.e. the state of Strombolian eruptions from September 1989 to January 1990, from November 1990 to January 1991, and from January to February 1993; the incandescent state at the crater from November 1988 to June 1989; the state of the crater lake and mud eruptions from 1987 to September 1988, February to October 1990, April 1991 to December 1992, and from May 1993 to now. In order to compare the volcanic activities with this figure, the activities are summarized as follows. **1989:** After the eruptive activity in 1985, a hot crater lake had appeared in 1st Crater. In October 1988, the crater floor was first seen to be incandescent. At the end of 1988, ash ejections were observed. In April 1989, ash ejections became gradually more active and small blocks were ejected. In July numerous eruptions occurred at irregular intervals with ash columns of 2.5 km height. The flames of burning gases and glows were frequently observed. From September to November many large eruptions occurred with ash falls as far as about 40 km to 50 km from the crater. In October there were ash eruptions every day and scoria ejections, including bombs greater than 1 m in size, reached a height of several hundred meters. In late October rumbling sounds became stronger and were audible around the caldera at a distance about 10 km from the crater. In late November strong Strombolian explosive eruptions recommenced. In December these eruptive activities became a little weaker and rumbling sounds were not heard but ash emissions continued. Associated with these activities, the amplitude of volcanic tremor was high from March to December. In October and November, low frequency and large amplitude tremors were generated and they were recorded by seismic stations more than 100 km from the crater. **1990:** The 1989 activity continued intermittently until February 1990. Thereafter no eruption was observed until April. In April an eruption occurred with a lot of ash. The eruptive activity continued until June with heavy ashfalls. In June the crater lake appeared again. From July to early December no eruptive activity occurred. In November the crater floor became incandescent. In December the activity again became eruptive. Strong rumbling sounds were heard in the caldera as in the preceding year. Responding to this volcanic state, the tremors increased in amplitude and remained at a high level. **1991:** The 1990 activity continued until early January 1991. Thereafter the amplitude remained at a low level. In March the crater bottom was buried with mud and sand, and a pool of water was formed. Through most of 1991, emissions from the crater were limited white clouds of water vapor. **1992:** From June to October 1992 the tremor-regime was characterized by isolated tremors corresponding to individual mud eruptions. In December a small new vent opened with emission of ash and flames. **1993:** At the beginning of 1993 the crater lake dried up and the ash eruptions continued. The plume of steam and ash rose to about 1,000 m to 1,500 m above the vent. This activity continued, with tremor amplitude remaining at a high level, until the early of February 1993. Then a small lake again formed and the whole surface of the crater gradually occupied by the hot water. **1994:** The quiet state continued to the end of March 1994. In March and May small mud eruptions occurred. From June to August the crater was calm. However, from September to October the tremor amplitude increased with mud eruptions. Then in December mud eruptions occurred again and the amplitudes further increased. This activity continued until April 1995. **1995:** Sometimes the tremors amplitudes increased with the small mud eruptions. From July to the following year the activity remained at a low level. **1996:** The activity remained at a low level through this year. There was a hot water pool in the crater. From June to August the amplitude began gradually increasing. This phenomenon was associated with the occurrence of volcanic earthquakes. In the entire period from 1989 to 1996, the volcanic activity was most vigorous from September to November 1989. At the depth of 150 m, where there were large long-period temperature fluctuations, with only small quasi-annual variations, the temperature reached a maximum in November and December 1989 and then fell gradually, and so could be the result of these volcanic activities with a delay of about one month.

#### ***Amplitude Ratio Variation between Low and High Frequencies***

The ratio change of 2.0Hz band tremor to 6.3Hz band (the bottom of figures) indicates also the volcanic activity. The ratio gradually increased from the end of 1988. This pattern can be explained that the low frequency band tremors is dominant according to the volcanic activity. As seen in figures and already mentioned, the volcanic activity at October 1989 was vigorous. The amplitude of tremors closely correspond to the states of volcanic activity in 1st Crater. During the active state, when the crater was ejecting a lot of ash and scoria-blocks as Strombolian eruptions, or producing very strong rumbling sounds or mud eruptions, the amplitude of volcanic tremor was always at a high level.



### Precursors and Seismic Sequence of 1999 Guagua Pichincha Eruption

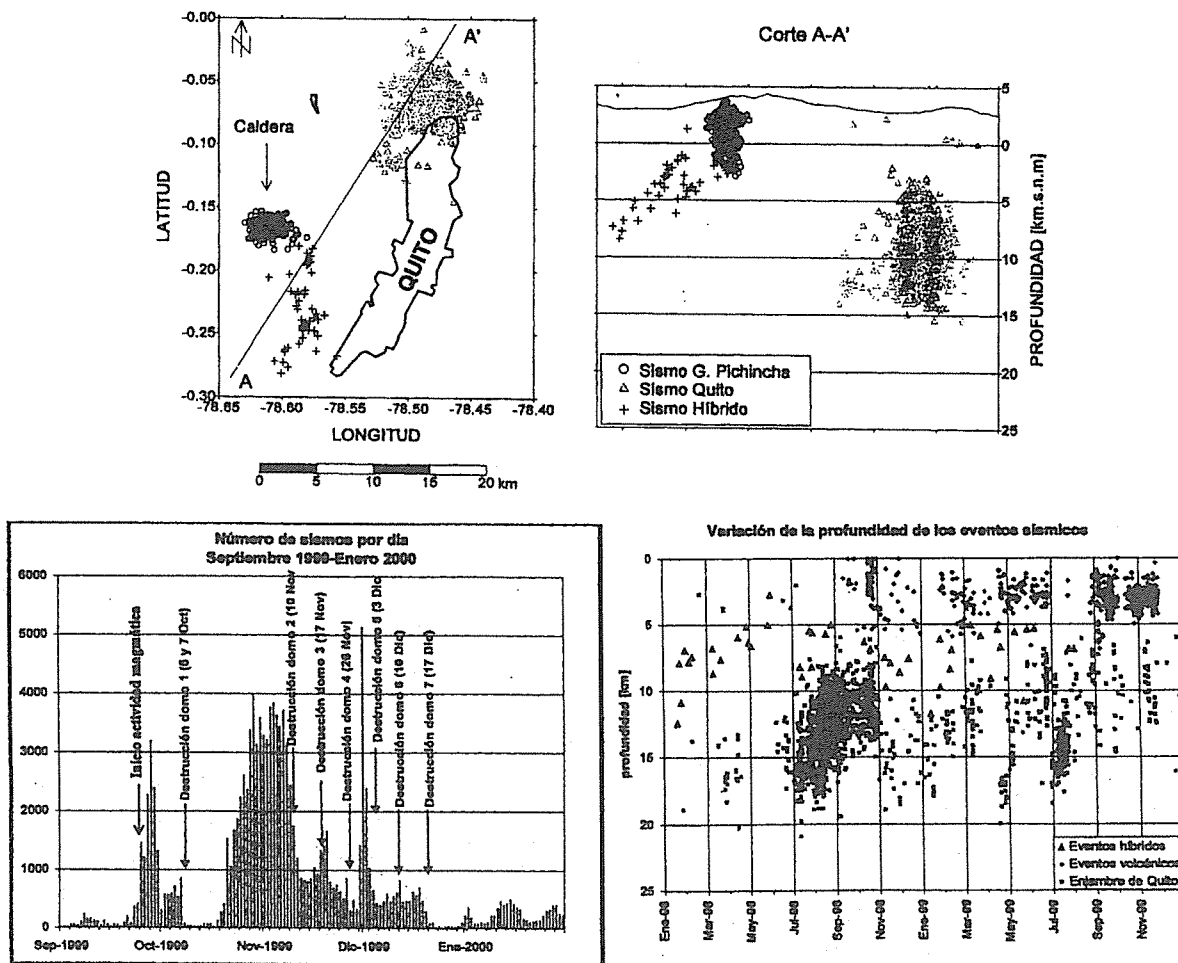
*Y. Sudo, T. Hashimoto, M. Ruiz-Romero, H. Yepes, D. Villagomez and D. Viracucha*

The 18 years-long period phreatic activity and the occurrence of swarms of tectonic events have characterized the precursory activity of Guagua Pichincha volcano. We present a brief description of this activity in order to discuss its significance for comparison with other volcano's precursors.

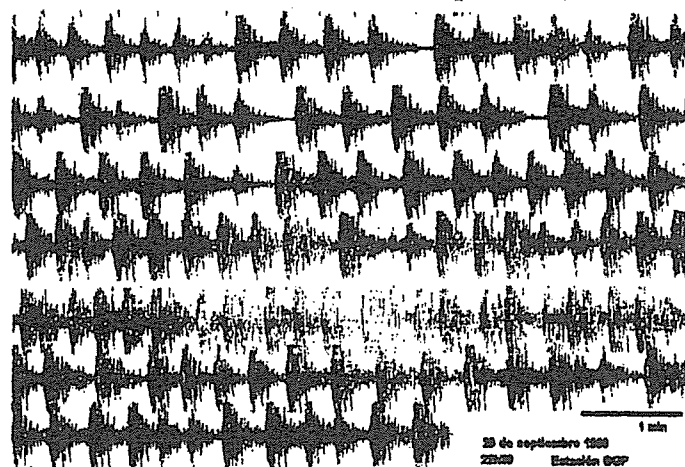


The first renewal signal on Guagua Pichincha was noticed in 1981 with the appearance of a new fumarolic field and the occurrence of phreatic explosions. Since 1981 up to 1997 the activity remained with few phreatic explosions per year especially during rainy seasons. Meanwhile in August 1988 a swarm of 200 events per month occurred below the southern flank at 8-10 km depth. Besides, since June 1989 an increase of seismicity of Quito fault was showed. In August 1990, a 5.1 Ms earthquake caused important damage in Pomasqui town, 20 km far from the crater. In June 1998 begun a very energetic swarm of tectonic events in the northern segment of Quito fault. Between July 24 and October 31, the swarm showed an average of 1200 events per month, a few of them with a magnitude larger than 4.0. A strong phreatic activity started in August 7, 1998 in the dry season. This activity was characterized by the occurrence of 19 phreatic explosions per month and a high number of seismic events. Phreatic activity showed three main phases, one from August to November 1998, the second one from December 1998 to April 1999 and the last one from July to September 1999. A monthly average of seismic events reached 1160 events. Upon their waveforms and spectral contents, the seismic events were classified in volcano-tectonic, long period, medium period and hybrid and explosion events. Since September 22, very energetic swarms of long period events precede the eruptions with magmatic origin. Until December 17, nine eruptions were detected. They allowed the formation of eight domes in the western edge of the caldera and their further destruction. The eruptions provoked five important ash falls in Quito city, the capital of Ecuador.

### Distribution of Volcanic and Tectonic Events near Quito (1998-1999)

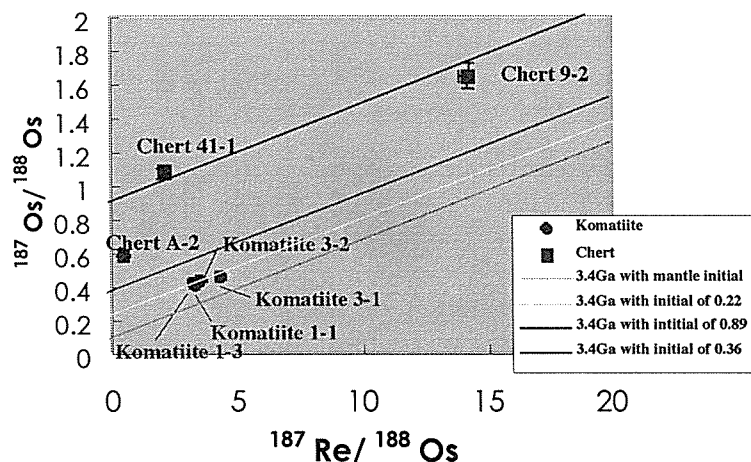
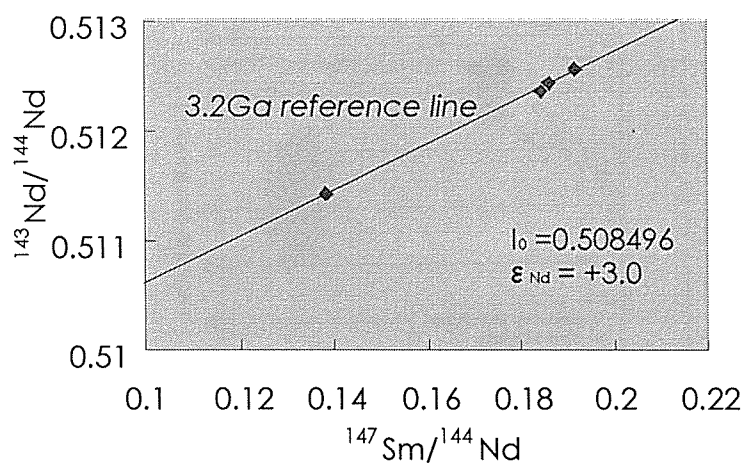


# LP EVENT Swarm on 29 September, 1999



## Re-Os and Sm-Nd systematics of basaltic komatiites and banded cherts in Pilbara, NW Australia: Implications for early continental growth

*K. Suzuki, H. Shimizu, M. Okamoto, Y. Hattori, M. Minami, G. Shimoda, Y. Tatsumi, and M. Adachi.*



Re-Os and Sm-Nd isotopic data of Marble Bar mafic volcanic rocks (komatiitic basalts) and cherts in Pilbara, NW Australia, were obtained in order to investigate chemical evolution of the Archean crust and mantle. The Re-Os and Sm-Nd isotopic ratios of mafic volcanic rocks of Marble Bar have been plotted on the 3.4 Ga Re-Os and 3.2 Sm-Nd reference lines, respectively (Fig. 1, 2), which is consistent within analytical uncertainties with 3.4 Ga U-Pb age of the zircon in dacite, strata between komatiitic basalts and cherts in Marble Bar. These results indicate that the volcanic rocks were formed around 3.4 Ga.

The initial  $^{187}\text{Os}/^{188}\text{Os}$  ratio of the reference line of the mafic volcanic rocks is around 0.22 (Fig. 2), much higher than that of the upper mantle (ca. 0.125, Shirey and Walker, 1998). Therefore, probably these mafic volcanic rocks are closely associated with the crustal materials which possess

Fig. 2. Re-Os diagram of Marble Bar komatiites and cherts.

much higher Os isotopic ratios than the mantle components ( $^{187}\text{Os}/^{188}\text{Os} = 0.1 - 0.14$ , e.g., Shirey and Walker, 1988). However, further investigation is required to make conclusion on this matter, because the Re-Os isotope ratio of komatiite-37 with relatively large analytical uncertainties defines the slope and initial Os ratio of the 3.4 Ga reference line. Therefore, the initial  $^{187}\text{Os}/^{188}\text{Os}$  ratio may include a large error.

Marble Bar cherts contain banded iron formation (BIF). Results of the Sm-Nd isotope analyses (Minami et al., 1995) revealed that the banded and yellowish cherts gave isochrons ages of  $3.23 \pm 0.29$  with  $\epsilon_{\text{Nd}}$  of  $1.0 \pm 3.0$  and  $2.54 \pm 0.20$  with  $\epsilon_{\text{Nd}}$  of  $-5.4 \pm 2.0$  (Fig. 3). They suggested that the yellowish cherts record the event of reset of the Sm-Nd isotopic system at around 2.54 Ga. The  $^{187}\text{Os}/^{188}\text{Os}$  ratios of banded (Chert 41) and yellowish cherts (Chert 9) are 1.08 and 1.65, respectively (Fig. 2). These values are extremely high (Fig. 2), which strongly implies involvement of the continental crust component with high Os isotopic ratios in the formation of the cherts. Both Re-Os isotopic data of the banded and yellowish cherts are roughly plotted on the 3.4 Ga reference line (Fig. 2), which supports the idea that the cherts were formed at ca. 3.4 Ga. This result is consistent with the Sm-Nd data (Fig. 3). If true, the initial  $^{187}\text{Os}/^{188}\text{Os}$  ratio yields an extremely high value of approximately 0.9, indicating that involvement of the continental crust is the essential process in formation of the cherts. In contrast, the initial Nd ratio is identical within analytical uncertainties to that of the chondritic mantle,

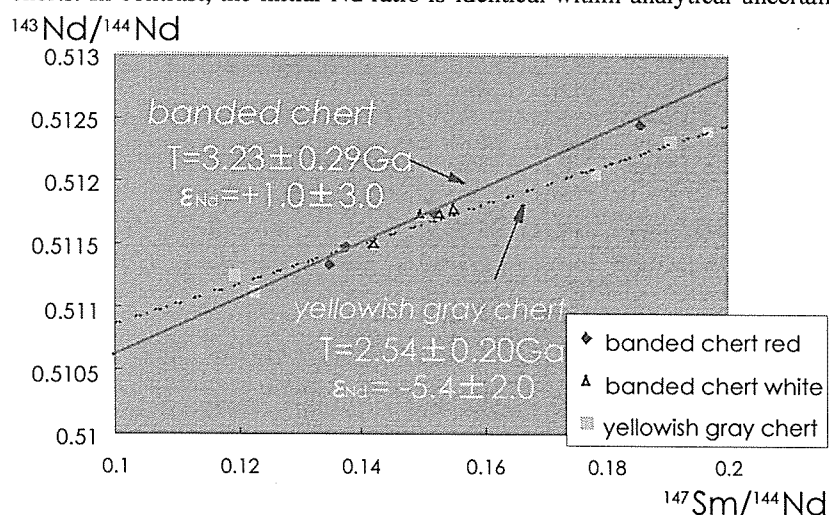


Fig. 3. Sm-Nd diagram of two types of Marble Bar cherts from Pilbara. (Minami et al., 1995)

indicating the cherts were formed from the hydrothermal solution originated from the mantle component (Minami et al., 1995). We propose that the crustal component is more likely associated with the formation of Marble Bar cherts. The Nd isotope evolve slowly in the early Earth system, because both Sm and Nd belong to REEs, Sm/Nd could not be fractionated much. It results in difficulty in detection of deviation in Nd ratios of the Archan cherts from the chondritic evolution curve. On

the contrary, much higher resolution of the Re-Os system can be obtained, because Re/Os is highly fractionated in geological processes and the  $^{187}\text{Os}/^{188}\text{Os}$  ratio evolve at much higher rate. As a result, the Re-Os isotopic data obtained for the cherts in the present study strongly suggest the cherts are originally associated with the continental crust. Also, it may be important that the continental crust had been already developed at 3.4 Ga.

Rhenium loss during later alteration of the cherts is the possible process to shift the Re-Os isotopic data plot to the left region of the reference line of komatiitic basalts. If true, the original Re concentration of the cherts may several times higher than the present value, which is unreasonable.

The above result suggest that the Re-Os isotopic system may be more resistant to later alteration, because the Re-Os plot of the yellowish cherts, whose Sm-Nd system was reset and Rb-Sr system was disturbed, are located near the 3.4 Ga Re-Os reference line of the banded chert without disturbance of the Sm-Nd system.

# **Re-Os isotopic systematics of Setouchi high-Mg andesites, SW Japan: Evidence for slab melting**

*K. Suzuki, and Y. Tatsumi*

Re-Os isotopic compositions have been determined for the primitive high-magnesian andesites (HMAs) and basalts in the Setouchi volcanic belt, SW Japan. The HMAs possess higher Os isotopic ratios and lower Os concentration (0.1718 - 0.2236 and 8.1 – 11.9 ppt) than basalts (0.1556 - 0.1769 and 31.0 – 53.7 ppt), indicating that the composition of Setouchi magma source lies on a mixing line of a rather depleted upper mantle and an enriched component (Fig. 1). One of the candidates of such an enriched endmember would be the subduction component from the sinking lithosphere, because the Setouchi primitive lavas show little evidence for crustal contamination. The observed Os isotopic compositions of HMAs are consistent with overprinting of slab (sediment)-melt not slab-fluids, because aqueous fluids cannot transport radiogenic Os effectively. Mixing calculations based on isotopic signatures reveals that the addition of several percent of terrigenous and/or pelagic sediment-derived melt can account for the Os-Pb-Sr-Nd isotopic compositions of Setouchi magma source.

(To be submitted to Geology)

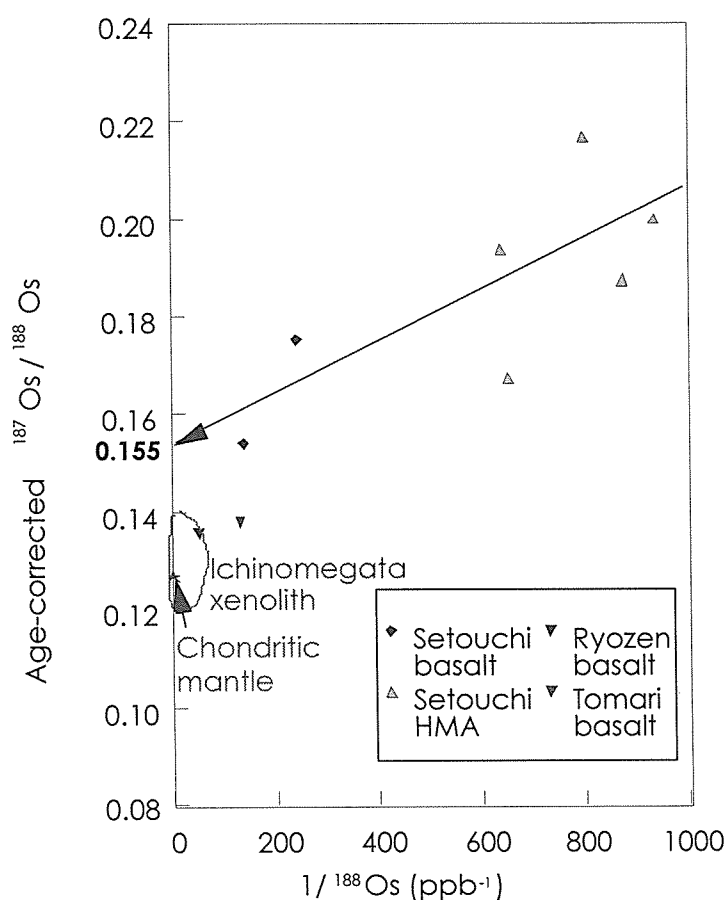


Fig. 1.  $1/^{188}\text{Os}$  vs.  $^{187}\text{Os}/^{188}\text{Os}$  diagram of the Setouchi basalts and HMAs and Ryozen and Tomari basalts. □

# **Osmium transport during serpentinite dehydration at 1.0 GPa: Experiments and implications for the Os isotopic compositions of arc magmas**

*K. Suzuki, Y. Aizawa and Y. Tatsumi*

Dehydration experiments on natural serpentinites were conducted at 1.0 GPa and 850 °C in order to examine the behavior of osmium during dehydration processes in subduction zone. The results (Table 1) confirm that 20% of Os in the starting serpentinite is moderately transported with aqueous fluids in the absence of sulfide phases during dehydration processes. If we consider two stage model where Os in the slab moves into overlying hydrous peridotite layer and is subsequently transferred into mantle wedge (Fig. 1), only less than 5 % Os is likely transferred from the subducting slab to the mantle wedge. It is thus suggested that arc lavas having higher  $^{187}\text{Os}/^{188}\text{Os}$  ratios than the mantle value may be produced by overprinting of slab-derived melts, not fluids, onto the original mantle wedge, although possible effect of crustal contamination cannot be ruled out.

Table 1. Os concentration of serpentinite used as starting material and run products of dehydration experiment.

	Os conc (ppb)	Re conc (ppb)
Starting material A	2.74 ± 0.19	0.676 ± 0.002
run product	2.42 ± 0.07	0.4 ± 0.02
Escaped water corrected	2.1 ± 0.06	0.34 ± 0.02
Mobility (%)	23 ± 2	49 ± 2
	Os conc (ppb)	Re conc (ppb)
Starting material B	0.4 ± 0.07	0.46 ± 0.08
run product	0.42 ± 0.07	0.31 ± 0.07
Escaped water corrected	0.36 ± 0.06	0.27 ± 0.09
Mobility (%)	9 ± 2	42 ± 16

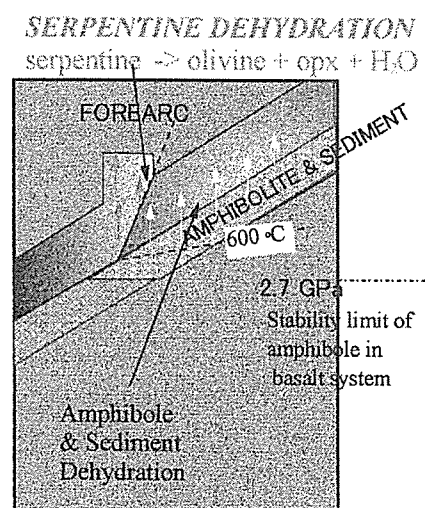


Fig. 1. A model for fluid migration and magma generation in subduction zones, after Tatsumi and Eggins (1995).

(Submitted to Geophy. Res. Lett. 2001/04/20)

## **Os-Sr-Nd-Pb systematics of tholeiites and alkali basalts in Weichang, NE China: Implications for the intracontinental magmatism**

*K. Suzuki, T. Shibata, and Y. Tatsumi*

The Cenozoic basaltic rocks are widely distributed in NE China, which has been called “Hot region” (Fig. 2, Miyashiro, 1986). The mechanism of the basaltic rock production under the thick and cold continental crust is poorly constrained. Here we have analyzed Os, Sr, Nd, and Pb isotopic abundance of the tholeiites and alkali basalts in Weichang, NE China, in order to investigate the volcanic activity in NE China.

Sr-Nd and Pb-Pb isotopic diagrams (Fig. 1 (a), (b)) imply mixing of the DMM-like depleted mantle reservoir and enriched sediments. However, the tholeiites possess the enriched feature in the Nd isotope, whereas they

show the depleted characteristics in the Pb isotopes, which cannot be explained by simple mixing of the depleted mantle source and the enriched component.

The very high Os isotopic ratios (0.2 – 1.1) beyond those of ocean island basalts were obtained for both the Weichang tholeiites and alkali basalts (Fig. 3). This strongly suggests that the enriched component such as crustal materials were involved in formation of Weichang volcanic rocks, because none of the mantle component known at present possess such high Os isotopic ratios. The possible enriched component is material in the subducting slab and the continental crust through which Weichang magma ascended.

Results of mixing calculation between Os abundance and isotopic ratios of Weichang basalts reveal that more than 95 % continental crust materials are required to generate Os signature of the Weichang basalts. It is unlikely, because 95 % continental crust involved would not produce rocks with basaltic chemical compositions.

It is difficult at present to explain all the data consistently. Further consideration such as the behavior of Re and Os in the subducting slab under the continental crust and the isotopic signatures of the lower crust is required.

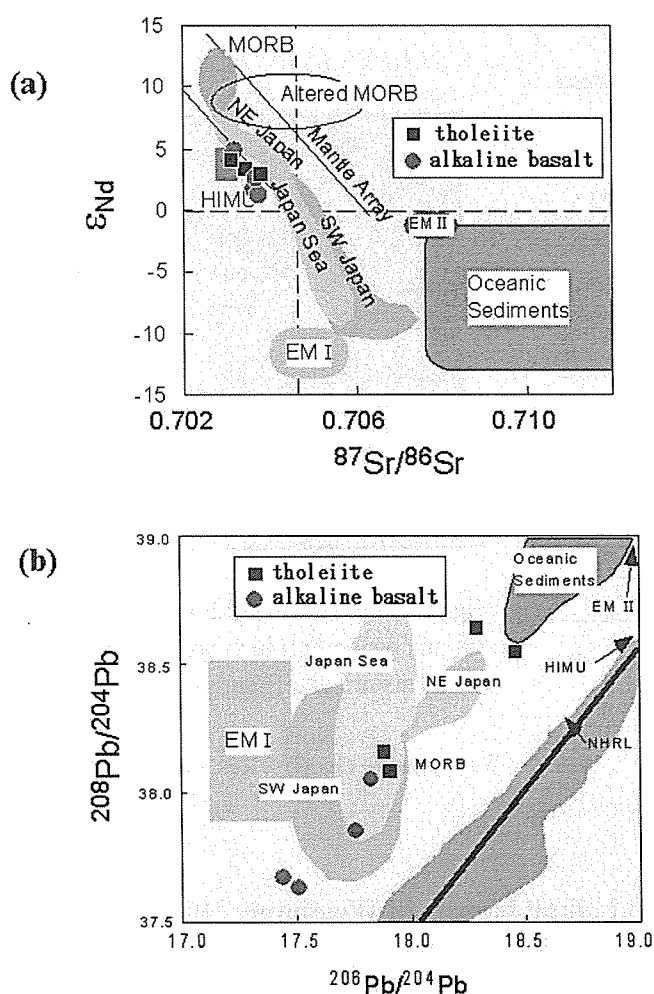


**Fig. 1. Sr-Nd-Pb isotopic signatures of Weichang basalts, NE China.**

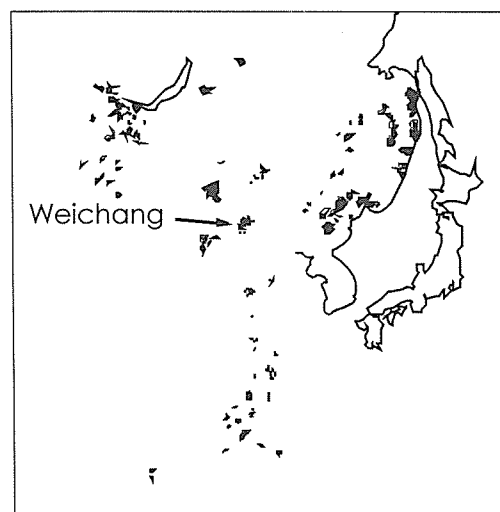


**Fig. 2. Distribution of Cenozoic basalts in Eastern China and Russia. Weichang basalt forms plateau of 10,000 km².**

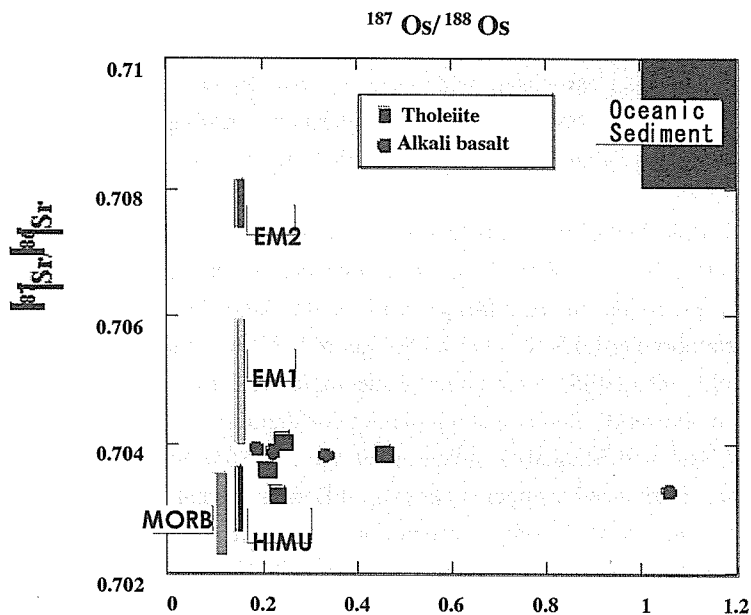
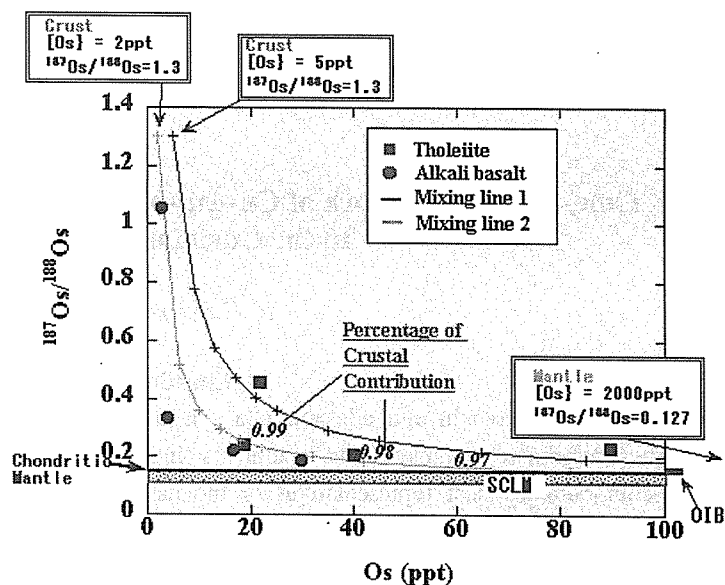


Fig. 3. Os-Sr correlation of Weichang tholeiites and alkali basalts.

Fig. 4. Mixing calculation using correlation between Os abundance and  $^{187}\text{Os}/^{188}\text{Os}$  ratios.



### Proterozoic Cu-Au systems of the Curnamona Province, Australia: geological and stable isotope constraints on timing and origins

*R. G. Skirrow, P. M. Ashley, and K. Suzuki*

The Curnamona Province in New South Wales and South Australia, including the Broken Hill and Olary Domains, is emerging as a significant Proterozoic Cu-Au as well as Pb-Ag-Zn metallogenic province. Mineralization styles range from shear-hosted magnetite-ironstone associated Cu-Au styles (e.g. Copper Blow deposit), through stratabound vein/replacement Cu-Au(-Mo) mineralization with locally developed Fe-oxides (e.g. Kalkaroo, Portia prospects), to high temperature(?) Au(-Cu-Mo) deposits with very minor Fe-oxides (e.g.

White Dam prospect). Key shared characteristics, in addition to the Cu-Au +/- Mo +/- As +/- REE +/- Ba +/- F signature, include an association with potassic +/- Fe alteration (biotite, K-feldspar +/- magnetite), combined structural - stratigraphic controls, and syn- to late-tectonic timing. The Cu-Au mineralization and alteration overprint regionally extensive pre- or early-tectonic sodic alteration effects in the Willyama Supergroup, although albitization and calcsilicate alteration are also associated with some Cu-Au deposits. A significant proportion of deposits occur near the regional interface between albitic to calcsilicate-bearing and variably magnetic metapsammitic lithologies, and overlying relatively reduced metapelitic rocks with low magnetic susceptibility.

Based on stable isotope and reconnaissance fluid inclusion results, copper - gold at Kalkaroo and Waukaloo were deposited at probable maximum temperatures of  $\sim 420\text{--}460^\circ\text{C}$  from hypersaline Na-K-Ca-Cl fluids. Oxygen and hydrogen isotope compositions of fluids in equilibrium with sulfide-associated biotite and amphibole overlap with both magmatic and metamorphic fluids ( $\delta^{18}\text{O} = 5.5\text{--}8.5$  per mil,  $\delta\text{D} = -44$  to  $-67$  per mil), and are distinctly lighter than metamorphic fluids responsible for regional syntectonic Na-Ca-Fe metasomatism at around 1583-1588 Ma. In conjunction with molybdenite Re-Os isotopic dating constraints for Mo and Cu-Au mineralization at the Portia, Kalkaroo, White Dam and Waukaloo prospects (9 ages,  $\sim 1632$  Ma to  $\sim 1612$  Ma), we infer that Cu-Au mineralization was introduced syntectonically at differing crustal levels during inversion of the Willyama Supergroup basin, and was broadly synchronous with the Olarian Orogeny. Emplacement of granitoids with I-type characteristics may have occurred at  $\sim 1630\text{--}1640$  Ma, although their role in the mineralizing systems remains unknown. The Cu-Au mineralized systems of the Curnamona Province are considered to be variants within the diverse global family of Fe-oxide associated Cu-Au deposits.

(Submitted to Mineral. Dep.)

## **Time-Space framework of Cu-Au(-Mo) and regional alteration systems In the Curnamona Province**

*R. G. Skirrow, P. M. Ashley, N. J. McNaughton, and K. Suzuki*

### **Introduction**

The Broken Hill Domain and adjacent Olary Domain in the Curnamona Province experienced broadly similar lithostratigraphic, magmatic and tectonic evolution during the Palaeoproterozoic and Mesoproterozoic. Although both domains host representatives of the major mineral deposit styles in the province, the Olary Domain contains the greater share of known Cu-Au(-Mo) mineralization, whereas Pb-Zn-Ag resources discovered to date are localized primarily in the Broken Hill Domain. Robust and predictive exploration models for Cu-Au-Bad Pb-Zn-Ag ore systems in the Curnamona Province will build on a framework of quantitative information on the timing of hydrothermal events relative to tectonism and magmatism, the geometry of fluid flow pathways, and fluid and host rock physicochemical properties. Here, we present a summary of geochronological, stable isotopic and preliminary fluid inclusion constraints on the timing, character and distribution of fluids responsible for Cu-Au(-Mo) mineralization and regional Na-Ca-Fe alteration, and conclude with comments on the significance of the results for exploration models. Reviews of the Regional geology and metallogenesis of the Olary Domain by Ashley (2000) and Ashley et al. (1998) provide a background to our results.

### **Conclusions and Exploration Implications**

Cu-Au(-Mo) introduction in the epigenetic Fe-oxide associated systems may have commenced during the period -1612-1632 Ma, based on high-precision Re-Os dating. This timing would have overlapped with possibly the earlier stages of the Olarian orogeny as marked by granitoid emplacement (e.g., at 1616 +/- 9 Ma, Fanning et al. 1998). However, improvement in the accuracy of Re-Os dating, and further age dating and characterization of -1620-1580 Ma S-type and/or I-type and -1630-1640 Ma I-type granitoids (Ashley et al., 1998; Wyborn et al.



1998), are required to fully reconcile results on the temporal relationships between mineralization and magmatism

Regional-scale flow of -450-550°C Na-Ca-Fe metamorphic brines between -1595 Ma and -1583 Ma was controlled principally by D3 structures.

The regional alteration event temporally overlaps with magmatism of the Hiltaba Suite - Gawler Range Volcanics and Cu-U-Au mineralization (Olympic Dam) in the Gawler Craton, and is within error of the age of volcanism on the Benagerie Ridge (Fanning et al, 1998)-

Syntectonic Na-Ca-Fe regional alteration is prominent in the southern, higher metamorphic grade parts of the Olary Domain, whereas Cu-Au(-Mo) mineralization and associated Fe-oxide and potassic alteration are best developed in the lower metamorphic grade, northern Olary - Benagerie Ridge.

The White Dam Au(Cu-Mo) mineralization may be a high-temperature style associated with quartzofeldspathic veins in a high-grade metamorphic area.

Although the Cu-Au-Mo-As-F-LREE geochemical signature and stable isotope compositions of proximal alteration minerals in the Fe-oxide associated systems are consistent with magmatic fluid input possible 'causative' magmatism has yet to be identified.

(AGSO Record 2000/10, 83-86)

### **Geochemical modeling of partial melting of subducting sediments and subsequent melt-mantle interaction: generation of high-Mg andesites in the Setouchi volcanic belt, southwest Japan**

*Y. Tatsumi*

A possible mechanism for high-Mg andesite formation, including melting of subducting sediments and subsequent melt-mantle interaction, was examined by geochemical formulation of partial melting and melt-solid reactions. The modeling results demonstrate that a sediment-melt produced at 1050°C and 1.0 GPa changes its composition from rhyolitic to andesitic, as it dissolves olivine and clinopyroxene and crystallizes orthopyroxene. Such a reaction product possesses major and incompatible trace element compositions close to high-Mg andesites in the Setouchi volcanic belt, southwest Japan.

(Geology, in press.)

### **Slab melting: its role in continental crust formation and mantle evolution**

*Y. Tatsumi*

A possible mechanism for continental crust formation, slab-melting and subsequent melt-mantle interaction, was examined by geochemical formulation of partial melting and melt-solid reactions. The modeling results suggest that such a process can reasonably explain the major and trace element compositions of the andesitic bulk continental crust. However, the Sr-Nd-Pb isotopic compositions of melting residues in the subducting slab, which may have foundered and been stored in the deep mantle, do not match those of any proposed geochemical reservoir. This may lead to the conclusion that the slab melting did not play the major role in the continental crust formation during the Archean.

(Geophys. Res. Lett., in press.)

## Constraints on Arc Magma Genesis

*Y. Tatsumi*

Improved understanding of the complex processes associated with subduction zone magmatism requires the identification and explanation of tectonic, petrological, geochemical, and geophysical characteristics common to most subduction zones. These characteristics include: (1) the presence of dual volcanic chains within a single volcanic arc, (2) the constant depths to the surface of the subducting lithosphere beneath trench- and backarc-side volcanic chains, ~110 km and ~170 km, respectively, (3) greater volume of magma production beneath the trench-side volcanic chain (4) selective enrichment of particular incompatible elements, (5) systematic across-arc variations in incompatible element concentrations and isotopic/element ratios, (6) location of a high-temperature (>1350°C) region within the mantle wedge, (7) occurrence of localized high-temperatures (~1300°C) immediately beneath the crust/mantle boundary, (8) location of very low-velocity regions within the mantle wedge. It is suggested here that dehydration processes and associated selective element transport, which take place in both the subducting lithosphere and the downdragged hydrated peridotite layer, and secondary convection within the mantle wedge induced by plate subduction are largely responsible for the observed characteristics of subduction zone magmatism.

(AGU Monograph, in press)

## Aeromagnetic survey in Aso Volcano

*M. Utsugi, Y. Tanaka, T. Hashimoto and H. Hase*

To investigate the magnetic structure of the central cones of Aso Volcano, we conducted the aeromagnetic surveys using helicopter in November of 2000. We measured along 18 parallel N-S lines with 250 m spacing around the center part of the central cone of Aso Volcano (Fig. 1) using portable Overhauser effect magnetometer. The altitude of flight was kept about 200 to 300 m above the terrain.

To determine the distribution of rock magnetization, we divided the crust with a number of cubic blocks (length=250m, width=250m and height=250m) with 3 layers. Using the joint inversion of the observed data and the topography, we determined the intensity of the magnetization of each cubic block. The effect of the topography is corrected from a digital terrain model by integrating analytically in the vertical direction and then numerically in horizontal plane. The distribution of the surface

magnetization around Mt. Nakadake is shown in Fig.2. One of the low magnetized areas is shown in the

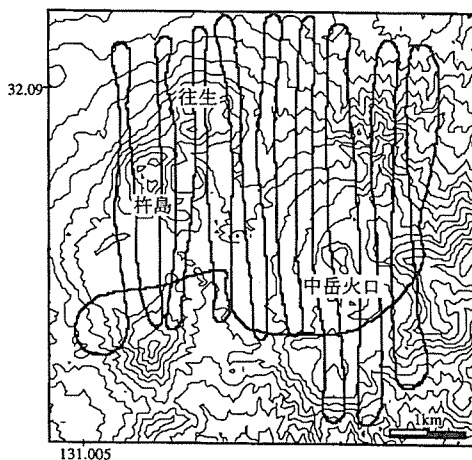


Fig. 1 Flight course of aeromagnetic survey

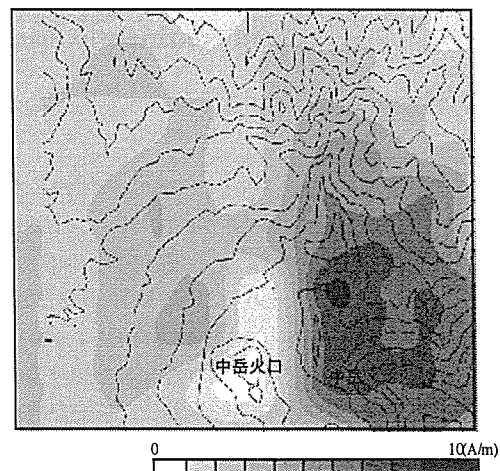


Fig.2 Distribution of the surface magnetization around Mt. Nakadake.

vicinity of the active crater of Mt. Nakadake. This low magnetization may be caused by that the higher temperature under the Nakadake crater reduces the underground rock magnetization.

## The Sr, Nd and Pb isotopic ratios of GSJ standard rocks

*M. Yoshikawa, T. Shibata, and Y. Tatsumi*

The analytical procedure for chemical separation and mass spectrometry basically followed *Yoshikawa and Nakamura* [1993] for Sr isotopic ratio and *Shibata et al.* [1989] for Nd isotopic ratio and *Koide et al.* [1990] for Pb isotopic ratio. The samples were decomposed by HF + HNO<sub>3</sub> + HClO<sub>4</sub> in a 7ml teflon beaker. Sr and Nd were separated with 2.5N HCl using 1ml cation-exchange chromatography in H<sup>+</sup> form (Muromac AG50W-X8 resin). Sr was purified with 0.06M DCTA in 0.5N pyridine, distilled water and HCl using 0.3ml cation-exchange chromatography in pyridinium form. Nd was purified with 0.22M hydroxy-alpha-isobutyric acid using 0.3ml cation-exchange chromatography in pyridinium form. Pb was separated with 0.5M HBr and distilled water using 0.1ml anion-exchange chromatography in Br<sup>-</sup> form. Pb was purified using the same column with the same procedure described above.

Mass spectrometry was carried out on a Finnigan MAT 261 and Triton TI instruments. Normalizing factors to correct for isotopic fractionation for Sr and Nd are  $^{86}\text{Sr}/^{88}\text{Sr} = 0.1194$  and  $^{146}\text{Nd}/^{144}\text{Nd} = 0.7219$ , respectively. The averaged correction factor is 0.116 ‰ per mass unit ( $n = 8$ ). Measured ratios for standard materials were  $^{87}\text{Sr}/^{86}\text{Sr} = 0.710279 \pm 0.000028$  ( $2\sigma$ ) for NIST SRM987 ( $n = 5$ ),  $^{143}\text{Nd}/^{144}\text{Nd} = 0.511851 \pm 0.000013$  ( $2\sigma$ ) for La Jolla ( $n = 9$ ),  $^{208}\text{Pb}/^{204}\text{Pb} = 36.708 \pm 0.011$  ( $1\sigma$ ),  $^{207}\text{Pb}/^{204}\text{Pb} = 15.494 \pm 0.004$  ( $1\sigma$ ), and  $^{206}\text{Pb}/^{204}\text{Pb} = 16.938 \pm 0.003$  ( $1\sigma$ ) for the NIST SRM951 ( $n = 8$ ).

Measured Sr, Nd and Pb isotopic ratios of Geological Survey of Japan (GSJ) standard rocks are listed in Table 1.

Table 1. Sr, Nd and Pb isotopic ratios of GSJ rock standards

Sample name	$^{87}\text{Sr}/^{86}\text{Sr}$	$2\sigma_m$	$^{143}\text{Nd}/^{144}\text{Nd}$	$2\sigma_m$	$^{208}\text{Pb}/^{204}\text{Pb}$	$2\sigma$	$^{207}\text{Pb}/^{204}\text{Pb}$	$2\sigma$	$^{206}\text{Pb}/^{204}\text{Pb}$	$2\sigma$
JB-1	0.704144	$\pm 0.000005$								
JB-1a	0.704136	$\pm 0.000005$	$0.512750 \pm 0.000013$							
JB-2			$0.513097 \pm 0.000011$		38.267	$\pm 0.007$	15.565	$\pm 0.003$	18.354	$\pm 0.004$
JB-3	0.703446	$\pm 0.000006$	$0.513048 \pm 0.000009$							
JA-1	0.703566	$\pm 0.000007$	$0.513102 \pm 0.000018$		38.281	$\pm 0.020$	15.552	$\pm 0.009$	18.328	$\pm 0.010$
JA-2	0.706338	$\pm 0.000006$	$0.512558 \pm 0.000013$		38.694	$\pm 0.017$	15.622	$\pm 0.007$	18.419	$\pm 0.008$
JA-3	0.704183	$\pm 0.000008$	$0.512859 \pm 0.000014$		38.265	$\pm 0.014$	15.551	$\pm 0.006$	18.315	$\pm 0.007$

# Temporal Change of P wave Velocity at Kuju Volcano, Kyushu, Japan

*M. Yoshikawa., Y. Sudo., H. Masuda. and S. Yoshikawa.*

The northwestern area of Kuju Volcano is one of the most active geothermal fields in Japan, where seismic swarms have been observed. The  $V_p/V_s$  ratio changes with time and increases before the seismic swarm.

On the other hand, a temporal change of travel time of P-wave was able to be detected. Travel time of P-wave before April 1996 was slower than after the time (Fig.1, Fig.2). It indicates that P-wave velocity changed with time in this area.

Kuju Volcano in the central Kyushu came to life with a phreatic ash eruption on 11 October 1995. So this change with time of travel time seems to be associated with this eruption and the interaction of geothermal fluids inside the volcano.

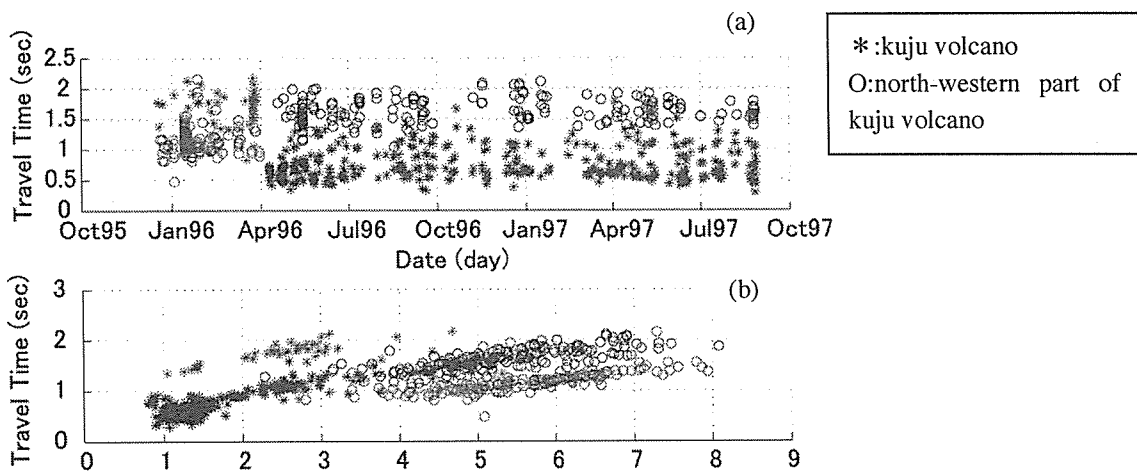


Fig.1(a)Temporal change of P arrival time and (b)Travel time curve at station kj2.

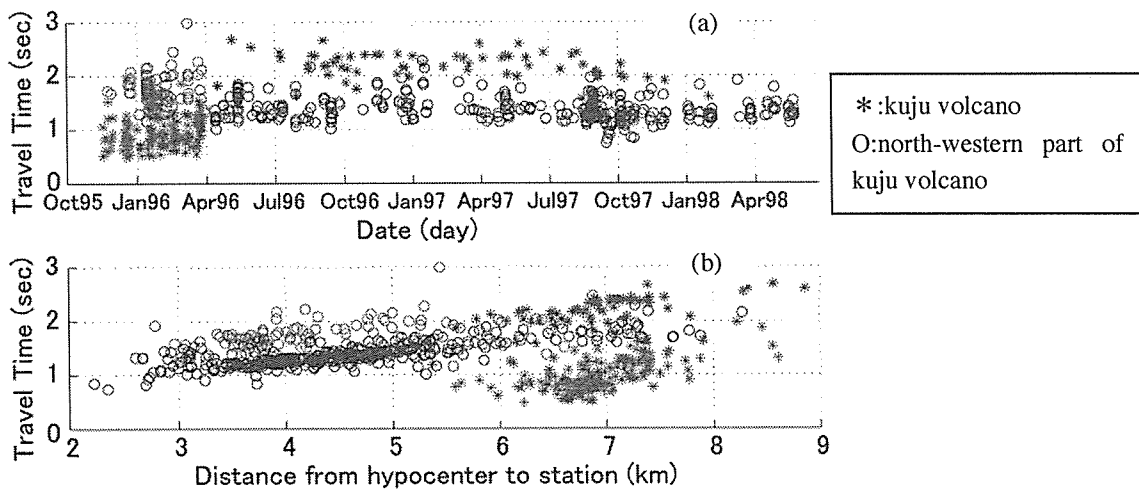


Fig.2(a)Temporal change of P arrival time and (b)Travel time curve at station 1ms

## Thermal Springs in Shargaljuut, Bayankhongor Province, Mongolia

*Y. Yusa and K. Tagomori*

The Shargaljuut Thermal Spring Area is located at the foot (about 2000 meters above the sea level) of the Hangayn Mountains in a distance of about 60 km to the North-East from Bayanhongor City, Mongolia.

Thermal waters are discharged through about 200 holes/fissures of granitic rocks covering an area of 350×170 meters at the north bank of Shargaljuut River. Water temperatures are in a range of 45 – 90°C, and high temperature waters are accompanied by bubbles containing mainly nitrogen. Total outflows are 0.05 m<sup>3</sup>/s for water and 18.5 MW for heat respectively. Thermal waters are alkaline and in low chemical concentration of Na - HCO<sub>3</sub>•SO<sub>4</sub> type. Stable isotope compositions of hydrogen and oxygen in thermal waters indicate that they are originated from meteoric water.

The Shargaljuut Hydrothermal System is interpreted to be that infiltrated meteoric water heated up to about 170°C by terrestrial heat flow at about 4000 meters depth and given chemical substances by water-rock interaction under a limited CO<sub>2</sub> supply uprises through narrow holes of 0.1 - 1 cm in radius.

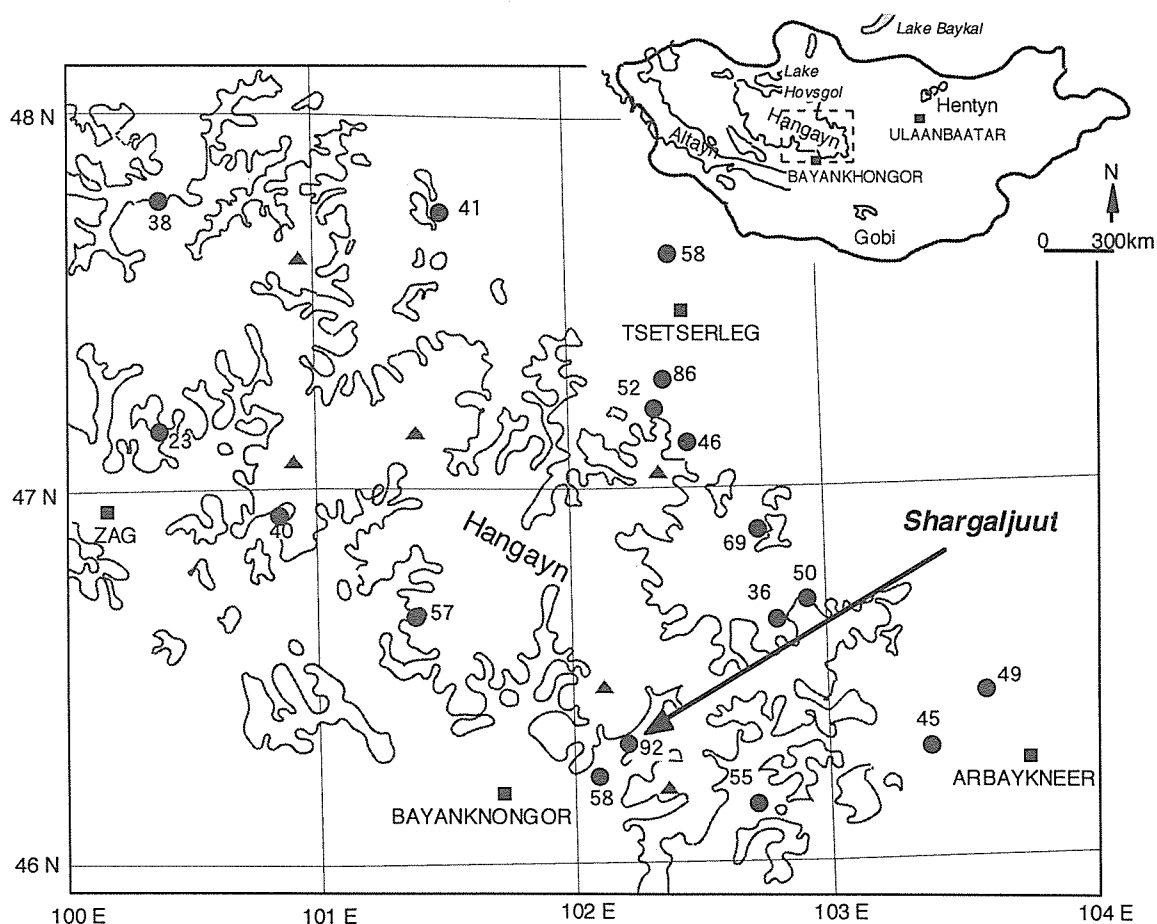


Fig. 1. Location map of thermal springs around Hangayn Mountains. Numerals show discharging temperatures (°C).

<査読有>

- 相澤 義高・伊東 和彦 (22001) ピストンシリンダー型装置を用いた高温高压下における P 波速度の測定のための新手法,地震, 53, 385-387.
- Fukuda Y., M. Itahara, S. Kusumoto, T. Higashi, K. Takemura, H. Mawatari, Y. Yusa, T. Yamamoto and T. Kato (2000) Crustal movements around the Beppu Bay area, East-Central Kyushu, Japan, observed by GPS 1996-1998. *Earth Planets Space*, 52, 979-984.
- Furukawa, Y., H. Mawatari, and T. Kuroda, (2000) Seismic activities in Beppu, Kyushu, *Bull. Seism. Soc. Japan*, 53, 487-490.
- Hashimoto, T. (2001) Detection of Crustal Inhomogeneity in Nojima Fault Zone Using the Earth Current Noise, *Island Arc* (in press).
- Honda, S., T. Nakakuki, Y. Tatsumi, and T. Eguchi (2000) A simple model of mantle convection including a past history of yielding, *Geophys. Res. Lett.*, 27, 1559-1562.
- 岩倉 一敏・大沢 信二・高松 信樹・大上 和敏・野津 憲治・由佐 悠紀・今橋 正征 (2000) 長湯温泉 (大分県) から放出される二酸化炭素の起源. *温泉科学*, 49, 86-93.
- Kawakatsu, H., S. Kanashima, H. Matsubayashi, T. Ohminato, Y. Sudo, T. Tsutsui, K. Uhira, H. Yamasato, H. Ito, D. Legrand (2000) Aso94: Aso seismic observation with broadband instruments. *J. Volcanol. Geotherm. Res.*, 101, 129-154.
- Kimura, S., T. Nanba, T. Sada, M. Okuno, M. Matsunami, K. Shinoda, H. Kimura, T. Moriwaki, M. Yamagata, Y. Kondo, Y. Yoshimatsu, T. Takahashi, K. Fukui, T. Kawamoto and T. Ishikawa (2000) Infrared spectromicroscopy and magneto-optical imaging stations at SPring-8. *Nucl. Sci. Instr. A*, 467-468, 893-896.
- Kumagai, I. and K. Kurita (2000) On the fate of mantle plumes at density interfaces, *Earth Planet. Sci. Lett.*, 179, 63-71.
- 熊谷 一郎・栗田 敬 (2000) レイリー・テイラー不安定の実験～ダイアピル間の相互作用による波長の変化について～, 火山, 45, 331-335.
- Lentz, D., and K. Suzuki (2000) A low-F, pegmatite-related Mo skarn from the southwestern Grenville Province, Ontario, Canada: phase equilibria and petrogenetic implications. *Econ. Geol.*, 95, no. 6, 1319-1338.
- 森健彦・須藤靖明・筒井智樹・中坊真・吉川慎 (2000) 鶴見火山群伽藍岳泥火山における間欠的地震動 "Heart Beat" の震源メカニズム. 火山, 2, 45, 2, 107-117.
- Murakami, H., T. Hashimoto, N. Oshiman, S. Yamaguchi, Y. Honkura, and N. Sumitomo (2001) Electrokinetic phenomena associated with the water injection experiment at Nojima earthquake fault in Awaji Island, Japan, *The Island Arc* (in press).
- Nakashima, T., G. Shimoda, and Y. Tatsumi (2000) Porphyritic magnesian andesites in the Setouchi volcanic belt, SW Japan, *Bull. Volcanol. Soc. Japan*, 45, 259-269.
- Ohkura T. (2000) Structure of the upper part of the Philippine Sea plate estimated by later phases of upper mantle earthquakes in and around Shikoku, Japan, *Tectonophysics*, 321, 17-36 (2000)
- Ohsawa, S., T. Kawamura, N. Takamatsu, and Y. Yusa (2000) Geothermal Blue Water Colored by Colloidal Silica. *Proc. World Geothermal Congress 2000*, 663-668.
- Ohsawa, S., Y. Yusa (2000) Isotopic characteristics of typhonic rainwater: Typhoons No.13, 1993 and No.6, 1996 struck Japan. *Limnology*, 1, 143-149.
- 佐藤 佳子 (2000) 極東ロシア・シホテアリン地域北部における新生代の火山活動とその日本海拡大に対する意義, 地球化学, 242.
- Skirrow, R. G., P. M. Ashley, N.J. McNaughton, and K. Suzuki (2000) Time-space framework of Cu-Au(-Mo) and regional alteration systems in the Curnamona Province. *AGSO Record 2000/10*, 83-86.

- Sudo, M., E.L. Listanco, N. Ishikawa, T. Tagami, H. Kamata, Y. and Tatsumi (2000) K-Ar dating of the volcanic rocks from Macolod Corridor in southwestern Luzon, Philippines: toward understanding of the Quaternary volcanism and tectonics, *J. Geol. Soc. Philippines*, 55, 89-104.
- 周藤正史・石原和弘・巽好幸 (2000) 始良カルデラ地域の先カルデラ火山活動史ーカルデラ北縁部加治木, 国分地域及び南縁部牛根地域の溶岩流試料の K-Ar 年代測定, *火山*, 45, 1-12.
- Suzuki, K., and Y. Tatsumi (2001) Osmium concentrations and isotopic compositions of GSJ reference rocks, JB-1a, JA-2 and JP-1. *Geochem. J.*, 35, 207-210.
- Suzuki, K., M. Feely, and C. O'Reilly (2001) Disturbance of Re-Os chronometry in molybdenites from the late-Caledonian Galway Granite, Ireland, in post-depositional alteration. *Geochem. J.*, 35, 29-35.
- Takano, B., Q. Zheng, and S. Ohsawa (2000) A telemetering system for monitoring aqueous polythionates in an active crater lake. *J. Volcanol. Geotherm. Res.*, 97, 397-406.
- 田中麻貴・須藤靖明・筒井智樹 (2000) 九重火山で観測された S 波の先行相. *火山*, 2, 45, 2, 65-73.
- Tatsumi, Y. (2000) Continental crust formation by delamination in subduction zones and complementary accumulation of the EMI component in the mantle, *G-cubed*, 1, Dec.
- Tatsumi, Y. (2000) Slab melting: its role in continental crust formation and mantle evolution, *Geophys. Res. Lett.*, 27, 3941-3944.
- Tatsumi, Y. (2001) Geochemical modeling of partial melting of subducting sediments and subsequent melt-mantle interaction: generation of high-Mg andesites in the Setouchi volcanic belt, southwest Japan, *Geology*, in press.
- Tatsumi, Y., K. Sato, T. Sano, R. Arai, and V.S. Prikhodko (2000) Transition from arc to intraplate magmatism associated with backarc rifting: evolution of the Sikhote Alom volcanism, *Geophys. Res. Lett.*, 27, 1587-1590.
- Tatsumi, Y., N. Ishikawa, K. Anno, K. Ishizaka, and T. Itaya (2001) Tectonic setting of high-Mg andesite magmatism in SW Japan: K-Ar chronology of the Setouchi volcanic belt, *Geophys. J. Intern.*, 144, 1-11.
- Tatsumi, Y., T. Kani, H. Ishizuka, S. Maruyama, and Y. Nishimura (2000) Activation of Pacific mantle plumes during the Carboniferous: evidence from accretionary complexes in southwest Japan, *Geology*, 28, 580-582.
- Yamamoto, M., H. Kawakatsu, S. Kaneshima, T. Iidaka, J. Oikawa, S. Watada, Y. Morita, T. Mori, T. Tsutsui, Y. Sudo, M. Yoshikawa, T. Hashimoto and M. Nakabo (1999) ASOBOI97: Aso Seismic Observation with Broadband Instruments in 1997. *Bull. Earthq. Res. Inst.*, 74, 267-285.
- Yusa, Y. and S. Ohsawa (2000) Age of of the Beppu hydrothermal system, Japan. *Proc. World Geothermal Congress 2000*, 3005-3008.
- Yusa, Y., S. Ohsawa, and K. Kitaoka (2000) Long-term changes associated with exploitation of the Beppu hydrothermal system, Japan, *Geothermics*, 29, 609-625.

<査読無>

- 火山研センター (2000) 火山噴火予知連絡会会報九重火山の火山活動について (1999 年 5 月~10 月), 75, 97-99.
- 火山研センター (2000) 阿蘇火山の最近の活動 (1999 年 5 月~10 月), 74, 102-104.
- 長谷 英彰・田中 良和・橋本 武志・坂中 伸也 (2000) 阿蘇火山中央火口丘における自然電位観測, 京都大学防災研究所年報, 43, 47-53.
- 村上 英記・橋本 武志・大志万 直人, 山口 寛 (2001) 注水試験時の電磁気観測(2)-流動電位計測-, 月刊地球総特集「野島断層注水実験と誘発地震」, 23, 250-255.
- 大沢 信二 (2000) 噴気ガスの化学・同位体組成からみた別府温泉の地熱流体の起源及び性状. 大分県温泉調査研究会報告, 51, 19-28.
- 下泉 政志・半田 駿・網田 和宏・田中 良和・茂木 透・鈴木 貞臣 (2000) 男女海盆での O B E M 観測 (序報) C A 研究会 2000 年論文集, 61-66.
- 下泉 政志・半田 駿・田中 良和・茂木 透・湯元 清文 (2000) 浅海用海底電位磁力計の開発 (1), C A 研究会 2000 年論文集 54-60.
- 下泉 政志・田中 良和・歌田 久司・濱野 洋三 (2000) N T T 海底ケーブルを用いた地電位差測定, C A 研究会 2000 年論文集 46-53.

- 田部井 隆雄・木股 文昭・大倉 敬宏・加藤 照之・小竹 美子(2001), GPS 観測から見たフィリピン・インドネシア東部の地殻変動, 月刊地球, 23, 70-75
- 高倉 伸一・橋本 武志・小池 克明・小川 康雄 (2000) MT法による阿蘇カルデラの比抵抗断面, C A研究会論文集, 23-30.
- 巽 好幸 (2000) 統合国際深海掘削計画 (IODP) の科学目標 ―新しい地球観の創成を目指して―, OD21 Newsletter, 4, 2-5.
- 吉川 美由紀・須藤 靖明・筒井智樹・田口幸洋 (2000) 九重火山周辺部地熱地域における地震活動. 京都大学防災研究所年報, 43 B-1, 37-46.
- 由佐 悠紀 (1999) 地熱開発の水文学的側面, 地熱エネルギー, 24, 224-231.
- 由佐 悠紀・大沢 信二 (2000) 別府温泉の年齢, 大分県温泉調査研究会報告, 51, 1-9.

### 学 会 発 表 Conference Presentations

- Aizawa, Y., Compressional wave velocity measurements of mantle rocks at high pressures and temperatures, SEDI 2000, Exeter, UK, 2000 年 8 月
- 相澤 義高, 伊東 和彦, 地殻物質の部分溶融の P 波速度への影響, 地球惑星科学関連学会 2000 年合同大会, 東京都代々木オリンピックセンター, 2000 年 6 月
- 網田 和宏・大沢 信二・長谷 英彰・坂中 伸也・大上 和敏・下田 玄・橋本 武志・由佐 悠紀, 「別府温泉の地熱流体供給域における比抵抗構造」, 地球惑星科学関連学会合同大会 (2000 年 6 月: 東京代々木オリンピックセンター)
- 網田 和宏・大沢 信二・長谷 英彰・坂中 伸也・大上 和敏・下田 玄・橋本 武志・由佐 悠紀「別府温泉の比抵抗構造とその解釈」, 日本温泉科学会 (2000 年 8 月: 香川県琴平温泉琴参閣)
- Hase, H., Hashimoto, T., Sakanaka, S., Tanaka, Y., Self-potential Measurements on the Central Cone of Aso Volcano: WPGM (June 27-30, Tokyo)
- Hashimoto, T., Y. Tanaka and T. Kagiya, Self-Potential Variability of 10 Years Observed at Unzen Volcano, Japan, Western Pacific Geophysics Meeting, Tokyo, 2000.
- Hashimoto, T., W. Kanda, S. Takakura, S. Sakanaka and Y. Tanaka, Resistivity Structure of the Central Cones of Aso Volcano, Japan, VIII workshop on geoelectromagnetism, Maratea, Italy, 2000.
- 橋本 武志, 電場磁場変動から推定される火山浅部の流体変動, 京都大学防災研究所研究集会「火山の浅部構造と火山流体」(代表者・鍵山恒臣), 宇治, 2001 年 1 月 14 日.
- 橋本 武志・田中 良和・宇津木 充, 最近 10 年間の阿蘇火山の地磁気変化について, 京都大学防災研究所研究発表講演会, 京都市, 2001 年 2 月.
- 橋本 武志・田中 良和・宇津木 充, 最近 10 年の阿蘇火山の地磁気変化について, 平成 12 年度防災研究所研究発表講演会, 13/2/23 京都市リサーチパーク
- 市来 雅啓・橋本 武志・網田 和宏・田中 良和ほか「九州地域におけるネットワーク MT 観測 (第 3 報) 九州地方のデータコンパイルと解析」(108 回地球電磁気・地球惑星圏学会, 11/23, 板橋区文化会館)
- 市来 雅啓・橋本武志・上嶋 誠・網田 和宏・神田 径・馬渡 秀夫・下泉 政志・笹井 洋一・田中 良和・歌田 久司, 九州地域におけるネットワーク MT 観測 (第 3 報) 九州地方のデータコンパイルと解析, 地球電磁気・地球惑星圏学会, 東京, 2000.
- 神田 径・橋本 武志・網田 和宏・半田 駿・長谷 英彰・生駒 良友・鍵山 恒臣・小山 崇夫・増田 秀晴・茂木 透・宗包 浩志・小河 勉・小野 博尉・坂中 伸也・下泉 政志・田中 良和・Djedi S. Widarto, 阿蘇火山における TDEM 法電磁気構造調査, 地球惑星科学合同学会, 東京, 2000.
- 神田 径・橋本 武志・網田 和宏・長谷 英彰・増田 秀晴・小野 博尉・坂中 伸也・田中 良和 ほか「阿蘇火山における TDEM 法電磁気構造調査」(2000 年地球惑星科学関連学会合同大会, 青少年総合センター)



- 神田 径・田中 良和「桜島およびその周辺に於ける長基線地電位差観測（２）」（日本火山学会秋季大会 9/13 茨城大学）
- 神田 径・田中 良和・宇津木 充ほか、「口永良部島火山の集中総合観測 ―電磁気観測編―」（2001 年 1 月 29 日 C A 研究会,伊東市富戸コミュニティ・センター）
- 神田 径・田中 良和・宇津木 充ほか,通信衛星を利用した口永良部島火山における地磁気全磁力連続観測,平成 12 年度防災研究所研究発表講演会,13/2/23 京都リサーチパーク
- 川本 竜彦, 外熱式 DAC を用いたマグマの分光学, 高圧討論会, 2000 年 11 月, 東京
- 川本 竜彦, 高温高圧条件下でのマグマの分光学へ, 平成 12 年度特定領域研究「超高压地球科学」シンポジウム「プレート・マントル・核相互作用の超高压物質科学研究の現状と今後の研究戦略」2001 年 2 月, 仙台
- 川本 竜彦,「地球内部の水とマグマ：実験マグマ学への招待」熊本大学理学部地球科学科談話会,2001 年 2 月 16 日
- 恵口 泰秀・田部井 隆雄・高谷 卓司・橋本 学・細善信・大倉 敬宏・木股 文昭・平原 和朗・松島 健・田中 寅夫・宮崎 真一・越智 久巳, 西南日本の地殻変動場と中央構造線の活動様式—GPS 稠密トラバース観測より—,日本地震学会秋季大会（2000 年 11 月,つくば国際会議場）
- Kumagai, I. (2000) Laminar entrainment and mixing in compositionally buoyant plumes: effect of viscosity ratio, The 7th SEDI (the Study of the Earth's Deep Interior) symposium (July 2000, Exeter, United Kingdom).
- Kurita, K. and Kumagai, I. (2001) Possibility of a stagnant layer between upper and lower mantle, OHP/ION joint symposium (January 2001, Yamanashi, Japan).
- 茂木 透・田中 良和・橋本 武志ほか「雲仙溶岩ドーム（平成新山）周辺の浅部抵抗構造」（2000 年地球惑星科学関連学会合同大会,青少年総合センター）
- 茂木 透・田中 良和・橋本 武志・宇津木 充ほか「有珠火山における電磁気観測」（日本火山学会秋季大会 9/14 茨城大学）
- Murakami, H., T. Hashimoto, N. Oshiman, and S. Yamaguchi, Electrokinetic Observations during Water Injection Experiments at the Nojima Fault, Japan, Fall Meeting, AGU, San Francisco, 2000.
- 村上 英記・橋本 武志・大志万 直人・山口 覚, 野島断層注水試験に伴う自然電位変化(2), 地球電磁気・地球惑星圏学会, 東京, 2000.
- 西田 泰典・茂木 透・佐藤 秀幸・谷元 健剛・佐波 瑞恵・高田 真秀・田中 良和・橋本 武志・宇津木 充・笹井 洋一, 有珠火山における電磁気観測, 日本火山学会, 水戸, 2000.
- 西田 泰典・茂木 透・佐藤 秀幸・谷元 健剛・佐波 瑞恵・高田 真秀・田中 良和・橋本 武志・宇津木 充・笹井 洋一, 2000 年有珠噴火における電磁気観測, 地球電磁気・地球惑星圏学会, 東京, 2000.
- 西田 泰典・田中 良和・橋本 武志・宇津木 充ほか「2000 年有珠火山に於ける電磁気観測」（108 回地球電磁気・地球惑星圏学会,11/21,板橋区文化会館 p）
- 大倉 敬宏, 四国およびその周辺におけるフィリピン海プレート上面の構造, 日本地震学会秋季大会（2000 年 11 月,つくば国際会議場）
- Ohsawa, S., Kawamura, T., Takamatsu, N., Yusa, Y.: “Geothermal Blue Water Colored by Colloidal Silica”, Oral presentation, World Geothermal Congress, Beppu, May-June 2000
- Ohsawa, S., Iwakura, K., Takamatsu, N.: “Mixing of Volcanic CO<sub>2</sub> with Groundwater Originating in a Non-volcanic Sedimentary Basin, Oita Plain, Middle Eastern Kyushu, Japan”, Oral presentation, Western Pacific Geophysics Meeting, Tokyo, May 2000
- 大沢 信二・由佐 悠紀:小笠原硫黄島の噴気 CO<sub>2</sub> の同位体地球化学的特徴, 第 50 回日本温泉科学会, 琴平, 2000 年 8 月
- 岡元 正久, 鈴木 勝彦, 南 雅代, 下田 玄, 清水 洋, 足立守, 西オーストラリア Pilbara 地域の先カンブリア紀 komatiite, banded chert の Re-Os 及び Sm-Nd 同位体システムティクス, 2001 年度日本質量分析学会同位体比部会（2000 年 11 月 23~24 日:大分県湯布院ハイツ）
- 大島弘光, 森濟, 前川徳光, 吉田邦一, 田村真一, 一柳昌義, 岡田弘, 浜口博之, 西村大志, 青山裕, 辻浩, 植平賢司, 宮町宏樹, 八木原寛, 須藤靖明, 高山鐵朗: 2000 年有珠山噴火に伴う地震活動. 2000 年度日本火山学会秋季大会（2000 年 9 月:茨城大学）

- 坂中 伸也・田中 良和・宇津木 充ほか「カリフォルニア州オーエンスバレーにおける自然電位測定」  
(108 回地球電磁気・地球惑星圏学会,11/21,板橋区文化会館 p)
- 笹井 洋一・田中 良和ほか「伊豆半島東部地域の全磁力観測：1976-2000」(2001 年 1 月 29 日 C A  
研究会,伊東市富戸コミュニティ・センター)
- Sato, K., Y. Tatsumi, T. Sano, R. A. Tsurudome, V. Prikhodko, T. Tagami., Cenozoic volcanism in northern  
Sikhote Alin and its implication for the opening of the Japan Sea, 地球惑星関連学会(青少年オリンピ  
ック総合センター) 2000 年 6 月
- Sato, K., Kazuo Saito, Bretstein Yuri, S., ベトナム地域の玄武岩類における K-Ar 年代測定, 質量分析学  
会同位体比部会, 湯布院ハイッ, 2000 年 11 月
- 須藤 靖明・橋本 武志, Mario Ruiz-Romero, Hugo Yepes, Darwin Villagomez, Diego Viracucha, 1999 年エ  
クアドル・グアグアピテンチャ火山の活動について, 地球惑星科学合同学会, 東京, 2000.
- 須藤靖明, 池辺伸一郎: 阿蘇カルデラ内で見出された落差 1m の新鮮な活断層と最近の地震活動. 京  
大防災研究所研究発表講演会(2000 年 2 月: 京都)
- Suzuki, K., and Tatsumi, Y., Re-Os isotopic systematics of Setouchi high-Mg andesites, SW Japan: Evidence  
for slab melting. Goldschmidt 2000 (Sep. 3-8, 2000: Oxford (UK))
- Suzuki, K., Aizawa, Y., and Tatsumi, Y., Osmium transport during dehydration processes in the subducted slab:  
Experiments and implications for the Os isotopic compositions of arc magmas. Goldschmidt 2000 (Sep. 3-8,  
2000: Oxford (UK))
- Suzuki, K., and Tatsumi, Y., Rhenium-Osmium isotopic systematics of Setouchi high-Mg andesites, SW Japan:  
Evidence for slab melting. AGU Fall Meeting (Dec. 15-19, 2000: San Francisco (USA))
- 鈴木 勝彦,相澤 義高,巽 好幸,沈み込むスラブの脱水過程とオスミウムの挙動: 高温高圧実験と島弧  
火山岩のオスミウム同位体組成,2000 年度日本地球化学学会年会 (2000 年 9 月 25~27 日: 山形大学)
- 鈴木 勝彦,Roger, G. Skirrow, 巽 好幸,Broken Hill(オーストラリア)鉍床モリブデナイトの高精度,高分  
解能レニウム-オスミウム年代,2000 年度日本地球化学学会年会 (2000 年 9 月 25~27 日: 山形大学)
- 鈴木 勝彦,柴田 知之,巽 好幸,東北中国の tholeiite,alkali basalt のオスミウム同位体: プレート内マグ  
マ活動に関する示唆,2000 年度日本地球化学学会年会 (2000 年 9 月 25~27 日: 山形大学)
- 鈴木 勝彦,柴田知 之,巽 好幸,東北中国 Weichang 地域 tholeiite,alkali basalt の Re-Os システムティク  
ス,2001 年度日本質量分析学会同位体比部会 (2000 年 11 月 23~24 日: 大分県湯布院ハイッ)
- 鈴木 勝彦,巽 好幸,瀬戸内玄武岩,高マグネシウム安山岩のオスミウム同位体とスラブ溶融,2000 年度  
日本地球化学学会年会 (2000 年 9 月 25~27 日: 山形大学)
- 鈴木 勝彦,巽 好幸,JB-1a, JA-2, JP-1 のオスミウム濃度と同位体組成,2000 年度日本地球化学学会年会  
(2000 年 9 月 25~27 日: 山形大学)
- Tabai, T., Kimata, F., Ohkura, T., Kotake, Y. and Kato, T. "Active Deformation in the Philippines-Eastern  
Indonesia From GPS Measurements", Western Pacific Geophysical Meeting ( June 2000, Tokyo)
- 田中 良和・橋本 武志・宇津木 充・長谷 英彰「最近 10 年の阿蘇火山における地磁気変化」(2001  
年 1 月 29 日 C A研究会,伊東市富戸コミュニティ・センター)
- Tatsumi, Y., Scientific targets of OD21, WPGM Symposium (2000 年 6 月 30 日, 東京)
- Tatsumi, Y., Continental crust formation in subduction zone and mantle evolution. (2000 年 8 月 22 日; ユー  
ジーン)
- Tatsumi, Y., The role of subduction factory in the evolution of the solid Earth, Hayashibara Symposium (2000  
年 9 月 7 日, 岡山)
- Tatsumi, Y., Ancient activity of Pacific plume, Geol. Soc. America Annual Meeting (2000 年 11 月 15 日, リ  
ノ)
- 巽 好幸, 高 Mg 安山岩の生成と大陸地殻成の因論,三鉍学会シンポジウム (2000 年 11 月 6 日,徳島大  
学)
- 巽 好幸, サブダクションファクトリー: 地球進化における役割, 玉城教授記念講演会 (2000 年 12  
月 8 日,京都大学)
- 筒井 和男・由佐 悠紀・福田 洋一,別府における地下水変動と重力の時間変化の関係,日本陸水学会第  
65 回大会 (2000 年 9 月,福岡大学)

- Utsugi M., Volcanomagnetic Field Considering the Inhomogeneity of the Crustal Magnetization, (2000 Western Pacific Geophysics Meeting, 2000 年 6 月 27-30 日, 国立オリンピック記念青少年総合センター)
- 宇津木 充, 田中 良和, 雲仙普賢岳における地場変化-1995 年~2000 年 6 月-, 日本火山学会(2000 年 9 月 13~15 日, 茨城大学)
- 宇津木 充, 笹井 洋一, 田中 良和, 坂中 伸也, Malcolm J. S. Johnston, Jacques Zlotnicki, 上嶋 誠, 後藤 忠徳, ロング・バレー・カルデラの電磁気共同観測 (3) - 地磁気全磁力観測について -, 地球電磁気・地球惑星圏学会(2000 年 11 月 20~23 日, 板橋区立文化会館)
- 宇津木 充・田中 良和ほか「ロングバレー・カルデラにおける磁場変化」(2001 年 1 月 29 日 C A 研究会, 伊東市富戸コミュニティ・センター)
- 宇津木 充・田中 良和・橋本 武志・長谷 英彰, 阿蘇火山における空中磁気測量について, 平成 12 年度防災研究所研究発表講演会, 13/2/23 京都市サーチパーク
- 山本 希・川勝 均・金嶋 聡・大湊 隆雄・加藤 護・須藤 靖明・橋本 武志・森 健彦・中坊 真・吉川 慎・吉川 美由紀, 二つの高密度アレイによる阿蘇火山火山性微動の解析, 地球惑星科学合同学会, 東京, 2000.
- 吉川美由紀, 須藤靖明, John M Londono, 増田秀晴, 吉川 慎, 田口幸洋: 九重火山とその北西部における P 波速度構造の時間変化. 2000 年度日本火山学会秋季大会 (2000 年 9 月: 茨城大学)
- Yusa, Y. and Ohsawa, S. (2000) Age of of the Beppu hydrothermal system, Japan. Proc. World Geothermal Congress 2000 (2000 年 5 月~6 月, 別府ビーコンプラザ) .
- Yusa, Y., Ohsawa, S. and Kitaoka, K., Effects of exploitation in the Beppu hydrothermal field, Japan, World Geothermal Congress 2000 (2000 年 5 月~6 月, 別府ビーコンプラザ) .

### 共同研究 Collaboration

#### 国内

- 橋本武志: 「高速サンプリングデータロガーを使った阿蘇火山における自然電位連続観測」(京大理, 地質調査所地殻熱部)  
: 「雲仙科学掘削計画 (自然電位・地磁気)」
- 橋本武志・宇津木充: 「三宅島火山における電磁気観測 (磁力計の設置)」(京大理, 東大震研)
- 橋本武志・宇津木充・田中良和: 「有珠火山における電磁気観測 (磁力計携帯電話テレメータの開発と設置)」(京大理, 北大理, 東大震研)
- 大倉敬宏: 「中央構造線における稠密 GPS トラバース観測」
- 大沢信二: 「山地斜面の地下水に関する研究」(京都大学防災研究所研究担当)
- 大沢信二・網田和宏・下田玄・山田誠: 「阿蘇火山中岳湯溜の地球化学的・色彩学的研究」(東邦大学理学部化学科)
- 須藤靖明: 阿蘇火山火山性微動観測 A S O 2000 (震研・東工大, 川勝・山本・金嶋・高木・須藤・吉川) 2000 年 6 月 5 日-8 日; 10 月 27 日-31 日; 2001 年 3 月 28 日-31 日.  
: 第 7 回国際火山ガス野外研究集会 (2000 年 10 月 23-25 日, 九重火山: 須藤, 吉川, 中坊)  
: 東大地震研究所研究集会九州の活火山における火山研究の到達点と今後の課題\_雲仙・阿蘇・九重・霧島・桜島・南西島弧の噴火機構と地下構造\_ (2000 年 9 月 26 日-27 日, 代表者: 須藤靖明, 所内担当: 鍵山恒臣)
- 鈴木勝彦: 「Pilbara chert, komatiite の Re-Os, Sm-Nd システムティクス: 初期大陸の生成」(広大, 清水・岡元・服部, 名大, 足立)  
: 「Pt-Os, Re-Os 放射壊変系を Hawaii, Iceland などの玄武岩に適用し, プルームの発生深度を探る」(東工大, 高橋, 岡山大学, 河野)  
: 「ダブル  $\beta$  壊変  $^{100}\text{Mo}$ - $^{100}\text{Ru}$ : ニュートリノの質量」(広大, 日高・Chi)

- :「EXAFS による天然岩石中の白金族元素の存在状態」(広大, 高橋・清水)
- 田中良和: 理化学研究所併任 (地震国際フロンティア研究プログラム)
- : 京都大学防災研究所研究担当
- : 工業技術院地質調査所地殻物理部併任
- :「有珠火山の電磁気観測 7/11-15」
- :「秋の宮地域の電磁気調査 9/9-9/11」
- :「地磁気日変化と電離層電場, 風の関係」(京都大学宙空電波研究所)
- 田中良和・橋本 武志・宇津木充:「地震に伴う電磁放射の観測 (火山研に機器の設置)」(京大理, 広島工業大学)
- 田中良和・宇津木充:「岩手火山の空中磁気測量 12/19-12/23」
- :「口永良部島の電磁気観測 8/8-8/12」
- :「口永良部島の空中磁気測量」
- :「ロングバレーカルデラの電磁気観測 8/17-8/30」(米国地質調査所)
- 田中良和・宇津木充・長谷英彰:「岩手火山の電磁気観測 6/30-7/3」
- 巽好幸: 京都大学防災研究所研究担当 (始良カルデラにおける大規模火砕流マグマの成因)
- : 海洋科学技術センター併任研究員
- : 岡山大学固体地球研究センター嘱託研究員

## 国際

- 橋本武志:「地球電磁気学的手法による火山流体の調査」(Istituto Internazionale di Vulcanologia, Catania, Italy)
- 大倉敬宏:「フィリピン・マコロド回廊における GPS 観測」(フィリピン火山地震研究所)
- :「インドネシア北スラベシにおけるジオダイナミクス」(名古屋大学, 高知大学, バンドン工科大学, フィリピン火山地震研究所)
- 鈴木勝彦:「フィリピン ophiolite の Re-Os 年代と Os 初生同位体比による多段階生成モデル」(フィリピン環境鉱床研究所, Santos, R.A., 東大総合文化, 高野, 東大海洋研, 野崎, 宮田)
- :「モリブデナイトの超高分解能 Re-Os 直接年代決定法によるオーストラリア Olary-Broken Hill 地域の鉱床生成論」(オーストラリア地調, Skirrow, R. G.)
- :「カナダ Grenville 地域のモリブデナイトの高精度 Re-Os 年代」(カナダ地調, Lentz, D.)
- :「オーストラリア東南地域のモリブデナイトの Re-Os 年代」(オーストラリア国立大学, Blevin, P.)

## A brief report on routine observations at AVL

*Aso Volcanological Laboratory*

### **Purpose of routine observations**

One of the major activities of AVL is geophysical research on structure and dynamics of active volcanoes.

In case of unrest, integrate and intensive observations are necessary in order to have an accurate grasp of volcanic activity and to forecast impending eruption. However, routine observations at an inactive stage of a volcano are also important to establish a baseline for evaluation of possible eruptive activity. In order to obtain simple and general set of laws to predict an eruption, we need comparative studies with other volcanoes which are equipped with basic and common tools, such as seismic monitoring and measurements of ground deformation, gravity and magnetism. Routine observations as well as strategic temporal observations are necessary for hypothesis testing and constructing of a theory. Because the time scales of some volcanic phenomena are long, we need long-term observations and homogeneous data for a better understanding of these phenomena.

AVL has been taking charge of continuous monitoring of Aso volcano since its foundation. Recently, other active volcanoes such as Kuju and Tsurumi have been under monitoring. Exact data and detail description of Aso and Kuju volcanoes are regularly reported to Coordinating Committee for Prediction of Volcanic Eruption. Also they are published in “Report of Coordinating Committee for Prediction of Volcanic Eruption” by JMA. For further information about these two volcanoes, please refer to these publications.

### **Routine observation crew( #:part time)**

<Research Staffs> Yoshikazu TANAKA, Yasuaki SUDO, Hiori ONO, Takahiro OHKURA, Takeshi HASHIMOTO and Mitsuru UTSUGI<sup>#</sup>

<Technical Staffs> Teruaki HOKA, Mikio SAKO, Shin YOSHIKAWA and Hideharu MASUDA<sup>#</sup>

<Graduate Students>

Takehiko MORI, Makoto NAKABOH, Hideaki HASE, Miyuki YOSHIKAWA and John Makario LONDONO

### **Items of routine observations and persons in charge**

<Seismology>

A control of the regional network: Y. SUDO

Analysis of data from the regional network: Y. SUDO

A control of the network around the active crater in Aso: H. ONO

Analysis of data from the network around the active crater: H. ONO and T. MORI

A control of the network around Kuju volcano: Y. SUDO

Analysis of data from the Kuju network: Y. SUDO and M. YOSHIKAWA

Maintenance works on instruments: T. HOKA, M. SAKO, S. YOSHIKAWA and H. MASUDA

Maintenance works on seismic stations: T. HOKA, M. SAKO, S. YOSHIKAWA and H. MASUDA

Volcanic tremor accumulator in Aso: Y. SUDO and M. SAKO

<Ground deformation>

Tiltmeters and extensometers in Aso: H. ONO and M. SAKO

Tiltmeters in Kuju: M. SAKO

GPS and EDM in Aso: H. ONO and M. NAKABOH

GPS and EDM in Kuju: H. ONO and M. NAKABOH

Leveling survey in Aso: M. NAKABOH and others

Super Conductivity Gravimeter: Y. SODO, S. YOSHIKAWA and T. MORI

<Geomagnetism>

Fulltime monitoring of total force in Aso: Y. TANAKA , T. HASHIMOTO and M. UTSUGI

Fulltime monitoring of total force in Kuju: Y. TANAKA , T. HASHIMOTO and M. UTSUGI

<Miscellaneous>

Geothermal observation nearby the active crater in Aso: Y. SODO and S. YOSHIKAWA

## Volcanic activity and geophysical observations at Aso during the past ten years

*T. Hashimoto, Y. Tanaka, Y. Sudo, H. Ono, T. Ohkura, T. Tsutsui, T. Hoka,  
M.Sako, H. Masuda, S. Yoshikawa, S. Sakanaka, M. Utsugi, and T. Mori*

We investigated changes in some geophysical data observed around the active crater of Nakadake, Aso Volcano during the period of 1990-2000 with special attention to the relationship between geomagnetic changes, tremors and superficial activities of the volcano. The followings are suggested.

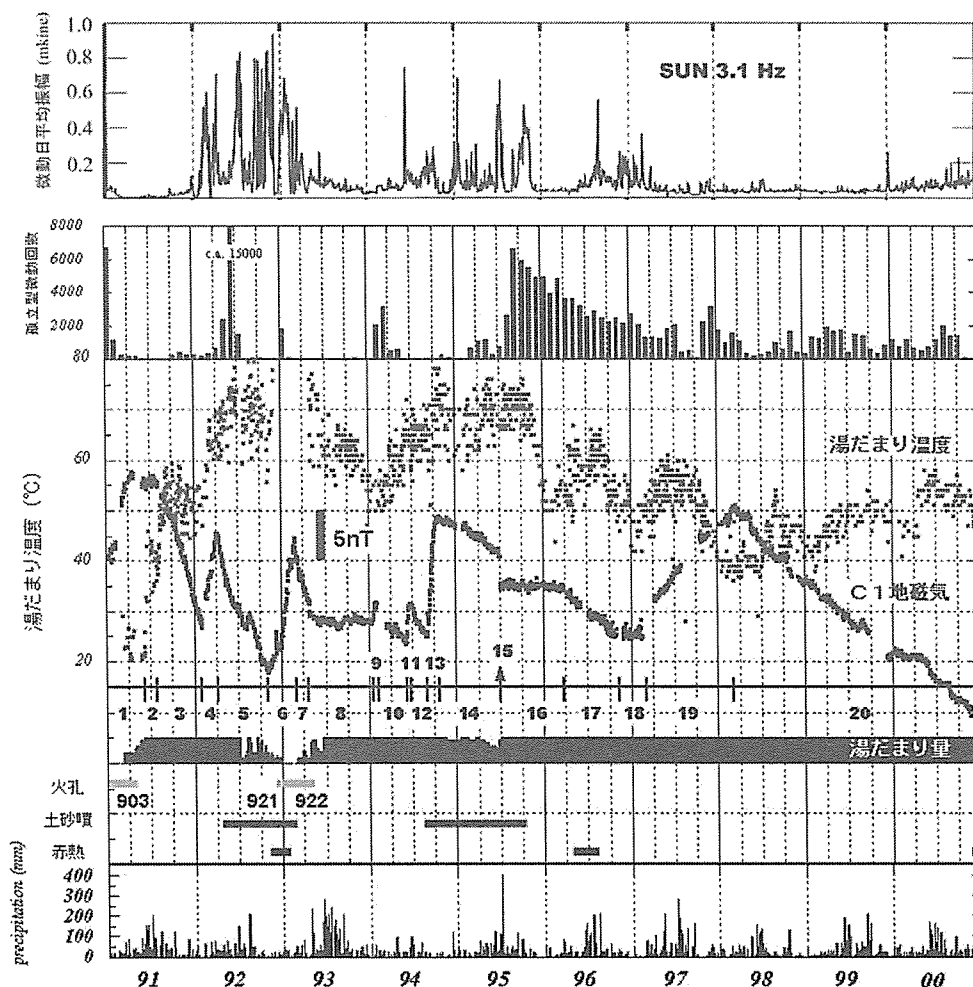


Fig.1 (From top to bottom) Geophysical variations observed at Nakadake, Aso Volcano during the period of 1990-2000. Amplitude variations of tremors (AVL), cumulative number of isolated tremors (JMA), surface temperature of the crater lake (JMA), geomagnetic total force (AVL), water level of the crater (JMA), existence of pit craters, mud flow and incandescence (AVL and JMA), and precipitation (JMA).

- (1) An onset of magnetization (cooling) period frequently coincides with a burst of continuous tremor, mud eruption, or opening of a vent. Such events seem to be strongly related to heat and material transport from the shallow part to the ground surface. Inversely, it is frequently observed that the burst of continuous tremor does not coincide with geomagnetic change.
- (2) Increase of the cumulative number of isolated tremors does not seem to coincide with an onset of magnetization (cooling) but that of demagnetization (heating).
- (3) Condition of the crater bottom severely affects the heat-transfer system at shallow part.

## Seismicity in the Beppu graben in 2000

*Y. Furukawa, H. Mawatari, and K. Takemura*

In the Beppu graben we have observed seismic activity (See the section “Observation of seismic activity in the Beppu graben” in this issue). In 2000 we have located 228 events; the hypocenter and vertical sections in the E-W and N-S directions are shown in Fig. 1. In 2000 we have three major seismic swarms in this graben. The first swarm activity began in January 1999 in the area between the Kannawa and the Asamigawa faults, which occurred just after a large swarm in December 1999. The second one was occurred in April 2000 in the area between the Beppu-Kita and the Kannawa faults. The last one was occurred in May just after the duration of the second one in the area ~2 km north of the area of the second one.

In the areas of the swarms in Dec. 1999 and 2000 swarm-like seismic activity has been observed; the maximum magnitude of these swarms is less than ~3.0. The swarms from Dec. 1999 till May 2000 have several events with magnitude of >3.0, and the number of events was one order of magnitude larger than that of the previous year.

In Fig. 2 the maximum depth of focus become deeper with the distance from the volcanoes, which is considered to simulate the temperature of the brittle-ductile transition in the crust (See the section “Seismic Activity in the Beppu graben, Kyushu, Japan: implications for earthquakes triggered by magmatic fluids” in this issue). In a area in the Beppu bay near the northern swarm area, a dome structure was detected by reflection studies, which is considered to be magmatic intrusion. The swarm areas, the volcanoes, and the magmatic dome structure are approximately on a line, and the deeper swarm activity could be related with magmatic intrusion.

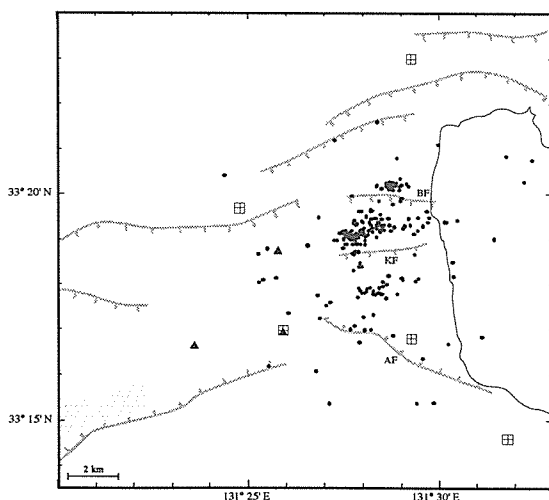


Fig. 1 Epicenter distribution located in the period from April 1993 to Dec. 1999 for events with magnitude greater than 1.0. The shaded oval represents the location of the estimated high electric conductivity body. Fault structures estimated from gravity survey are also shown as shaded straight lines. Open rectangles and filled triangles denote seismic stations and volcanoes, respectively. BF, KF, and AF represent the Beppu-kita, Kannawa, and Asamigawa faults.

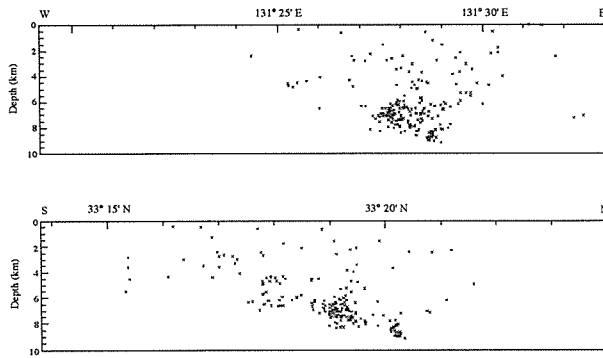


Fig. 2 Vertical cross sections of focal distribution in the N-S and E-W directions.

## Volcanic earthquakes near Mt. Naka-dake, Aso Volcano in 2000

*H. Ono*

The first crater of Mt. Naka-dake, Aso Volcano has been covered with hot water pool since 1993. The incandescent state was appeared at the south part of the first crater on October in 2000 and continued through the year.

Volcanic earthquake activity was calm near the active crater of Mt. Naka-dake in 2000.

The foci of volcanic earthquake distributed under the first crater as yet. The source location and daily number histogram of volcanic earthquakes were shown in Fig. 1 and Fig. 2.

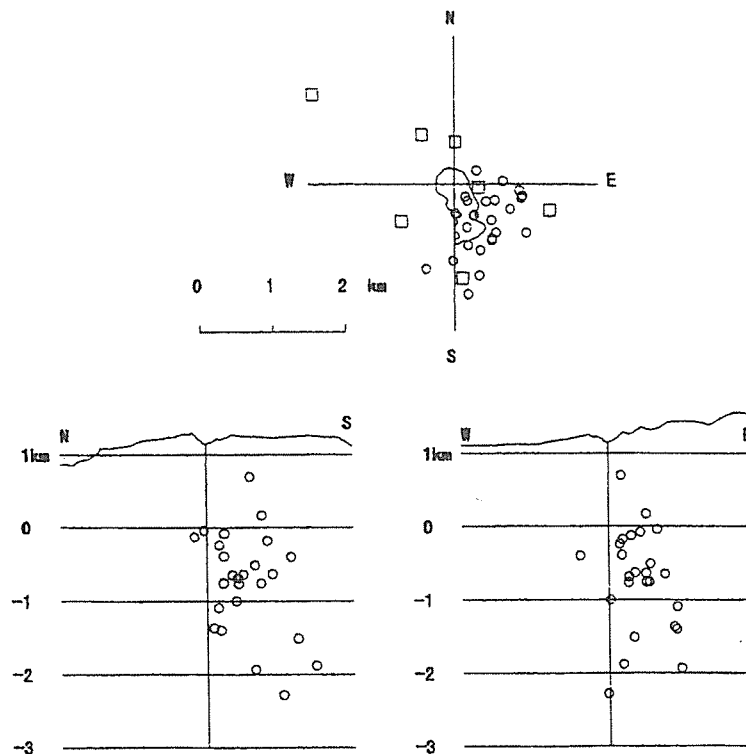


Figure 1. Source distribution of volcanic earthquakes near Naka-dake in 1999.  
○ : location of volcanic earthquake, □ : seismic station.



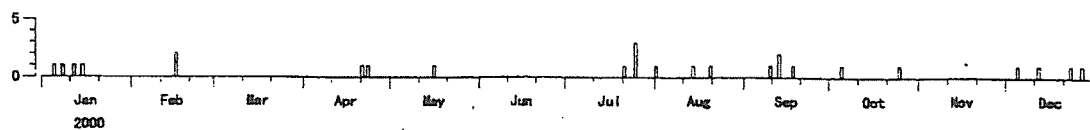


Figure 2. Daily number histogram of volcanic earthquakes in 1999.

## Ground deformation observation in 2000

*H. Ono*

The tunnel for ground deformation observation locates in 30m underground at about 1km south-west from the first crater of Mt. Naka-dake and consists of horizontal tunnels forming equilateral right-angled triangle. Watertube tiltmeters of 25m span (WT1 and WT2) and extensometers of 20m span (E1 and E2) and 25m span (E3) have been installed.

The ground deformation observed by tiltmeters and extensometers in 2000 is shown in Fig. 2 with precipitation by Aso-san Weather Station, JMA.

Extensometers recorded annual variation with strain amplitude of  $10^{-6}$  order.

The northwest uplift of  $5 \mu\text{radian}$  was observed by tiltmeters for the later 5 months in 2000. It is doubtful whether this uplift will progress to volcanic eruption, because the uplift direction is perpendicular to the active crater.

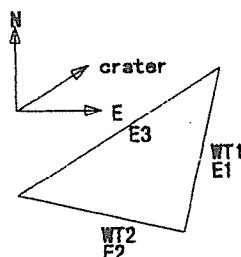


Figure 1. Tunnel and setting of watertube tiltmeters (WT1, WT2) and extensometers (E1, E2, E3).

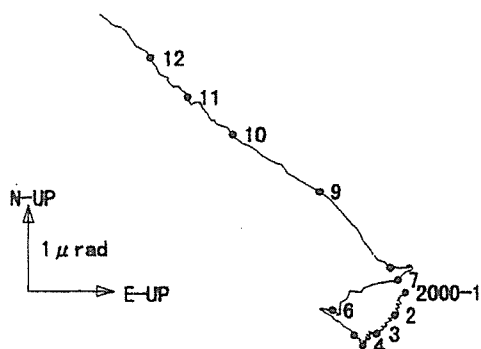


Figure 3. Upward vector from watertube tiltmeter observation. Attached numbers show months (1st day).

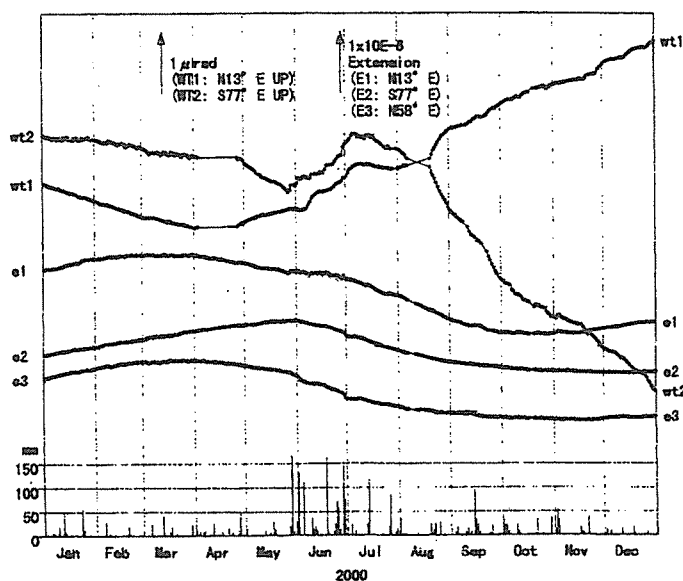
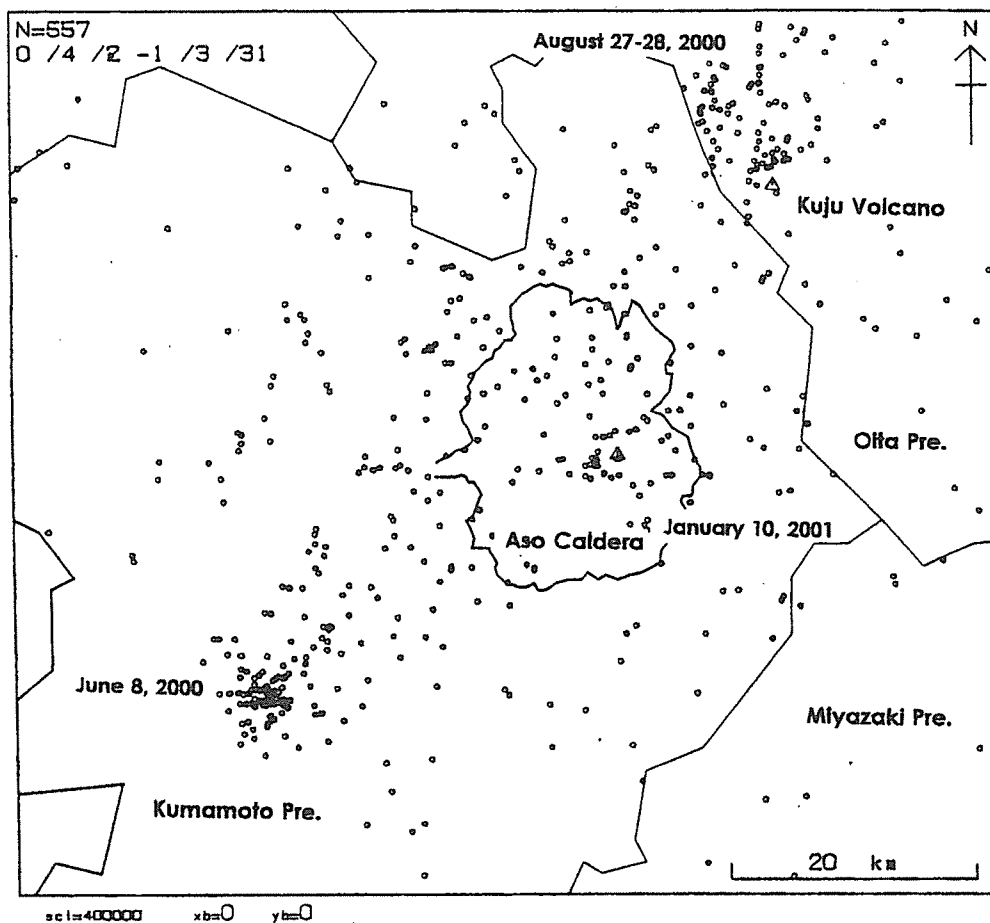


Figure 2. Ground deformation records in 2000. Lower is daily precipitation by Aso-san Weather Station, JMA.

## Seismic Activity around Aso Caldera and Kuju Volcano during the period from April in 2000 to March in 2001

Y. Sudo

A telemetrically seismic network around Aso Caldera and Kuju Volcano is composed of 17 stations. Several earthquake swarms have occurred at the southwestern region of Aso Caldera and the northwestern side area of Kuju Volcano. In June 2000, at the southwestern region of Aso Caldera the big swarms occurred, some vents were felt. The largest event occurred at 09:32 on 8 June, its magnitude was 4.8. In Aso Caldera, on 10th January, 2001, the felt event (mag=4.0) occurred at the southeastern side near Takamori Town. This seismic event was very interest, because it had a few aftershocks (only three events) and at its hypocentral region no earthquake has occurred recently. The mechanism of this event indicates the reverse fault. At Kuju Volcano, many earthquakes occurred during this period. The swarm-like events occurred on August 27 and 28, 2000. The mechanisms of their events indicate a combination of both normal and right lateral strike-slip type faults. The tension axis maintains a horizontal north-south orientation.



## A new system for sound velocity measurements under high P-T conditions

Y. Aizawa and K. Ito

Using a piston cylinder type high pressure and temperature apparatus in this institute we can carry out runs at 1 ~ 1.5 GPa, room temperature ~ 1200 °C, which is suitable for investigation of the crust and the upper mantle. We have constructed a system for measurements of sound velocity under the crustal and the upper mantle conditions.

We used a piston-cylinder with 24 mm inner diameter and 80 mm thickness. The cell assembly is shown in Fig. 1. A sample with 6 mm diameter and 6 mm length was put between two platinum rods with 6 mm diameter and 18 mm length. Two LiNbO<sub>3</sub> transducers (6 mm diameter, 0.5 mm thickness, and 36° Y-cut) were attached at the far side of the platinum rods. These rods are indispensable especially for wave-pattern observation under high temperatures to keep the temperature of transducers low enough to prevent the breakdown of the transducers.

Figure 2 illustrates the paths of the ultrasonic pulses. We can observe the pulse that goes through the rods and the sample without reflection (path I) and one that is reflected at the interfaces between the sample and the rods (path II). The travel time is obtained from the measurement of the delay time between these echoes, which gives us the precise travel time in the sample [Birch, 1961; Fujisawa et al., 1974]. A difference of acoustic impedance between the platinum rods and the sample is large, and platinum is stable under temperatures >1000 °C. For these reasons we used platinum as the buffer rods. In our experiments, the uncertainty of the temperature was estimated to be  $\pm 20^\circ\text{C}$  at 1000°C.

We measured the travel time of a quartz glass sample at 1 GPa, room temperature ~ 1185°C. Error of the travel time measurements is less than  $\pm 0.4\%$ . Error of usual methods is  $\sim \pm 1\%$  and this method is considered to be useful for measurements of sound velocity under conditions of the crust and the upper mantle.

### References

- Birch, F., 1961, The velocity of compressional waves in rocks to 10 kilobars, 2, J. Geophys. Res., **66**, 2199-2224.
- Fujisawa, H., H. Kinoshita, T. Hachimine, 1974. New apparatus for measurements of velocity and attenuation of elastic waves in minerals, Jishin, **27**, 57-64.

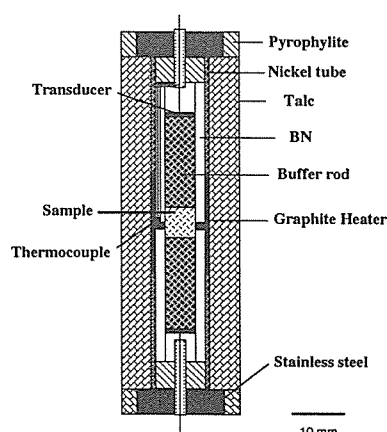


Fig. 1 Sample assembly.

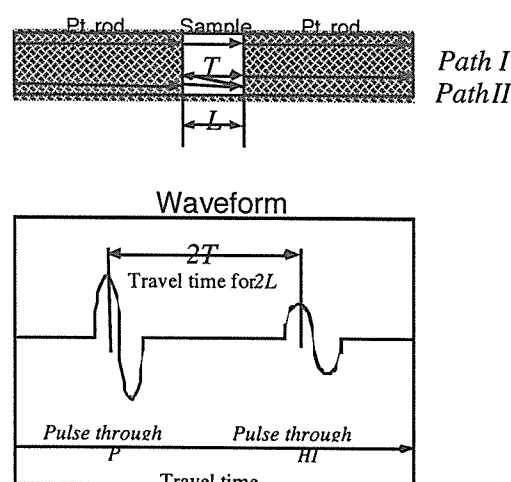


Fig. 2 Paths of the pulses and an observed waveform.

# Observation of seismic activity in the Beppu graben

*Y. Furukawa and H. Mawatari*

We have installed four seismic stations at the Institute for Geothermal Sciences, Kyoto University (IGS), Mt. Karaki (KRK), Mt. Tsurumi (TRM), and Mt. Takasaki (TKS) in March 1993, and one station at Amama (AMA) in October 1993; these stations are located in and around the Beppu graben. The location of the seismic stations is shown in Fig. 1. We have used the earthquake observation system: MICROSEIS-100 of Japex Geoscience Institute, Inc. A 3-component 1 Hz geophone was installed at each seismic station; the data is digitized at a sampling rate of 200 Hz, and is telemetered from each station to the host part of this system installed at the IGS station.

Earthquake is automatically detected by the host system when the amplitude of the vertical signal of three or more stations becomes larger than a threshold value set for each station. The first arrivals have been manually picked, and detected earthquakes have been located using a maximum-likelihood method [Hirata and Matsu'ura, 1987]. The crustal velocity structure used in this study is based on those estimated from refraction seismic studies in the Beppu graben and reflection seismic studies in the central and the southern Kyushu [Ono et al., 1978; Kubotera et al., 1982]. Uncertainty of epicenter location is estimated to be less than 0.5 km in the area between the KF and the AF, but larger than 2 km in the west of 131° 23' E, and error of focal depth will increase with depth and is estimated to be less than 2 km in depths shallower than ~10 km [Hirata and Matsu'ura, 1987].

## References

- Hirata, N. and Matsu'ura, M. (1987) Maximum-likelihood estimation of hypocenter with origin time eliminated using nonlinear inversion technique. *Phys. Earth Planet. Inter.*, 47: 50-61.
- Kubotera, A., Ito, K., Murakami, H. and Mitsunami, T., (1982) Crustal structure of Kuju volcano group as revealed by explosion seismology. *Bull. Volcano. Soc. Japan*, 27: 81-95.
- Ono, K. et al. (1978) Explosion seismic studies in south Kyushu especially around the Sakurajima volcano. *J. Phys. Earth*, 26: S309-S319.

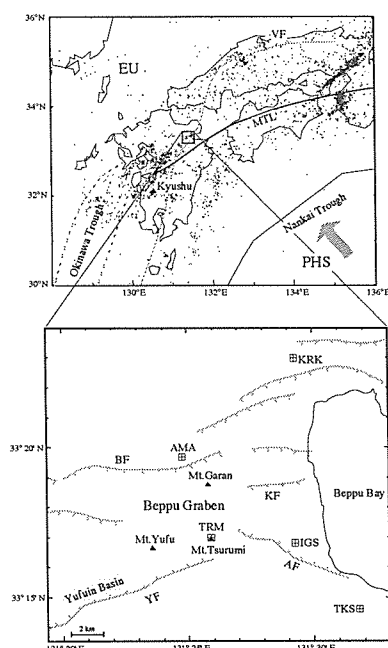


Fig. 1 Schematic tectonic map of the Beppu graben. Top: EU and PHS denote the Eurasian plate and the Philippine Sea plate, respectively. The Median Tectonic Line (MTL) and the volcanic front (VF) are also shown. The Beppu-Shimabara rift zone is shown as hatched zone. The hatched arrow indicates the convergence direction of the PHS. Epicenter of shallow earthquakes (<20 km) located by JMA from Jan. 1993 to July 1996 is also shown. Bottom: the rectangles and the solid triangles indicate the seismic stations (KRK: Mt. Karaki; AMA: Amama; IGS: Institute for Geothermal Sciences; TRM: Mt. Tsurumi; TKS: Mt. Takasaki) and the Quaternary volcanoes. The shaded

## Experimental geochemistry laboratory

*T. Kawamoto*

In Beppu, you can conduct the following two types of experiments:

- 1 **Quench experiments.** Using piston cylinder type high pressure and temperature apparatus you can carry out runs at 1~1.5 GPa, room temperature ~1700 °C. A typical capsule size is less than 3.9 mm outer diameter and 5 mm height.
- 2 **In-situ observation under high pressure and high temperature.** By the use of Bassett's type hydrothermal diamond anvil cell (DAC), you can conduct in-situ observation of materials of your interest up to 1050 °C in a range from 0.1 GPa to about 5 GPa. Pressure at high temperature can be estimated by luminescence of SrB<sub>4</sub>O<sub>7</sub>:Sm<sup>2+</sup> or an equation of state of H<sub>2</sub>O at lower pressures than 2 GPa. You can use an optical microscope, FT-IR microscope (2000 - 10000 cm<sup>-1</sup>), and Raman microscope (532 nm excited) with a combination of DAC.

### Magma characterization system

#### FT-Infrared microscope (JASCO Micro-20 and FTIR 610)

Abundance of total H<sub>2</sub>O and speciation of molecular H<sub>2</sub>O and OH ion in melts, glasses, and crystals. W and globar light sources, CaF<sub>2</sub> beam splitter, InSb detector, 25 mm plus 25 mm working distance and x10 Cassegrainian mirror system are used for 2000 ~ 10000 cm<sup>-1</sup> analysis.

#### Raman microscope (Kaiser HoloLab 5000)

Information of structure of crystals, glasses and melts. Total H<sub>2</sub>O abundances in glasses and melts. 532 nm YAG laser, 21 mm working distance and x20 objective lens are used for 100 ~ 4500 cm<sup>-1</sup> Raman shift analysis.

### Chemical analysis of run products

Electron microprobe analyser (JEOL superprobe), SEM-EDS (JEOL) .

### High temperature and pressure apparatus

#### Diamond anvil cell (Bassett type)

Direct observation of melts and crystals under the conditions up to 1050 °C and 5 GPa.

#### Piston cylinder apparatus (Senyo)

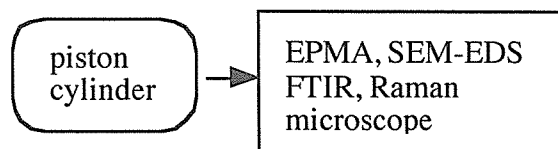
Phase equilibrium experiments up to 1700 °C and 1.5 GPa.

#### Heating stage (Linkam 1500)

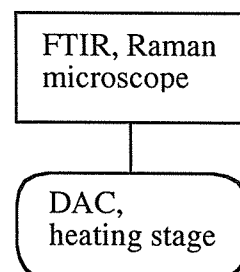
Heating stage under microscope up to 1500 °C at atmospheric pressure.

### *Quench experiments*

### *Characterization*



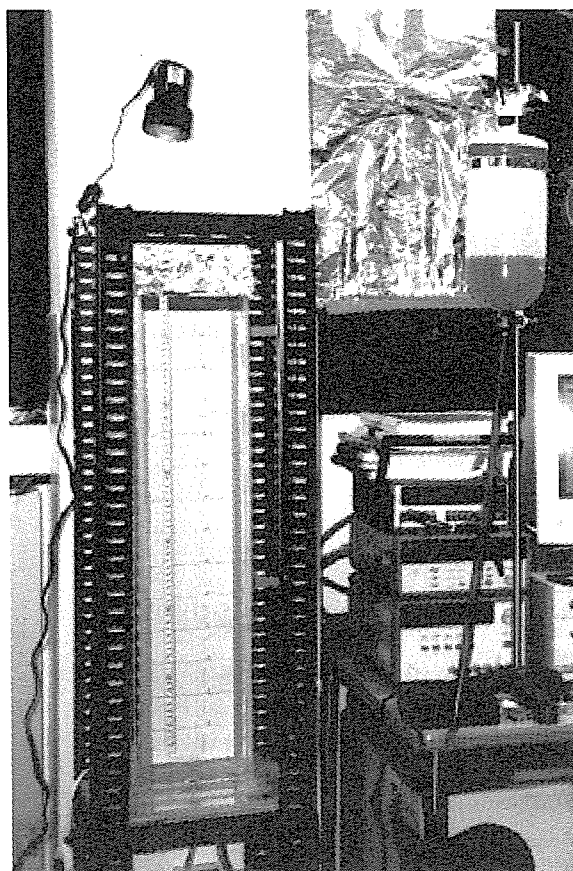
### *In-situ observation*



## The fluid dynamics laboratory

*I. Kumagai*

The fluid dynamics laboratory is equipped with instruments for the measurement of fluid properties and the study of fluid motions. Facilities include a built in kitchen unit, a multi-meter, a dc power supply, a water circulator, gravimeters, a viscometer, a refractometer, heaters, pumps, acryl glass tanks, a 3-channel CCD video camera, tracers for flow visualization and laboratory computer systems for the recording and analysis of data and for digital image analysis, etc.



Experimental apparatus for laminar plumes

## Analytical Procedure of Osmium and Rhenium

*K. Suzuki*

The analytical procedure used here is based on the Carius tube digestion (Shirey and Walker, 1995) combined with bromine-extraction of Os (Birk et al., 1997) or carbon tetroxide extraction (Cohen and Waters, 1996; Pearson and Woodland, 2000) with some modifications. The Carius tube method (Shirey and Walker, 1995) is an effective decomposition technique for achieving complete isotopic equilibration of sample-derived Os with the enriched spike in a wide range of geological materials, although the possibility of accidental sample loss by explosion exists. 2.5 to 5 g of the reference rocks were weighed and added with Re (typically 0.1 – 0.5 ml) and  $^{190}\text{Os}$  spike solutions (0.1 – 0.5 ml) and heated in inverse aqua regia in a sealed Carius tube at 220 °C for

at least 24 hours. After cooling, the tube was opened carefully. In case of bromine extraction, the solution was transferred into a 60 ml PFA vessel, into which 2 ml of liquid bromine and 0.5 ml of a 40 %  $\text{CrO}_3$  solution in 8N  $\text{HNO}_3$  were added. The closed vessel was then placed on a hotplate and heated to approximately 60 °C. Bromine boiling under the aqueous phase scavenged volatile  $\text{OsO}_4$  at the top of the vessel and flowed back to the bottom (Birck et al., 1997). After three hours of bromine extraction, the vessel was cooled in a freezer. The Os-bearing liquid bromine at the bottom was then pipetted into another container with 1 ml water. The water in the vial was discarded and  $\text{HBr}$  (0.5 ml) was added to the bromine containing separated Os, which was then gently evaporated.

As for  $\text{CCl}_4$  extraction, we followed the methods developed by Cohen and Waters (1996) and Pearson and Woodland (2000). The solution and sample residue is transferred to 30ml PFA vessel and added with 4 ml of chilled carbon tetrachloride. This mixture is allowed to warm and shaken for 2 min. The organic fraction is then filtered by solvent extraction filter paper. The filtrate organic phase containing Os extracted. Organic extraction of the aqua regia fraction is performed twice more to ensure consistent Os recovery, which was added with 9N  $\text{HBr}$ . Then, the mixture was tightly capped in a Teflon vessel, allowed to warm to room temperature and then shaken for 2 min and kept under a heat lamp for 1 h. On cooling, the Os-bearing  $\text{HBr}$  was pipetted from the organic phase and dried. In both bromine and carbon tetroxide extraction, the residue was further purified by microdistillation (Roy-Barman, 1993) and ready for mass spectrometry. After extraction of Os described here, the aqueous phase was added with ethanol to reduce  $\text{CrO}_3$  to  $\text{Cr}^{3+}$ . Rhenium was separated from the aqueous phase left behind the  $\text{Br}_2$ -extraction of Os, using Muromac AG 1X8 anion exchange resin. Both Re and Os were corrected for blanks. Total procedural blanks for Os and Re are 6.318 pg with  $^{187}\text{Os}/^{188}\text{Os} = 0.1744 \pm 0.0070$  and 20 pg, respectively.

All measurements presented here were performed on a Finnigan MAT<sup>R</sup> 262 mass spectrometer in a negative ion detection mode (Creaser et al., 1991; Volkening et al., 1991) equipped with a gas leak valve and an ion counting multiplier. A high purity Pt filament (99.999 %, 0.5 mm x 0.025 mm, H. Cross Co. or 99.99 %, 1 mm x 0.025 mm, Tanaka Precious Metal Co.) was baked in air to a bright red temperature for more than three minutes. Osmium loaded on the Pt filament was covered with 10  $\mu\text{g}$  Ba and 2  $\mu\text{g}$  Na. Custom-made 10,000 ppm  $\text{Ba}(\text{NO}_3)_2$  solution (SPEX) was used. Both Re and Os blanks in the solution used were less than 0.01 pg. The filament was then heated in air until the loaded material started to melt and then quickly cooled, which reduces the organic interferences at masses 233-235 in Os isotopic measurements (Birck et al., 1997). This step was omitted in the Re isotopic measurements. Osmium and Re isotopic compositions were measured in the static multiple Faraday collector mode or in the pulse counting electron multiplier mode. Instrumental mass fractionation of Os was corrected by normalizing the  $^{192}\text{Os}/^{188}\text{Os}$  ratio to 3.08271 (Nier, 1937). The subtraction of oxygen contributions for Os and Re was conducted using the ratios of  $^{17}\text{O}/^{16}\text{O} = 0.00037$  and  $^{18}\text{O}/^{16}\text{O} = 0.002047$  (Nier, 1950).

A high blank of Re in mass spectrometer would cause serious troubles for isotopic measurements of low-level Re (e.g., Shen et al., 1996; Birck et al., 1997). We found the major source of high Re blank in mass spectrometry is the sample magazine,

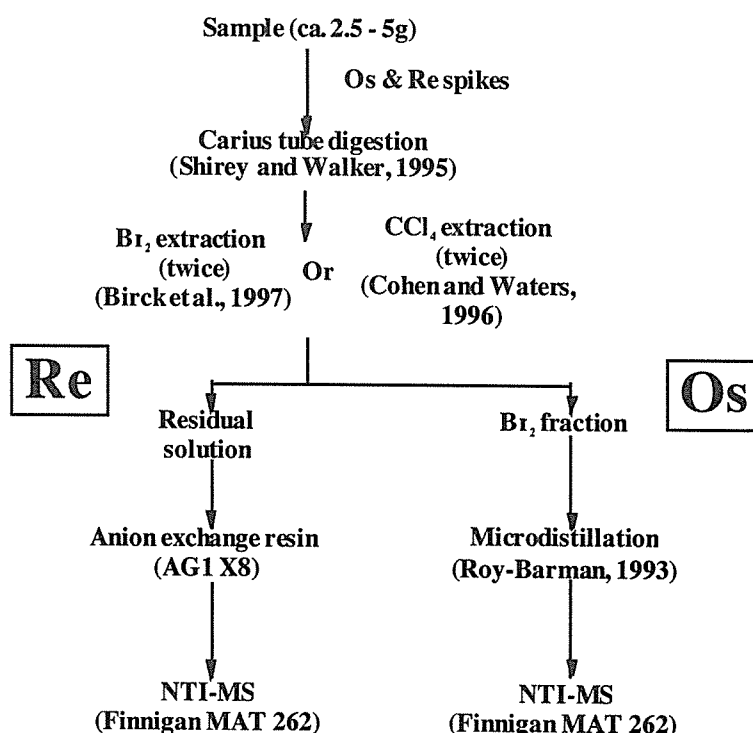


Fig. 1. Analytical procedure.

which supports filament holders. When the magazine was employed which had been used for Pb and Nd measurements on Re filaments, at first high Re loading blank of 10 – 15 pg was observed. Rhenium emitted from Re filaments is possibly attached on the surface of the sample magazine and may be ionized at high temperature caused by following filament heating. The Re blank was reduced to 0.3 pg after 12 months operation of the TIMS without Re filaments.

#### References

- Birck, J. L., Roy-Barman, M. and Capmas, F. (1997) Re-Os isotopic measurements at the femtomole level in natural samples. *Geostand. Newslett.* **21**, 19-27.
- Cohen A. S., and Waters G. G. (1996) Separation of osmium from geological materials by solvent extraction for analysis by thermal ionization mass spectrometry. *Anal. Chim. Acta* **332**, 269-275.
- Creaser, R. A., Papanastassiou, D. A. and Wasserburg, G. J. (1991) Negative thermal ion mass spectrometry of osmium, rhenium, and iridium. *Geochim. Cosmochim. Acta* **55**, 397-401.
- Nier A.O. (1950) A redetermination of the relative abundances of the isotopes of carbon, nitrogen, oxygen, argon and potassium. *Phys Rev B* **77**, 789-793.
- Pearson D. G., and Woodland S. J. (2000) Solvent extraction / anion exchange separation and determination of PGEs (Os, Ir, Pt, Pd, Ru) and Re-Os isotopes in geological samples by isotope dilution ICP-MS. *Chem. Geol.* **165**, 57-107.
- Roy-Barman, M. (1993) Mesure du rapport  $^{187}\text{Os}/^{188}\text{Os}$  dans les basaltes et les peridotites: contribution a la systematique  $^{187}\text{Re}$ - $^{187}\text{Os}$  dans le manteau. *Ph. D. thesis, Universite de Paris VII*
- Shen J.J., Papanastassiou D.A. and Wasserburg G.J. (1996) Precise Re-Os determinations and systematics of iron meteorites. *Geochim Cosmochim Acta* **60**, 2887-2900.
- Shirey, S. B. and Walker, R. J. (1995) Carius tube digestion for low-blank rhenium-osmium analysis. *Anal. Chem.* **67**, 2136-2141.
- Suzuki and Tatsumi (2001) Osmium concentrations and  $^{187}\text{Os}/^{188}\text{Os}$  ratios of GSJ reference samples, JB-1a, JA-2 and JP-1 *Geochem. J.*, in press.
- Volkening, J., Walczyk, T. and Heumann, K. G. (1991) Osmium isotope ratio determinations by negative thermal ionization mass spectrometry. *Int. J. Mass Spectrom. Ion Processes* **105**, 147-159.
- (After Suzuki and Tatsumi, 2001, *Geochem. J.*, in press)

## An analysing system of Sr, Nd and Pb isotopes from rock and mineral samples

*M. Yoshikawa and T. Shibata*

- 1) Rock samples are crushed and then rock chips are pelverized to powder or minerals are separated by isodynamic separator (Franz) at the Rock Crushing and Mineral Separation room.
- 2) Chemical preparations for Sr, Nd and Pb isotope analyses (e.g. acid leaching, decomposition, ion chromatography) are carried out in the class 100 clean room at BGRL.
- 3) The isolated elements are analyzed by thermal ionization mass spectrometer (Finnigan MAT 262). The reproducibility of Sr (100 ng), Nd (150 ng) and Pb (100 ng) isotope measurements were 0.002%, 0.0013% and 0.029% (relative standard deviation: RSD%) , respectively.



## 教育活動 Education

### 学位・授業 Academics

#### 学位審査

大沢信二

(学識確認) 齊藤隆志 (博士 京都大学大学院理学研究科)

須藤靖明

(主査) 森健彦 (博士 京都大学大学院理学研究科)

(審査員) 森真陽 (修士 京都大学大学院理学研究科)

田中良和

(審査員) 森健彦 (博士 京都大学大学院理学研究科)

由佐悠紀

(審査員) 筒井和男 (修士 京都大学大学院理学研究科)

北川大祐 (修士 京都大学大学院理学研究科)

斎藤隆志 (博士 京都大学大学院理学研究科)

#### 講義・ゼミナール

科目

担当教官

##### 学部

地熱学

田中良和, 巽好幸, 由佐悠紀, 須藤靖明, 大沢信二, 古川善紹

陸水物理学

由佐悠紀, 諏訪浩<sup>1</sup>

火山物理学

田中良和, 須藤靖明

陸水物理学

由佐悠紀 (分担)

地球惑星科学 I

巽好幸 (分担)

地球科学実験 B

大倉敬宏 (分担)

##### 大学院 (修士課程)

水圏地球物理学 II

由佐悠紀, 大沢信二, 奥西一夫<sup>1</sup>, 諏訪浩<sup>1</sup>

地球熱学・地熱流体学 I

由佐悠紀, 田中良和, 大沢信二

地球熱学・地熱流体学 II

巽好幸, 須藤靖明, 古川善紹, 竹村恵二<sup>2</sup>

応用地球電磁気学

田中良和, 大志万直人<sup>1</sup>

環境地球科学 II

巽好幸, 井口正人<sup>1</sup>, 石原和弘<sup>1</sup>

##### 大学院 (修士・博士課程)

水圏地球物理学ゼミナール III

由佐悠紀, 大沢信二, 奥西一夫<sup>1</sup>, 諏訪浩<sup>1</sup>, 齊藤隆志<sup>1</sup>

地球熱学・地熱流体学ゼミナール I

由佐悠紀, 田中良和, 大沢信二, 川本竜彦, 鈴木勝彦

地球熱学・地熱流体学ゼミナール II

巽好幸, 須藤靖明, 古川善紹, 小野博尉, 橋本武志, 竹村恵二<sup>2</sup>

応用地球電磁気学ゼミナール

田中良和, 橋本武志, 大志万直人<sup>1</sup>, 神田径<sup>1</sup>

環境地球科学ゼミナール II

巽好幸, 井口正人<sup>1</sup>, 石原和弘<sup>1</sup>, 山本圭吾<sup>1</sup>, 西潔<sup>1</sup>, 神田径<sup>1</sup>

固体地球物理学ゼミナール IV

大倉敬宏, 尾池和夫<sup>2</sup>, 中西一郎<sup>2</sup>

(<sup>1</sup> 防災研究所, <sup>2</sup> 地球物理学教室)

#### 野外実習

地熱学野外実習 (7月31日～8月3日)

別府：温泉井の温度検層, 水質測定

阿蘇：阿蘇火山巡検, 水準測量

地球電磁気学 3 回生野外実習 (7月31日～8月5日)

阿蘇火山自然電位測定  
阿蘇火山地磁気測定  
地磁気3成分絶対値測定  
阿蘇火山AMT比抵抗測定

#### 講義（他大学）ほか

大倉敬宏 非常勤講師：神戸学院大学  
大沢信二 非常勤講師：大分大学（教育福祉科学部後期「温泉学」）  
小野博尉 九州東海大学非常勤講師（農学部後半期「地学」）  
巽好幸 集中講義：大阪府立大学，放送大学  
由佐悠紀 集中講義：九州大学工学部

#### 特別講義

西田泰典（北海道大学理学研究科教授）「火山における熱的及び電磁気的研究」（9月26～28日）  
平 朝彦（東京大学海洋研究所教授）「白亜紀の温暖地球」（10月30日）

### セミナー Seminars

#### BGRLセミナー

8月 3日 真島英壽（九大・理）  
10月 13日 Gary Thompson "The petrogenesis of Rarotonga, South Pacific: A maverick ocean island"  
11月 20日 川本竜彦「コマチアイトマグマはどうやって出来たと考えるか」  
岡元正久（広大・理）「西オーストラリア Pilbara 地域の先カンブリア紀 komatiite, banded chert の Re-Os 及び Sm-Nd 同位体システムティクス」  
11月 27日 丸山誠史（岡山大学固体地球研究センター）「紫外レーザー掘削型同位体比質量分析法（UV-laser IRMS）による酸素同位体比局所分析法の開発と太陽系形成過程の解明」  
12月 22日 柴田知之「東北日本第四紀火山岩の微量元素・同位体組成の島弧横断方向の変化傾向からみた島弧マグマの起源」  
1月 19日 服部雄次（広大・理）「チベットの土壌の地球化学的特徴」  
篠塚一典（海洋科学技術センター）「コンドライト中の希土類元素存在度大気中トリチウムについて」  
2月 8日 相澤義高「高温高压下における岩石・鉱物のP波速度の決定」  
2月 15日 熊谷一郎「Anatomy of mantle plumes—マールブルーケーキとレイヤーケーキ，あなたはどちらがお好き？—」  
3月 1日 芳川雅子「幌満マントルかんらん岩体の化学的進化過程」

#### 電磁気学セミナー

4月 7日 網田和宏「透水係数を変化させて，2次元流動計算を行う場合の計算方法」  
橋本武志「論文英語作成の注意点について（1）」  
長谷英彰「Matlab 言語で書かれた電場計算コードのC言語化」  
5月 17日 網田和宏「2次元領域内で透水係数を変化させる場合のレイリー数の取り扱いについて」  
宇津木充「 $1/R$  の関数の畳み込み無限2重積分を暗算で解く方法」  
橋本武志「論文作成のための英語に関する Tips（2）」「論文紹介 地殻深部を水はどう流れるか クラックの役割，中島善人・鳥海光弘 岩波科学 Vol.66, No.12, 1996」  
長谷英彰「電場計算コードのC言語化（2）」  
6月 8日 網田和宏「書籍紹介 Modeling Density-Driven Flow in Porous Media, Ekkehard Holzbecher,

- Springer, 1998, 3. Analytical Description」  
 宇津木充「食い違い弾性理論についての考察」  
 橋本武志「書籍紹介 Modeling Density-Driven Flow in Porous Media, Ekkehard Holzbecher, Springer, 1998」  
 長谷英彰「電場計算コードのC言語化 (3)」  
 7月 21日 網田和宏「Holtzbecher 式を用いた透水係数変化の試み (1)」  
 宇津木充「雲仙の全磁力観測」  
 橋本武志「論文紹介 “The heat source of Ruapehu Lake ; deductions from the energy and mass balances”, A.W.Hurst, H.M.Bibby, B.J.Scott and M.J.McGuinness, J.V.G.R, 46, 1-20, 1991.  
 長谷英彰「電場計算コードのC言語化 (4)」  
 8月 31日 網田和宏「Holtzbecher 式を用いた透水係数変化の試み (2)」  
 橋本武志「電磁気学ゼミ, これまでの整理と今後の方針」  
 長谷英彰「電場計算コードのC言語化 (5)」  
 9月 29日 網田和宏「Holtzbecher 式を用いた透水係数変化の試み (3)」  
 宇津木充「雲仙の全磁力観測 (続報)」  
 長谷英彰「電場計算プログラムのGUI化」  
 12月 26日 網田和宏「Holtzbecher 式を用いた透水係数変化の試み (4)」  
 宇津木充「阿蘇山における空中磁気測量」  
 橋本武志「界面動電現象に伴う電場・磁場計算 (レビュー)」  
 長谷英彰「電場計算プログラムのGUI化 (2)」  
 2月 2日 網田和宏「Holtzbecher 式を用いた透水係数変化の試み (5)」  
 橋本武志「2次元流動計算コードの円筒座標系化」  
 長谷英彰「電場計算プログラムのGUI化 (3)」  
 3月 30日 網田和宏「計算領域内で透水係数が増加する場合の流動について」  
 宇津木充「地形効果を考慮した自然電位場計算の方法について」  
 橋本武志「阿蘇の地磁気変化と火口湖からの熱放出量の関係について」  
 長谷英彰「地形効果を考慮にいたした場合の3次元電場計算について」

#### 他機関等

- 12月 13日 橋本武志「地殻活動電磁気学」(京大防災研究所地震予知研究センター)  
 11月 8日 橋本武志 “Electromagnetic study in Aso Volcano, Japan” (ウルビノ大学, イタリア)

## 学 会 活 動 Activities in Scientific Societies

巽好幸

編集委員長：The Island Arc  
編集委員：G-Cubed  
評議員：日本火山学会・日本地質学会  
学会賞選考委員：日本岩石鉱物鉱床学会

田中良和

運営委員：地球電磁気・地球惑星圏学会  
委員：地磁気観測作業委員会

由佐悠紀

会長・編集委員：日本温泉科学会  
学会賞選考委員：日本陸水学会，日本地熱学会  
評議員：日本温泉科学会，日本地熱学会  
運営委員長：陸水物理研究会

## 社 会 活 動 Public Relations

大沢信二

大分県温泉地保全検討委員（大分県生活環境部）  
新エネルギー財団地化学技術検討会委員  
大分県温泉調査研究会理事

小野博尉

阿蘇町町史編集委員  
長陽村立長陽西部小学校 3・4 年学級「ふるさとじまん」講師(2000 年 11 月)

須藤靖明

火山噴火予知連絡会委員  
阿蘇火山ガス安全対策専門委員会委員  
くじゅう山系（硫黄山）防災協議会委員  
九重山系硫黄山土石流発生基準雨量検討委員会委員  
熊本県議会災害対策委員会講師「熊本県内の地震活動状況について」(6 月 12 日)  
第 5 回エネルギー業界「ガス情報サロン」講師「阿蘇火山とエネルギー」(7 月 7 日)  
日本キリスト教保育所同盟第 4 2 回夏期大学講師「阿蘇火山について」(8 月 24 日)

巽好幸

ODP 国内研究連絡会委員  
IODP 国内連絡委員会委員  
OD21 科学計画策定 WG 長  
OD21 陸上施設検討 WG 委員  
IODP Scientific Planning Working Group

委員

大分県環境保全審議会委員

由佐悠紀

資源エネルギー庁環境審査顧問  
地熱開発促進調査委員会委員  
大分県環境審議会委員  
大分県自然環境保全審議会委員（温泉部会長）  
大分県土地利用審査会委員  
大分県温泉地保全検討委員会委員長  
大分県温泉調査研究会会長  
大分県温泉管理検討懇話会座長  
地熱発電所環境保全実証調査委員会委員  
地熱構造モデル構築スタンダード作成調査検討委員会委員長  
温泉影響予測手法導入調査検討委員会委員長  
日本温泉協会学術部委員  
別府子供たちセミナー「温泉と火山のはなし」講師（2000 年 4～6 月）  
日本電機工業会地熱セミナー講師（5 月）  
歴史と自然を学ぶ会土曜講座講師（9 月）  
大分合同新聞「21 世紀への遺産」（大分の温泉）執筆者（10 月）  
インターネット博覧会「温泉の科学」監修（12 月）  
韓国子供たち科学ツアー講演講師（12 月）  
平成 12 年度地熱開発管理者研修会講師（1 月）

## 装置・設備 Instruments and Facilities

### 装置 Instruments

#### 【別府】

ICP 発光分光分析装置  
 波長分散型電子プローブマイクロアナライザー  
 エネルギー分散型電子プローブマイクロアナライザー  
 波長分散型蛍光 X 線分析装置  
 エネルギー分散型蛍光 X 線分析装置  
 粉末 X 線回折装置  
 液体シンチレーションシステム  
 イオンクロマトグラフ  
 ガスクロマトグラフ

自動滴定装置  
 全自動微小地震観測システム  
 ピストンシリンダー型高圧発生装置  
 ICP-MS 用レーザーアブレーション装置  
 四重極型 ICP-MS 装置  
 表面電離型質量分析装置  
 外熱式ダイヤモンドアンビル  
 フーリエ変換型近赤外分光光度計  
 赤外顕微鏡  
 加熱ステージ

#### 【阿蘇】

阿蘇, 九重火山連続地震観測システム  
 地殻変動観測坑道  
 孔中温度観測システム  
 ビデオ映像監視システム  
 プロトン磁力計  
 フラックスゲート磁力計  
 地磁気絶対測定システム  
 傾斜計

可搬型地震計 (広帯域, 短周期)  
 人工震源車  
 重力計  
 超伝導重力計  
 地磁気地電流法測定装置 (広帯域型 ULF, ELF, VLF 型)  
 光波測距儀  
 水準測量システム (自動読み)

#### [Beppu]

ICP emission spectrometer  
 Wavelength dispersive electron microprobe  
 Energy dispersive electron microprobe analyzer  
 Wavelength dispersion type X-ray fluorescence analyzer  
 Energy dispersion type X-ray fluorescence analyzer  
 Powder X-ray diffractometer  
 Liquid scintillation system  
 Ion chromatography  
 Gas chromatography  
 Automatic titration system

Full-automated micro-earthquake monitoring system  
 Piston cylinder type high pressure apparatus  
 Laser ablation system  
 Inductively coupled plasma mass spectrometer (ICP-MS)  
 Thermal ionization mass spectrometer (TIMS)  
 Externally heated diamond anvil cell  
 FT-NIR spectrometer  
 IR microscope  
 Heating stage

#### [Aso]

Continuous seismic monitoring system for Aso and Kuju Volcanoes  
 Observation tunnel for ground deformation  
 Borehole temperature monitoring system for Aso  
 Video monitoring system of Aso and Kuju Volcanoes  
 Proton and fluxgate magnetometers  
 Geomagnetic absolute measurement system  
 Tiltmeters

Portable seismometers [broadband short-period]  
 Car-mounted seismicsource  
 Gravimeters  
 Super-Conducting Gravimeter  
 Magneto-Telluric measurement system (broad-band type, ULF, ELF, VLF-band)  
 Electronic distance measurement system  
 Leveling survey system (automatic reading)

## 設備 Facilities

### 岩石粉碎・鉱物分離室

バックミル・ディスクミルによる岩石粉碎やアイソダイナミックセパレータによる鉱物分離を行う。

### 器具洗浄室

実験に用いる器具の洗浄を行う。ドラフト 2 台・イオン交換筒・Milli-Q が設置されている。

### クリーンルーム

HEPA フィルターを設置し極力金属使用を抑えた設計で、クラス 100 のクリーン度を達成している。Sr・Nd・Pb 同位体比分析のための化学処理（試料の分解・イオン交換クロマトグラフィーによる目的元素の抽出）を行っている。

### 地下観測坑道（阿蘇火山地殻変動観測坑道）

阿蘇中岳第一火口から南西 1 km の、地下 30 m に設けられた、直角三角形の水平坑道で、1987 年度に竣工した。現在は、水管傾斜計（25 m）、伸縮計（20、25 m）、短周期地震計、長周期地震計、広帯域地震計、強震計、超伝導重力計が設置されている。

## 新規導入

### ラマン顕微鏡(Raman microscope)

Kaiser optical systems, HoloLab series 5000

カイザー社製のラマン顕微鏡はオリンパスの BX 60 金属顕微鏡と分光検出器で構成される。励起波長は YAG の倍波である 532 nm で、出力 50 mW、通常  $188\text{ cm}^{-1}$ （上付き）～ $4500\text{ cm}^{-1}$  までの波数範囲のラマン散乱光を測定する。検出器を物理的に移動させることで、下はスーパーノッチプラスフィルターの限界（ $100\text{ cm}^{-1}$  位か）、上は  $4600\text{ cm}^{-1}$  以上（限界未決定）測定することが可能である。顕微鏡には作動距離 2.1 mm の 20 倍の超作動対物レンズが装着されている他、作動距離が特に長い作動距離が必要ない場合は、50 倍、100 倍のレンズを用いて空間分解能 3 ミクロンのラマン分析が可能である。シングルモノクロであることと、透過型の回折システムで

あるため、ラマン顕微鏡としては、現在、最も明るい特長を持つ。

### 外熱式ダイヤモンドアンビルセル Externally heated diamond anvil cell

Foxwood 社製 106

コーネル大学バセット教授が開発制作したこのダイヤモンドアンビルセルは、常温から 1050℃ までの温度範囲で使用できる。圧力は現在のところ 5 GPa 程度であれば達成できる。H<sub>2</sub>O を圧力媒体として使用し、H<sub>2</sub>O の状態方程式を用いて圧力を測定する場合、2.5 GPa までの圧力範囲で使うことができる。それ以上の圧力範囲では SrB<sub>4</sub>O<sub>7</sub>:Sm<sup>2+</sup> などの蛍光物質を試料とともに封入しラマン顕微鏡で波長測定を行い圧力を計算する。

高温度での圧力決定については、圧力マーカの蛍光線の波長測定よりも、X 線を用いて標準物質の格子定数を求める方法が望ましいが、設備はない。

### フーリエ変換型近赤外分光光度計 FT-NIR spectrometer, IR microscope

日本分光社製 FTIR610+MICRO-20-16

近赤外顕微鏡は、外熱式ダイヤモンドアンビルセルを使用できるように、標準よりも長い作動距離と焦点距離（25 + 25 mm）を有するように改造されている。InSb ディテクターと CaF<sub>2</sub> ビームスプリッターの組み合わせることによって、波数 2000 cm<sup>-1</sup> から 8000 cm<sup>-1</sup> までの赤外～近赤外領域での測定に最適化されている。

加熱ステージ Heating stage

リンカム社製 TS1500

性能、1500℃までの温度範囲で、微小な液体包有物や流体包有物の加熱観察を実体顕微鏡下で行うことが可能である。アルゴンと水素の混合気体を用いて還元的な雰囲気で行うことが可能である。

## 研 究 費 Funding

### 科学研究費補助金

基盤研究(A) 須藤靖明・橋本武志（分担）「阿蘇山の火口直下に存在する圧力源の実体と噴火活動における役割の解明、代表：川勝均」3,500 千円

基盤研究(A) 大倉敬宏（分担）「変動するフィリピン島弧：地球物理および地質学的調査・研究、代表：安藤雅孝」4,800 千円

基盤研究(B) 大倉敬宏（分担）「地震発生の制御実験－南アフリカ金鉱山における－、代表：安藤雅孝」1,600 千円

基盤研究(B) 巽好幸・川本竜彦「含水珪酸塩溶融体の高温高压下におけるその場観察：マンツルの融解過程における水の役割の解明」700 千円

基盤研究(B) 田中良和（分担）「3次元深部地殻構造電磁探査システムの研究」300 千円

基盤研究(C) 大沢信二・由佐悠紀「火山体土壌空隙を介しての火山ガスと大気の相互作用」2,000 千円

基盤研究(C) 田中良和・橋本武志「海底電線を用いた九州西部海域の地殻電気抵抗の研究」700 千円

奨励研究(A) 大倉敬宏「引き裂かれるフィリピン島弧-マコロド回廊生成プロセスの解明-」1,200 千円

奨励研究(A) 川本竜彦「水を含んだマグマの構造の実験的解明」700 千円

奨励研究(A) 鈴木勝彦「白金-オスミウム、レニウム-オスミウム系を用いた海洋プレートの循環を追う試み」1300 千円

奨励研究(A) 橋本武志「地下浅部に貫入したマグマの冷却過程の解明」800 千円

特別研究促進費 田中良和（分担）「有珠山2000年噴火と火山防災に関する総合的観測研究」590 千円

### 受託研究

大沢信二「火山体水理構造のマグマ活動への影響の解明」1,923 千円

鈴木勝彦「高精度オスミウム同位体測定法の開発と地球化学的方法による白金-190-オスミウム-186壊変系列の壊変定数の決定」1800 千円

巽好幸「スーパープリュームの岩石学的研究」16,297 千円

### 奨学寄付金等

川本竜彦、京都大学学術研究奨励金「富士火山の下におけるマグマと熱水の溶解条件の実験的解明」1500 千円

川本竜彦、日本原子力研究所平成12年度黎明研究「高温度高圧力条件下におけるマグマの分光学」1800 千円

鈴木勝彦、日本科学協会「オスミウム同位体を用いた海洋底における有用金属硫化物鉱床の生成過程の研究」550 千円

田中良和・須藤靖明・小野博尉・橋本武志、京都大学創造開発研究（在外研究員）「活動的火山における流体流動モニタリングに関する調査研究」1,529 千円

## 共同研究等

田中良和（分担），日米科学協力事業「ロングバレーカルデラの電磁気共同観測」800 千円  
田中良和，東京大学地震研究所共同研究「伊豆半島における地殻活動電磁気学」248 千円

## 来 訪 者 Visitors

### 【別府】

- 4 月 1 日 岩屋毅（元衆議院議員），中井俊一・折橋（東大地震研）  
4 日 中城勝喜・寺司昭男（大分県生活環境）  
7 日 濱崎雅憲（大分地方気象台）  
8 日 別府子供セミナー（5 名），ケーブルテレビジョン別府，伊藤・牧ヶ野（キューバス）  
11 日 福富・古賀（株・カミナガ）  
12 日 岡洋一郎（大分モンゴル親善協会）  
17 日 川畑・野尻・荒巻（富士通）  
22 日 別府子供セミナー（15 名），ケーブルテレビジョン別府，牧ヶ野（キューバス）  
26 日 太田・御沓（大分県生活環境課）
- 5 月 9 日 大分放送取材班一行  
16 日 山崎芳直（21 世紀への遺産）  
19 日 衛藤良司（大分合同新聞）  
22 日 青池雄一（共同通信）  
23 日 花房篤司（朝日新聞）  
24 日 別府大学学生 4 名  
25 日 Ekkehard Holzbecher（元客員助教授，9 日間）  
26 日 豊田研吾（NHK 大分放送局）  
27 日 別府子供セミナー（子供 13 人），ケーブルテレビジョン別府，伊藤・牧ヶ野（キューバス）  
29 日 Wilfred Elders（元客員教授夫妻），Trevor Hunt（元客員教授夫妻）  
30 日 太田・木村・天野（京大経理部），西村（京大施設部），北野（理学部司計掛）  
31 日 Ian Graham（元客員助教授）
- 6 月 12 日 太田・御沓（大分県生活環境課）  
18 日 別府子供セミナー（10 名），ケーブルテレビジョン別府，伊藤・牧ヶ野（キューバス）  
21 日 岡洋一郎・亀山 哲・藤野健治（大分モンゴル親善協会）
- 7 月 3 日 堀江正治（名誉教授）  
4 日 八幡雅彦（別府大学短期大学部）  
12 日 木崎俊勝（読売新聞）  
13 日 河野 功・藤川将護（大分県情報企画室），エディ マリカ（2 日間）  
14 日 Jatmiko Prio Atmojo（九大），三浦祥子（ハヌマン）  
17 日 新名真裕美（北大）  
18 日 森山・竹中（出光大分地熱）  
28 日 三浦祥子（ハヌマン），栗原 稔（大分みらい信用金庫）  
31 日 鱈 嘉紀（朝日新聞），西村嘉晃・石井秀樹・苗村康輔（京大：地熱学実習，3 日間）
- 8 月 2 日 奥西一夫・Mihaela-Iuliana Constantin（京大，2 日間），青板邦之（元京大施設部長）  
3 日 Christian Schmidt and Michael Husman（ドイツ・ハノーバ大学，28 日間）  
4 日 田中秀雄（大分県文化企画部）  
7 日 Chi Vinh Ly（広大）  
7 日 太田・御沓（大分県生活環境課）  
21 日 鹿園直建（慶応大）



- 22日 大分大学附属中学校 PTA 一行
- 27日 新城竜一（琉大，5日間）
- 27日 渡慶次聡（琉大，4日間）
- 9月 18日 下池・八田・塩塚（西日本技術開発）
- 22日 太田・御沓（大分県生活環境課）
- 24日 西田泰典（北大，26日まで）
- 25日 岡洋一郎（大分モンゴル親善協会），バヤルマグナイ・ガンフヤグ（モンゴル・バヤンホンゴル県），アルタンツォジュ（大分大学），半田 駿（佐賀大学）
- 26日 高志徹（鶴見台中学校）
- 27日 川野哲也（院内町長），衛藤強（院内町振興課）
- 29日 松本，八田（西日本技術開発）
- 10月 3日 藤沢康弘（鹿児島大学，4日間），河上哲生（京大，6日間）
- 4日 清水洋・岡元正久（広大），橋口 智幸（鹿児島大学，5日間）
- 7日 山崎芳直（21世紀への遺産），小林記之（京大，2日間）
- 10日 松村絢子（京大，4日間）
- 11日 大倉敬宏（京大）
- 13日 徳田建司氏（別府市民）
- 16日 清田透（大分合同新聞）
- 18日 西裕季利他2人（NHK 大分放送局）
- 19日 藤川（大分県情報企画室），高野・百雲（大宣）
- 23日 太田・御沓（大分県生活環境課），坂本和一・若井ます江（立命館アジア太平洋大学 学長・アドミニストレーション・オフィス）
- 26日 九州大学地熱研修コース一行（12名）
- 30日 平朝彦（東大），川野田実夫・西垣肇・学生5名（大分大学）
- 11月 10日 高野・戸田（大宣）
- 15日 別府市民一行10人，筒井和男（京大）
- 16日 大野博司（韓国語通訳）
- 21日 曾我・藤原・米満・梅澤・丸岡・脇野（京大施設部），東辻（理学部施設掛）
- 25日 田中剛・谷水（名大）・松田准一・松本拓也（阪大）・西尾嘉朗（東大地震研）・平田 岳史・服部道成（東工大）・熊谷（海洋科学技術センター）
- 12月 4日 安藤茂信（湯布院ライオンズクラブ），マレーシア高校生1名，田川豊治（日出町民）
- 5日 加藤正信（別府市民）
- 8日 熊谷公生（九重町民）
- 11日 任鐘元（東工大，19日間）
- 12日 坂本富男・菅沼秀和・熊谷英憲（海洋科学技術センター）
- 15日 清英彦（電源開発豊肥地熱事務所），伊藤笙（キューバス）
- 1月 10日 清英彦・矢口稔明（電源開発豊肥地熱事務所）
- 13日 岡元正久（広大，7日間）
- 15日 服部雄次（広大）
- 18日 巽好幸（海洋科学技術センター，3日間）
- 22日 浜田亀太郎（地熱），河村建一（末広郵便局）
- 22日 Chi Vinh Ly（広大）
- 23日 吉岡正文（瀬戸臨海実験所）
- 24日 財津・中野（ケーブルテレビジョン別府），
- 27日 ケーブルテレビジョン別府一行（4名）
- 30日 三浦祥子（ハヌマン）
- 31日 堀江正治（名誉教授）
- 2月 2日 百雲ほか1名（大宣）
- 5日 Finke（ThermoFinnigan）
- 14日 佐藤裕之・笹原良宣（大分県別杵速見地方振興局），茅嶋（大宣），伊東和彦（南大阪

- 大学, 3 日間)
- 16 日 新宮一広 (環境衛生科学研究所) 藤田洋三 (カメラマン)
- 19 日 鎌嘉紀 (朝日新聞)
- 24 日 巽好幸 (海洋科学技術センター, 4 日間)
- 27 日 下岡・浦嶋・奥村・森川 (京大経理部), 井上・小原 (海洋科学技術センター)
- 28 日 太田・御沓 (大分県生活環境課): 広沢・梅木 (大分県統計情報課), 板井 (富士通), 和田至誠 (大分県議会議員)
- 3 月 1 日 大分大学附属小学校生徒一行
- 4 日 別府散策の会一行
- 12 日 宮田佳樹 (東大)
- 17 日 藤原博・秋吉哲幸 (昭和 24 年頃の技術補佐員)
- 19 日 鎌裕之 (東大)
- 21 日 中川 (京大附属図書館宇治分館), 島本・木村・浅野 (京大宇治地区事務部)
- 22 日 濱崎・日吉・中尾 (大分地方気象台)
- 26 日 巽好幸ほか 2 名 (海洋科学技術センター), 東辻 (京大理学部施設掛), 斉藤博・晃父子 (鹿児島県高山町)
- 27 日 鎌田浩毅・金子克哉・加藤護 (京大) 他
- 29 日 テレビ大分取材班一行
- 30 日 金庫検査; ・服部・森田 (京大経理部), 笹原・田中 (京大理学部)

【阿蘇】

- 4 月 10 日 城森 (ネオサイエンス)
- 5 月 26 日 加茂幸介 (名誉教授), 平林順一 (東工大), 長尾年恭 (東海大), 吉田・西 (広島市大)
- 30 日 宮内 (用度掛)
- 31 日 北野 (司計掛長), 西村 (施設掛), 九州財務局
- 6 月 7 日 金嶋 (東工大), 山本希 (地震研)
- 13 日 吉田 (広島市大, 2 日間), 松波孝治, 重富國宏 (防災研, 2 日間)
- 7 月 14 日 吉田 (広島市大), 立野ダム工事関係者 (2 名)
- 18 日 吉田 (白山工業)
- 8 月 21 日 財務局監査 (2 名, 3 日間), 北野司計掛長他 (4 名, 3 日間), Christian Schmitt・Michael Hussman (ドイツ・ハノーバ大学, 3 日間)
- 22 日 中山 (立野ダム工事事務所)
- 24 日 吉田・西 (広島市大)
- 29 日 小林・江浦 (国際電子工業)
- 11 月 16 日 長陽村立長陽西部小学校 3, 4 年学級 (15 名, 引率: 江口教諭)
- 30 日 大沢 (事務局長他 2 名)
- 12 月 9 日 坂中伸也 (秋田大学)
- 14 日 石原・井口・為栗 (桜島観測所), インドネシア留学生 (2 名)
- 1 月 17 日 宮縁 (森林総研)
- 19 日 大内 (西日本技術開発)
- 3 月 1 日 JICA 研修生 (5 名)・早水かほる (日本国際協力センター)・加藤孝志(気象庁)・田所敬一 (名古屋大学)・G.M.Besana(PHIVOLCS)
- 2 日 後藤他 3 名 (施設掛)
- 3 月 27 日 鎌田浩毅・金子克哉・加藤護 (京大) 他 (3 日間), 趙國澤夫妻 (2 日間)